DISTRIBUTION AGREEMENT

In presenting this thesis or dissertation as a partial fulfillment of the requirements for an advanced degree from Emory University, I hereby grant to Emory University and its agents the non-exclusive license to archive, make accessible, and display my thesis or dissertation in whole or in part in all forms of media, now or hereafter known, including display on the world wide web. I understand that I may select some access restrictions as part of the online submission of this thesis or dissertation. I retain all ownership rights to the copyright of the thesis or dissertation. I also retain the right to use in future works (such as articles or books) all or part of this thesis or dissertation.

_____

Rasagnya Viswanadha Date

Assembly and Transport of the Ciliary Inner Dynein Arm, I1 Dynein

By

Rasagnya Viswanadha

Doctor of Philosophy

Biochemistry, Cell and Developmental Biology

_____

Winfield S. Sale, Ph.D.

Advisor

_____

Maureen A. Powers, Ph.D.

Committee Member

_____

Tamara Caspary, Ph.D.

Committee Member

_____

Richard A. Kahn, Ph.D.

Committee Member

_____

Victor Faundez, MD, Ph.D.

Committee Member

Accepted:

_____

Lisa A. Tedesco, Ph.D.

Dean of the James T. Laney School of Graduate Studies

_____Date

Assembly and Transport of the Ciliary Inner Dynein Arm, I1 Dynein

By

Rasagnya Viswanadha

BSc., McMaster University, 2006

Advisor: Winfield S. Sale

An abstract of

A dissertation submitted to the Faculty of the James T. Laney School of Graduate Studies of Emory University in partial fulfillment of the requirements for the degree of Doctor of Philosophy

In

Graduate Division of Biological and Biomedical Sciences

2015

Abstract

Assembly and Transport of the Ciliary Inner Dynein Arm, I1 Dynein

By

Rasagnya Viswanadha

Motile cilia are essential for the development and for function of many organs in the adult. Large ATPase complexes called dyneins drive motility of cilia. Defects in the assembly of ciliary dyneins result in diseases including Primary Ciliary Dyskinesia (PCD). However, we are only beginning to understand the mechanisms of dynein assembly. To determine how ciliary dyneins are assembled, I focused on the *Chlamydomonas* inner dynein arm, I1 dynein. I1 dynein precursors in the cytoplasm assemble as a 20S complex similar to the 20S I1 dynein complex isolated from the axoneme. The intermediate chain subunit, IC140 (*IDA7*), and heavy chains (*IDA1, IDA2*) are required for 20S I1 dynein precursor assembly in the cytoplasm. Taking advantage of cytoplasmic complementation in zygotes, I determined that the I1 dynein complex is transported to the distal tip of the cilium before incorporating in the axoneme. In addition, cytoplasmic complementation in dikaryons using the conditional kinesin-2 mutant, *fla10-1,* revealed that transport of the I1 dynein precursor complex is dependent on kinesin-2 activity. Thus, I1 dynein assembly depends upon IFT and at least one additional factor, IDA3, for transport to the ciliary distal tip prior to docking in the axoneme. Together, these data indicate that ciliary axonemal dyneins assemble in a stepwise fashion beginning with precursor complex assembly in the cytoplasm followed by entry to the ciliary compartment and transport by IFT within the cilium before docking in the axoneme.

Assembly and Transport of the Ciliary Inner Dynein Arm, I1 Dynein

By

Rasagnya Viswanadha

BSc., McMaster University, 2006

Advisor: Winfield S. Sale, Ph.D.

A dissertation submitted to the Faculty of the James T. Laney School of Graduate Studies of Emory University in partial fulfillment of the requirements for the degree of

Doctor of Philosophy

In

Graduate Division of Biological and Biomedical Sciences

Biochemistry, Cell and Developmental Biology

2015

ACKNOWLEDGEMENTS

The last seven years has been a period of personal and intellectual transformation. I would like to express my special appreciation to my advisor, Professor Win Sale. You have been an incredible mentor and role model for me. Your advice, guidance and encouragement has enabled me to grow as a researcher and as a person.

I would also like to thank my committee members, Professors Victor Faundez, Maureen Powers, Rick Kahn and Tamara Caspary for the many engaging and enjoyable discussions of my project and for challenging me at every committee meeting.

Two special women facilitated my learning in the laboratory: Laura and Maureen. Laura, thank you for your patience and for meticulously teaching me the techniques in that laboratory. Maureen, thank you for teaching me how to be thorough with my thinking, questioning, experimentation and with interpretation of the data.

I am fortunate to have been mentored by two brilliant post-docs: Lea and Avanti. They are the finest examples of mentors and friends.

I am grateful to Emily, who has given me the pleasure of having numerous intellectually stimulating scientific discussions, and at many times, served as my "mirror" to bounce back experimental ideas.

I am blessed to have an incredibly strong support system: My family including my parents, sisters and in-laws. Thank you Dad, for instilling the passion for science - whether it be in the kitchen while cooking or on the tennis court while serving a ball. Thank you Mom for always being warm, compassionate and patient. You have influenced the person and the mother I am today. I am especially thankful to my sisters, Kavya and Prakriti for always being there! You know and feel me without me saying a word.

To my best friend, critic, confidant and husband, Rohit, thank you. You bring out the best in me at each and every step. This is your achievement as much as it is mine.

Finally, I am proud and grateful for my children, Neil and Nivin. It is for you, that I strive to the best I can be.

TABLE OF CONTENTS

List of Figures:

Chapter 1:

Chapter 2:

Chapter 4:

Chapter 1 – Introduction and Hypothesis

Overview

The overall objective of this dissertation is to determine the mechanisms of assembly of eukaryotic motile cilia/flagella. Cilia are generally classified as either immotile/primary/sensory or motile structures. Each plays essential roles in both vertebrate development and in a variety of functions of organs in the adult (Eggenschwiler and Anderson 2007; Hildebrandt et al. 2011; Drummond 2012; Oh and Katsanis 2012; Satir 2012). In this dissertation, I focus on the assembly of motile cilia that, in humans, are critical for embryonic development, sperm motility and movement of fluid in the airway, oviducts, and brain ventricles (Fig.1.1, (Satir and Christensen 2007; Brooks and Wallingford 2012; Satir et al. 2014). I am particularly interested in understanding how large and complex ciliary dynein motors, required for generating power and controlling ciliary motility, are assembled. The axoneme is a conserved microtubule scaffold that is comprised of several distinct dynein motors (Kikkawa 2013; Kamiya and Yagi 2014). The axoneme also harbors structures including the central pair (CP) apparatus (Goduti and Smith 2012), radial spokes (RS) (Pigino and Ishikawa 2012), Nexin-Dynein Regulatory Complex (N-DRC) (Porter 2012) and the calmodulin- and spoke-associated complex (CSC) (DiPetrillo and Smith 2013) that are responsible for regulating dyneins and ciliary motility (Fig. 1.4).

While significant progress has been made in understanding the composition and structure of the axonemal dyneins, we are only beginning to understand the mechanisms of assembly of the dyneins complexes. A collection of genetic disorders (such as Primary Ciliary Dyskinesia (PCD)) that result from defective assembly and function of motile cilia, have been linked to mutations in genes responsible for assembly of the axonemal

dyneins (Zariwala et al. 2011; Kobayashi and Takeda 2012; Knowles et al. 2013a; Kurkowiak et al. 2015). Although we have discovered only a small number of the genes responsible for PCD thus far, it is notable that the majority of the known mutations are in genes whose products contribute to assembly of axonemal dyneins (reviewed in (Zariwala et al. 2011; Hjeij et al. 2014). Thus, the central question of this dissertation is a crucial one: How are the ciliary axonemal dynein motors assembled? I include a brief review of a number of topics relevant to my thesis.

In this introduction, I will discuss: (1) the significance of cilia in human health and disease and will define (2) the structure of the motile axoneme, which is comprised of more than 400 proteins including at least 8 different dyneins each precisely positioned in the axoneme (Bui et al. 2012; Kamiya and Yagi 2014). I will discuss (3) the steps that lead to assembly of dyneins in the axoneme beginning with formation of the precursors in the cytoplasm (described in the literature as "preassembly") before transport and docking in the axoneme (Omran et al. 2008; Kobayashi and Takeda 2012). In addition, I will discuss (4) the highly conserved transport system in the ciliary compartment called Intraflagellar Transport (IFT) required for assembly of the primary and motile cilia (reviewed in (Scholey and Anderson 2006; Pedersen and Rosenbaum 2008; Ishikawa and Marshall 2011; Bhogaraju et al. 2013b; Scholey 2013b).

Here, I test the hypothesis that axonemal dynein complexes, as cargoes, depend on IFT for transport into and within the cilium before docking to the axoneme (Fig. 1.9). To achieve these aims, I focus on one axonemal inner dynein arm called I1 dynein (also known as dynein f; (Wirschell et al. 2007a), and I will explain the basis of using I1 dynein as model for defining assembly of axonemal dyneins. Based on my studies, I1

dynein assembly in the axoneme occurs in a stepwise fashion including: assembly of the dynein precursors complex in the cytoplasm; entry into the ciliary compartment; directed transport within the cilium by IFT and docking to precise positions in the ciliary axoneme (Fig. 1.9).

My work takes advantage of the model genetic organism, *Chlamydomonas reinhardtii* (Harris 2009). *Chlamydomonas* offers numerous genetic and biochemical advantages for the study of I1 dynein, and has been instrumental in defining conserved genes and mechanisms of ciliary assembly (Silflow and Lefebvre 2001; Ostrowski et al. 2011; Avasthi and Marshall 2012; Dutcher 2014). For example, IFT was discovered in *Chlamydomonas* (Kozminski et al. 1993), and this discovery alone has led to the identification of a large number of human diseases associated with cilia (Rosenbaum and Witman 2002; Scholey and Anderson 2006; Marshall 2008; Gerdes et al. 2009; Davis and Katsanis 2012; Drummond 2012; Oh and Katsanis 2012). *Chlamydomonas* has provided an informative series of mutant cells defective in I1 dynein assembly (Wirschell et al. 2007a; Wirschell et al. 2009) and has allowed me to test the hypothesis that I1 dynein is transported by IFT to the distal tip of the cilium before assembly in the axoneme. Additionally, experiments using *Chlamydomonas* have revealed the role of individual I1 dynein subunits and potential interacting partners of I1 dynein required for the assembly in the axoneme. For instance, our work revealed the identity of a new gene, *IDA3*, which appears to encode a protein specifically required for I1 dynein transport into the ciliary compartment (W. Sale lab., in preparation). The mutant *ida3*, and the gene *IDA3* are featured in Chapters 2 and 3 and additional analysis of *ida3* is presented in a recent publication (Viswanadha et al. 2014).

Significance of Cilia and Dyneins

We have experienced a surge in understanding of the importance of cilia in development and organ function (Smith and Rohatgi 2011). The discovery of IFT twenty years ago (Kozminski et al. 1993) has enabled an entirely new view of the primary cilium, a non-motile cilium responsible for cell signaling and sensory functions (Satir et al. 2010), as well on the importance of motile cilia in development and organ function (Drummond 2012; Brooks and Wallingford 2014). Evidence gathered in the last decade has revealed that mutations in genes encoding conserved IFT components, or associated proteins, result in developmental defects and failure in organ functions thus defining a class of diseases called ciliopathies (Marshall 2008; Veland et al. 2009; Hildebrandt et al. 2011; Davis and Katsanis 2012; Drummond 2012; Kim and Dynlacht 2013). In this introduction, I focus primarily on the PCD class of ciliopathies that is directly associated with defective assembly and function of motile cilia.

I also include brief discussion of a few landmark studies that contributed to our current view of the functional roles of cilia. Notable advances include: (1) analysis of mutations in the IFT genes in the mouse leading to the recognition that primary cilia are required for normal kidney function and (2) the discovery that failure in assembly of primary cilia results in polycystic kidney disease (PKD) (Pazour 2004; Yoder 2007; Lehman et al. 2008; Zhou 2009; Takiar and Caplan 2011; Huang and Lipschutz 2014). This second advance began with a pioneering study carried out by Pazour and colleagues who analyzed a hypomorphic mutation in IFT88, a component of the IFT complex, in the mouse (Pazour et al. 2000). Among the key observations was that these transgenic mutant mice (Tg737) died shortly after birth due to polycystic kidney disease (Pazour et al. 2000;

Taulman et al. 2001; Yoder et al. 2002). Pazour et al. observed that, in contrast to the kidneys from the control mice, which displayed a primary cilium on the apical surfaces, the assembly of the primary cilium was defective in Tg737 mice, presumably associated with the cystic kidneys. In addition to cystic kidneys, these mice also displayed pathologies in other organs that likely resulted from defective ciliary function (Taulman et al. 2001; Pazour et al. 2002a; Zhang et al. 2003). Genetic screens in *C. elegans* revealed major membrane proteins, PKD1 and PKD2, that are critical to normal kidney function, are localized to the primary cilia (Qin et al. 2001; Jauregui et al. 2008). These studies led to the recognition that proper targeting of the PKD proteins to the ciliary membrane is critical for normal functioning of primary cilia (Qin et al. 2001; Pazour et al. 2002b; Yoder et al. 2002; Nauli et al. 2003). Thus, studies such as these established the vital roles that primary cilia play in normal kidney function and began a completely new understanding of diseases in the kidney.

Another important advance comes from the forward genetic screens in the mouse by Anderson and colleagues that revealed that the primary cilium is also critical to the development of the central nervous system in vertebrate embryos (Caspary et al. 2002; Garcia-Garcia et al. 2005). Other investigators also discovered that components of the Hedgehog signaling, a highly conserved pathway critical for organism development are localized to primary cilia and that Hedgehog signaling also depends on IFT (Corbit et al. 2005, Haycraft et al. 2005, Huangfu et al. 2003, Liu et al. 2005 and reviewed in Scholey and Anderson 2006; Wang et al. 2006; Goetz and Anderson 2010). Additional mutants from the screen revealed that additional proteins important for the Hedgehog pathway, such as the small GTPase Arl13b, localized to the cilium and are critical for normal

development (Larkins et al. 2011). These pioneering studies led to a new view of the primary cilium as an organizing center for signaling proteins critical in vertebrate development, organ homeostasis (see review by (Goetz and Anderson 2010; Satir et al. 2010) and for further function of sensory cells including photoreceptor cells (Insinna and Besharse 2008; Malicki and Besharse 2012; Scholey 2012; Thomas et al. 2014; Wheway et al. 2014). Additional studies in the mouse and in other vertebrates have also demonstrated a role for the primary (Jones et al. 2008) and motile cilia in establishing planar cell polarity (PCP)(Marshall and Kintner 2008; Mitchell et al. 2009; Marshall 2010; Wallingford and Mitchell 2011; Wallingford 2012; Werner and Mitchell 2012).

Relevant to my thesis was the discovery that motile cilia are required for left-right pattern formation in early vertebrate development and important for body organization and heart morphogenesis during early development (McGrath and Brueckner 2003; Basu and Brueckner 2008; Drummond 2012; Hirokawa et al. 2012; Larkins et al. 2012; Wallingford 2012; Babu and Roy 2013; Komatsu and Mishina 2013; Koefoed et al. 2014; Yoshiba and Hamada 2014). It had been postulated that motile cilia play a key role in early development since it was recognized that patients with PCD (characteristic of defects in motile cilia and previously cited as “immotile cilia syndrome” or “Kartegener’s syndrome”) also exhibited a high probability of *situs inversus* (Afzelius 1981). Subsequently, the role of motile cilia at the embryonic node was confirmed in studies of transgenic mice in which a component of kinesin-II (Kif3), responsible for anterograde IFT was knocked out (Nonaka et al. 1998; Marszalek et al. 1999; Takeda et al. 1999). The mice had a high incidence of defects in neural tube closure and general problems of normal pattern formation, including defective heart morphogenesis. The authors also

directly observed motile cilia on the epithelial cells of the embryonic node. Thus, the discovery of the motile cilia on the node gave rise to new ideas for how asymmetry is established in the early vertebrate embryo. In addition, Brueckner and colleagues determined that an axonemal dynein called "left-right dynein (lrd)" is defective in the "inversus viscerum" mouse, also indicating a role for motile cilia in normal left-right patterning (Supp et al. 1997).

Other studies showed that motile cilia on the embryonic node are required to generate fluid flow across the epithelia during early phases of vertebrate development (reviewed in (Hirokawa et al. 2006). One of the most impressive and interesting experiments conducted by Nonaka and colleagues, directly demonstrated that fluid flow across the node is a key trigger for breaking symmetry in the developing mouse (Nonaka et al. 1998). In addition, Brueckner went on to determine that along with the motile cilia, primary cilia are also present at the node (McGrath et al. 2003). Brueckner proposed that primary cilia act as mechano-sensors that measure directed fluid flow generated by the motile cilia and translate this mechanical stimulus to downstream signals required in asymmetric growth and differentiation in the embryo (Basu and Brueckner 2008). Part of the foundation for Bruckner's proposal was based on evidence from other studies had demonstrated that primary cilia act as mechanosensors (Praetorius and Spring 2003b; Praetorius and Spring 2003a; Nauli et al. 2013).

Based on additional studies, the fluid flow generated by the motile cilia is also thought to move morphogens across the embryonic node and normal embryonic development (Tanaka et al. 2005). However the precise nature and role of the morphogens (discussed in (Tanaka et al. 2005) at the embryonic node is not understood.

What is understood is that proper assembly and function of the motile cilia is required for directed fluid flow across the embryonic node and normal development. One of the most severely affected organs in mice with defective motile cilia is the heart (Brueckner 2012; Keady et al. 2012; Larkins et al. 2012; Koefoed et al. 2014; Rao Damerla et al. 2014). Since this discovery, researchers studying heart development have focused much of their efforts on further understanding the role of cilia in early development (Larkins et al. 2012; Yuan et al. 2013; Koefoed et al. 2014).

The importance of normal assembly of ciliary dyneins is also well illustrated in mammals with PCD (Sharma et al. 2008; Zariwala et al. 2011). PCD manifests not only as developmental abnormalities, such as defective left-right pattern formation, but also with chronic respiratory infection and infertility in males (Kennedy et al. 2007; Zariwala et al. 2011; Knowles et al. 2013a; Horani et al. 2014). In some cases, defective motile cilia also result in hydrocephaly, presumably due to a failure in movement of the cilia on ependymal cells in the brain ventricles (Lechtreck et al. 2008; Olbrich et al. 2012). In many cases, PCD results from a failure in normal assembly of the outer dynein arms (ODA) (reviewed in (Knowles et al. 2013a). The diseases have revealed mutations in genes that encode ODA subunits and revealed additional novel conserved genes required for ODA assembly. For example, as indicated above and discussed in further detail below, ciliary dyneins including the ODA appear to be first assembled in the cytoplasm before transport to the cilium (Kobayashi and Takeda 2012). The assembly of the ODA complex in the cytoplasm requires a number of additional conserved proteins, which, when defective, result in a failure in ODA assembly in the axoneme and consequent problems of PCD (Hornef et al. 2006; Zariwala et al. 2006; Loges et al. 2008; Omran et

al. 2008; Loges et al. 2009; Horani et al. 2012; Kobayashi and Takeda 2012; Mitchison et al. 2012; Panizzi et al. 2012; Austin-Tse et al. 2013; Horani et al. 2013; Knowles et al. 2013b; Knowles et al. 2013c; Moore et al. 2013; Onoufriadis et al. 2014). In other studies, ODA fails to assemble in the axoneme due to defective docking proteins (Hjeij et al. 2014; Owa et al. 2014). Thus, studies of PCD in humans and in other mammals, has complemented and extended genetic analysis using model organisms such as *Chlamydomonas*, the mouse, zebrafish, *Tetrahymena*, etc. for study of the motile ciliary axoneme and assembly of the dyneins.

The dynein motors were discovered by Ian Gibbons in the 1960s while studying cilia from *Tetrahymena,* a ciliated protozoan and also an excellent genetic model for the study of ciliary biology (Gibbons 1963; Gibbons and Rowe 1965). In this pioneering work, Gibbons combined biochemical fractionation of the axoneme with electron microscopy to reveal the dynein ATPase complexes, and that these large ATPase complexes comprise arm-like structures that project from each outer doublet microtubule (Gibbons 1963). The term 'dynein' comes from the root terms, 'dyne' which means forces and 'in' which refers to a protein (Gibbons and Rowe 1965). Common features of all dyneins include the heavy chains (HC) that contain a large conserved motor domain with a series of P-loops in a ring-configuration (Carter and Vale 2010; Cho and Vale 2012; Ishikawa 2012; King 2012; Carter 2013; Kikkawa 2013). Also common to all dyneins are the intermediate and light chains (called the IC/LC complex) that associate with the heavy chains. Based on solving the structure of the motor domains (Carter et al. 2011; Kon et al. 2011; Kon et al. 2012; Redwine et al. 2012) and biophysical approaches to single motor domain activity (Reck-Peterson et al. 2006), we currently have a good

working model for how dyneins use ATP and generate force (Redwine et al. 2012). The IC/LC subunits are typically thought to mediate the dynein-"cargo" interaction where cargoes are the organelles or proteins carried by the dynein (Encalada and Goldstein 2014; Fu and Holzbaur 2014; Fu et al. 2014; Maday et al. 2014; Schroeder et al. 2014). Microtubules are not only the tracks upon which the dynein motors move (the B-microtubule), but are also cargos (A-microtubules) onto which axonemal dyneins are docked (Fig. 1.2). However, with the exception of the ODAs (Takada et al. 2002; Casey et al. 2003a; Wirschell et al. 2004; Owa et al. 2014) we have little understanding how dyneins are targeted and docked to cargo in the cell and on the axonemal microtubules.

Since the late 1980s, when the cytoplasmic dynein was definitively identified (Paschal et al. 1987), dyneins motors have been shown to perform a wide range of interesting and essential cellular functions (reviewed in (Kikkawa 2013; Roberts et al. 2013) including control of ciliary motility, "retrograde" movement of organelles and protein cargo in axons and within cilia (IFT), assembly and function of the Golgi, assembly and function of the mitotic spindle, transport and localization of mRNAs and transport of viruses and transcription factors (Karki and Holzbaur 1999; Vallee et al. 2004; Oiwa and Sakakibara 2005; Hook and Vallee 2006; Ori-McKenney et al. 2012; Encalada and Goldstein 2014; Fu and Holzbaur 2014; Schroeder et al. 2014). Thus, proper assembly of the dynein motors is critical to the cell functions listed here.

In this dissertation, I focus on a subset of dyneins localized exclusively to the ciliary axoneme (Kamiya and Yagi 2014). My goal is to understand how dyneins, as "cargoes", are transported and assembled in the ciliary axoneme (Fig. 1.2). My study is timely because of the growing list of mutations in PCD patients with defects in genes

encoding ciliary dyneins or factors necessary for the assembly of ciliary dyneins (Zariwala et al. 2007; Knowles et al. 2012). Additionally, the axoneme is an excellent model for the study of targeting of dyneins within the cell. This is because each of the 8 different dyneins is targeted to a unique position in the axoneme (see Fig. 1.4 and (Kamiya and Yagi 2014)). Thus, understanding targeting in the axoneme may reveal general principles for how the dyneins are targeted to diverse cellular locations and docked to cargo in general. In the next sections, I will review the structure of the motile cilia and discuss a few of the experimental advantages of *Chlamydomonas* for study of the axoneme.

Structural organization of motile cilia

In *vitro* reactivation studies have revealed that all components necessary for cilia movement are physically built into the structure of the axoneme (Gibbons and Gibbons 1972). Thus, biochemical and structural studies using isolated axonemes have identified many components required for the generation and regulation of ciliary motility. Defining the structural organization of the axoneme by electron microscopy has been essential for understanding the mechanism of ciliary bending (Satir et al. 2014). Key technical advances in electron microscopy include thin sectioning of axonemes embedded in plastic (Satir 1998), negative stain of whole-mount axonemes and purified dyneins (Burgess et al. 2003), computational approaches and image averaging (Kamiya et al. 1991; Mastronarde et al. 1992) and rapid-freeze, deep-etch rotary shadow electron microscopy (Goodenough and Heuser 1982; Goodenough and Heuser 1985c).

Most recently, high-resolution structural analysis using cryo electron tomography (cryo-ET) of axonemes and intact cilia has revealed an entirely new resolution of

structures in the axoneme (Nicastro et al. 2006; Bui et al. 2009; Nicastro 2009; Bui and Ishikawa 2013). For example, recent studies using cryo-ET revealed the MIA complex, a protein complex associated with I1 dynein and important for regulation of I1 dynein activity (Fig. 1.4 and (Yamamoto et al. 2013). In addition, the introduction of tagged proteins in the axonemes coupled with cryo-ET has shown much promise in defining the location of any subdomains or protein in the axoneme (Oda and Kikkawa 2013). For instance, Oda and Kikkawa expressed a tagged radial spoke protein to determine the location of the tagged domain in the radial spoke structure with the surprising result that the radial spoke protein 3 (RSP3) extends from its anchored position on the outer doublet microtubules to the spoke head, interacting with the central pair (Oda et al. 2014b). In an exciting new paper by Oda et al. (Oda et al. 2014a), a complex of two axonemal proteins, FAP59 (CCDC39) and FAP172 (CCDC40) form a 96 nm long complex. The authors used a range of additional approaches to definitively demonstrate that the FAP59/FAP172, complex is the 'molecular ruler' for establishing the 96 nm repeat. Thus, structural basis of the 96 nm repeat, one of the most important problems in understanding ciliary assembly, now appears to be resolved. Predictably, the continued combination of cryo-ET with tagged proteins will result in a complete map of proteins and protein domains in the axoneme.

When examined in cross section, motile cilia are characterized by a "9+2" axoneme consisting of nine outer doublet microtubules and a central apparatus built on two central pair singlet microtubules and their associated projections (Fig. 1.3). Each outer doublet microtubule is composed of a complete A tubule made up of 13 protofilaments, and the B microtubule, which is a partial structure, made of 10

protofilaments (Linck and Stephens 2007; Linck et al. 2014). Each outer doublet appears to be associated with the adjacent outer microtubule by connecting structures called the nexin interdoublet links. The nexin structure has recently been identified as a component of the Dynein Regulatory Complex (DRC), now called the N-DRC as described above (Fig. 1.4 and (Heuser et al. 2009). The dynein arm structures attached to the A tubule are categorized in two rows – the outer dynein arms (ODA) and the inner dynein arms (IDA; Fig. 1.4). The outer and inner rows of dyneins are structurally and functionally distinct: the ODAs are homogenous in composition and structure, whereas, the IDAs are more complex, composed of at least 7 distinct dynein isoforms (a-g) each localized in a fixed pattern related to the 96 nm axonemal repeat (Fig. 1.4 and (Kamiya and Yagi 2014)). Also clearly observed in the cross section are the radial spokes structures that are attached to the A tubule of the outer doublet microtubules and they project toward the two central pair microtubules.

The axoneme has an axis that is fixed relative to the bending plane and bend direction (Fig. 1.3). In *Chlamydomonas,* for instance, doublet #1 lacks the outer dynein arm (Hoops and Witman 1983) and other doublets, #2 through #9 are numbered in the direction the dynein arms point. Based on electron microscopic reconstruction, the bending plane passes through doublet #1 (Fig. 1.3) and between #5 and #6 (Bui et al. 2009; Heuser et al. 2009; Bui et al. 2012; Heuser et al. 2012). The central pair structure appears in random orientation in any given cross section. This is because in some organisms, including *Chlamydomonas*, the central pair structure rotates relative to the outer doublets 1-9 and this rotation appears to have a significant role in control of bending (Omoto and Witman 1981; Mitchell and Yokoyama 2003; Mitchell and

Nakatsugawa 2004). The central pair interacts with specific outer doublets through the radial spoke structures. The reader is referred to several recent publications for information on the radial spokes and central pair (Smith and Yang 2004; Pigino et al. 2011; Barber et al. 2012; Alford et al. 2013; Lechtreck et al. 2013; Nakazawa et al. 2014; Oda et al. 2014b).

When the outer doublet microtubules are examined in the longitudinal section, a 96 nm repeat pattern is observed in the cilia of all organisms (Warner and Satir 1974; Goodenough and Heuser 1985b). In Fig. 1.4, the outer doublet from *Chlamydomonas* is oriented with the proximal end to the left and the distal end to the right. In addition to the dyneins, each 96 nm repeat contains a pair of radial spokes (RS), the CSC (calmodulin spoke associated complex) and the N-DRC (nexin-dynein regulatory complex). All of the components in the 96 nm repeat in *Chlamydomonas* axoneme have a fixed stoichiometry and periodicity (Fig. 1.4). For example, each 96 nm repeat contains 4 copies of the ODAs (Fig. 1.4), and a single copy of each of the 7 different IDAs. This includes the inner dynein arm, I1 (dynein f) that is located at the proximal end of the 96 nm repeat, and is the focus of this dissertation.

Another prominent feature of the 96 nm repeat is that each of the components are localized to very precise positions, a feature that makes the axoneme ideal for image analysis and cryo-ET approaches (Nicastro 2009; Bui and Ishikawa 2013). Mutant cells that fail to assemble specific structures have been instrumental in defining these positions. For example, mutant cells defective in the assembly of I1 dynein results in a gap in the structure that repeats once every 96 nm (Fig. 1.4b and (Piperno et al. 1990; Porter et al. 1992; Yamamoto et al. 2013). This result indicated that I1 dynein is targeted

to a unique position on the outer doublet microtubule and assembles independent of the other IDAs. Consistent with this interpretation, *in vitro* reconstitution of IDAs with axonemes lacking a specific subset of inner arm structures also demonstrated that each IDA type is targeted to a unique position in the axonemal 96 nm repeat (Smith and Sale 1992; Yamamoto et al. 2006). However, the basis for such precise targeting is not understood. The recent discovery of the FAP59/172 protein complex that is responsible for establishing the 96 nm repeat pattern in the axoneme may provide new, testable models for how each IDA is targeted. For example, one hypothesis is that the FAP59/FAP172 ruler also contains docking domains for the IDAs (See Fig. 6 in Supplemental in (Oda et al. 2014a).

Critical to my dissertation is an understanding of the location and mechanisms of assembly of the 8 different axonemal dyneins (Kamiya and Yagi 2014). The ODAs are the best characterized of all dyneins in terms of structure, composition and assembly, and the ODAs are required for control of beat frequency of motile cilia (King and Kamiya 2009). The ODA is attached to the A microtubule towards the periphery of each doublet microtubule (Fig. 1.3). The subunit composition of the outer dynein arms in *Chlamydomonas* and humans is listed in Table 1; (Hom et al. 2011). This includes axonemal proteins required for the localization of the ODA and docking in the axoneme – the outer dynein arm-docking complex (ODA-DC) (Dean and Mitchell 2013; Owa et al. 2014). Although the ODA is not the main focus of my dissertation, many of the studies using ODA have been helpful in designing experiments to define I1 dynein assembly. For example, recent studies have revealed the ODA is assembled as a 23S complex in the cytoplasm before transport to the cilium (Kobayashi and Takeda 2012). As discussed in

Chapters 2, I also found that I1 dynein is preassembled in the cytoplasm before entry to the cilium.

Compared to the ODAs, which are relatively homogeneous in structure and composition, the IDAs are heterogeneous, organized into seven dynein structures and referred to as dyneins a, b, c, d, e, f/I1 and g (Fig. 1.4, Kamiya and Yagi, 2014). I1 dynein is the only IDA subspecies constructed with two distinct dynein heavy chains (DHCs) organized into a two-headed dynein structure (Fig. 1.5 and (Smith and Sale 1991; Toba et al. 2011). Based on motility analysis of *Chlamydomonas* mutants missing single IDAs, the IDAs appear to each contribute to regulation of bending waveform (Brokaw and Kamiya 1987; Kamiya 1991; Kamiya et al. 1991; Porter et al. 1992; Yagi et al. 2005; VanderWaal et al. 2011; Kubo et al. 2012; Bayly et al., 2010). Moreover, as indicated above, each IDA is distinct in composition and each is targeted to a unique position in the axonemal 96 nm repeat (Goodenough and Heuser 1985a; King and Kamiya 2009; Bui et al. 2012).

Based on a number of experimental advantages discussed below, the IDAs are excellent models for the study of how each dynein is targeted and docked on the outer doublet microtubules. In my dissertation I will focus on one of the IDAs, I1 dynein that is present on every outer doublet microtubule (Fig. 1.3) and targeted to a unique position at the proximal end of the 96 nm repeat (Fig. 1.4 and (Bui et al. 2009; Heuser et al. 2012; Yamamoto et al. 2013). As illustrated in Fig. 1.5, I1 dynein a large complex composed of 11 different subunits including two heavy chains (DHC 1α and DHC 1β), three intermediate chain subunits (IC140, IC138, IC97), a light-intermediate chain (FAP120) and five light chains (LC7a, LC7b, Tctex 2a, Tctex 2b, LC8) (Wirschell et al. 2007b;

Kamiya and Yagi 2014). Each of these subunits appears to have a special role in assembly and for regulating I1 dynein activity.

Chlamydomonas reinhardtii as a model genetic organism and discovery of IFT

Chlamydomonas has been on the forefront for defining conserved mechanisms of ciliary assembly and genes that, when defective, result in a wide range of diseases and developmental abnormalities in humans (reviewed in (Pazour and Witman 2003; Brown and Witman 2014)). Researchers have exploited the experimental advantages of *Chlamydomonas* to study ciliary motility and assembly. A few examples of important studies include: the work of J. Rosenbaum, G. Witman and colleagues in understanding the mechanisms of ciliary assembly and discovery of IFT in *Chlamydomonas*; D. Luck, B. Huang and colleagues in use of "dikaryon rescue", analysis of dyneins and discovery of extragenic suppressor mutants that restore motility to paralyzed ciliary mutants; U. Goodenough and W. Snell in analysis of differentiation of gametes and mating between plus (+) and minus (-) cells and R. Kamiya and colleagues in definition of the composition, functional role and regulation of the axonemal dyneins. Listed below are a few properties of *Chlamydomonas* that have been critical for my study of dynein assembly. Other experimental advantages of *Chlamydomonas* not discussed here, are mentioned in later chapters. These advantages include the amenability of *Chlamydomonas* to efficient genetic analysis, mapping of genes, introduction of exogenous DNA and rescue of mutant phenotypes, availability of a comprehensive nuclear genome database and a ciliary proteome and the ease of isolating pure cilia in large quantities. The nomenclature for mutants and mutant alleles is similar to that used

for yeast: the gene is indicated in all caps, italicized (*IDA3* – inner dynein arm mutant 3); mutant strains are indicated in lower case, italicized (*ida3*) and the protein is indicated in all caps (IDA3). In addition, an older nomenclature also appears in the databases and literature such as *pf14* (paralyzed flagella 14) or *fla10* (flagellar assembly 10).

As illustrated in Fig. 1.6, each *Chlamydomonas* cell contains two cilia that are ~10 um in length. Structural, genomic and proteomic studies have demonstrated that the axoneme is highly conserved in organisms that assemble cilia (Avidor-Reiss et al. 2004; Li et al. 2004). For example, comparative genomics have revealed conserved genes required for basal body (a microtubule-based organelle that serves as a template for the formation of all cilia) and ciliary assembly and function (Li et al. 2004). These studies also revealed that genes encoding the Bardet-Beidl syndrome (BBsome) proteins are associated with cilia (Zaghloul and Katsanis 2009). Notably, in *Chlamydomonas* the cilia are not required for viability. Thus, mutagenesis can result in viable cells defective in assembly or motility of cilia. The ciliary mutants can be isolated by simple motility (Kamiya 1991) or phototaxis screens (Horst and Witman 1993; Moss et al. 1995; Pazour et al. 1995; King and Dutcher 1997; Okita et al. 2005). Such screens have resulted in the identification of structural proteins of the axonemal dyneins as well as proteins required for the regulation, assembly and docking of axonemal dyneins.

Of particular relevance to my project are mutants defective in genes that encode structural proteins that constitute an inner dynein arm called I1 dynein and at least two additional genes required for I1 dynein assembly in the axoneme (*IDA3*; *PF23*). Examination of the I1 dynein mutants has allowed me to test the role of individual I1 subunits in the different steps of the assembly process. For example, *ida7* is defective in

the gene that encodes the I1 dynein intermediate chain IC140 and as discussed in Chapter 2 and 3, IC140 is required for I1 dynein assembly both in the cytoplasm as well as in the axoneme (Perrone et al. 1998). The availability of conditional mutants in *Chlamydomonas* has also been vital for my studies. In particular, mutants that contain a temperature-sensitive allele of the IFT motor, kinesin-II, called *fla10* (Walther et al. 1994; Kozminski et al. 1995; Piperno et al. 1996) has allowed me to test the hypothesis that I1 dynein, as a cargo, depends on IFT for transport within the cilium. This experiment is featured in Chapter 3. Additional mutant strains that are defective in assembly of the dyneins and used in this study are listed in Table 3.

In order to study the assembly of axonemal dyneins, I have taken advantage of an important stage of the *Chlamydomonas* life cycle called the "quadraflagellate dikaryon". The *Chlamydomonas* dikaryon is a zygote, resulting from the fusion of two opposite mating type gametes during sexual reproduction (Pan and Snell 2000; Lin and Goodenough 2007; Dutcher 2014). Like the yeast, *Chlamydomonas* is a haploid organism that can reproduce vegetatively or sexually (See Fig. 1.6 – *Chlamydomonas* life cycle). Vegetative cells can be differentiated into gametes by culturing the cells in nitrogen-deficient media. Mixing of the + and – mating type gametes (either a "+" or a "–" mating type) results in the formation of the dikaryon and includes a series of steps initiated by adhesion of the flagella by agglutinins and eventually leading to cell fusion (Ferris et al. 2005). The dikaryon has two nuclei, a shared cytoplasm and four cilia (i.e. quadraflagellate). The quadraflagellate dikaryon stage is temporary and lasts for 2.5 hours before cilia are resorbed and the cell completes meiosis and cell division (Fig. 1.6). During the 2.5-hour time period, mutant phenotypes, in certain cases, can be rescued by a

process referred to as “dikaryon rescue” (reviewed in (Dutcher 2014)). For example, in dikaryons formed by mating of wild-type cells with a paralyzed, radial spoke-deficient mutant such as *pf14*, cytoplasmic complementation resulted in the rescue of both motility and radial spoke assembly in the formerly paralyzed *pf14* cilia (Fig. 1.7, (Luck et al. 1977)). An important feature of this experiment is that rescued radial spoke assembly occurs on the otherwise full length and assembled ciliary axoneme (reviewed in (Dutcher 2014)). As discussed in depth in Chapter 3, and illustrated in Fig. 1.7, I also employed dikaryon rescue in other experiments to show that during the rescue process, the addition of axonemal subunits first occurs at the distal tip of the mutant cilium. Thus, I1 dynein complexes are transported to the distal tip of the cilium prior to docking to the axoneme.

Diverse studies have shown that during ciliary formation, the addition of ciliary precursors occurs at the distal end of the growing axoneme (Lefebvre and Rosenbaum 1986). For instance, original studies by Witman and colleagues using pulse labeling with [^{3}H] acetate followed by autoradiography, showed that majority of silver grains, (representative of newly synthesized proteins), appeared at the distal tip of the regenerating cilium ((Witman 1975). More recently, Johnson and Rosenbaum examined the incorporation of tubulin in regenerating cilia (Johnson and Rosenbaum 1992). Using a combination of ciliary regeneration and dikaryon rescue, they observed that new addition of tubulin subunits exclusively occurred at the distal end of cilia during ciliogenesis. In the same paper, the authors examined dikaryons formed between wild-type and radial spoke deficient mutant, *pf14* to show that during rescue, the assembly of the radial spokes first occurred at the distal tip of mutant cilia in dikaryons. These experiments, illustrated in Fig. 1.7, corroborated Witman’s earlier observations and indicated that ciliary

axonemal building blocks must be transported to the distal cilium before incorporation in the axonemes – analogous to constructing a skyscraper starting at the foundation. The authors predicted that a transport system was required to move ciliary precursors (e.g. tubulin dimers, radial spokes, dyneins etc.) from the cell body to the tip of growing cilia. Moreover, since there was no evidence of protein synthesis machinery such as the ribosomes or mRNA in the cilium, fully synthesized proteins had to be transported from the cytoplasm to and within the cilium. The important question is how the axonemal precursors reach the distal tip during ciliogenesis. One idea proposed by these researchers was that an active transport system, similar to that observed in neuronal axons is present in the cilium.

In 1992, a graduate student in Joel Rosenbaum's laboratory, Keith Kozminski working with Paul Forschner at Yale University, used video microscopy to examine the *Chlamydomonas* cilium. In doing so, they observed a rapid and bidirectional movement of particles along the entire length of the *Chlamydomonas* cilia (Kozminski et al. 1993). This bidirectional transport mechanism appeared strikingly similar to anterograde and retrograde movement in axons (see (Allen et al. 1982; Brady et al. 1982) for pioneering use of video microscopy to visualize axonal transport). Kozminski and Rosenbaum postulated that this movement served the purpose of transporting ciliary precursor protein components along the cilium and he called it "Intraflagellar Transport (IFT)". IFT appeared to be processive and the rate of movement was ~2.0um/sec in the anterograde direction and ~3.5um/sec in the retrograde direction. These velocities nearly matched the velocity of anterograde and retrograde organelle movement in axons (Kozminski et al. 1993). The discovery of Intraflagellar Transport (IFT) 20 years ago has provided answers

to how some axonemal precursors reach the distal tip during ciliogenesis (Kozminski et al. 1993; Kozminski et al. 1995; Kozminski et al. 1998; and reviewed in Cole 2003; Scholey and Anderson 2006; Pedersen and Rosenbaum 2008; Scholey 2008; Ishikawa and Marshall 2011; Kozminski 2012; Bhogaraju et al. 2013b).

Kozminski also combined video microscopy with electron microscopy to reveal particle "trains", electron dense complexes sitting between the axonemal microtubules and the ciliary membrane. Kozminski postulated that these trains comprised of IFT complexes and associated proteins (ciliary precursors) in transit. As indicated above, one of the chief advantages of *Chlamydomonas* is the isolation of pure cilia in large quantities (Craige and Witman, 2013). Two labs were able to isolate the IFT protein complexes from the detergent soluble "membrane matrix" (MM) fraction, obtained from isolated cilia (Piperno and Mead 1997; Cole et al. 1998; Behal et al. 2009; Richey and Qin 2013). Careful analysis of the membrane matrix fraction and biochemical isolation of the IFT complexes revealed that the IFT particles are composed of two conserved complexes: Complex A and B (Table 4 and Cole et al. 1998, Piperno et al. 1997, Piperno et al. 1998).

Based on models of axonal transport, it was postulated that cilia also contain kinesin-like proteins that interact with and move the IFT complexes. Diverse studies in several experimental systems revealed kinesin-like proteins in cilia (Fox et al. 1994; Verhey et al. 2011; Hirokawa et al. 2012; Scholey 2013b). Further investigation led to the discovery that the *FLA10* locus in *Chlamydomonas* encodes the motor subunit of the heterotrimeric kinesin, kinesin-2 (Walther et al. 1994). The *fla10* mutant is a temperature-sensitive allele of kinesin-2 that abolishes kinesin motor activity at restrictive temperature (Kozminski et al. 1995). Kozminski took advantage of the *fla10* cells to test the

hypothesis that IFT is driven by kinesin-2. When the *fla10* mutant was switched to restrictive temperature, IFT movement completely ceased. This was consistent with the role of kinesin-2 in the movement of IFT particles (Fig. 1.8). Subsequent analysis of sensory cilia in *C. elegans* (Scholey et al. 2004; Snow et al. 2004) and biochemical analysis revealed direct role of kinesin in IFT (Cole et al. 1998). In addition, genetic and biochemical analysis in *Chlamydomonas* also revealed that the IFT retrograde motor is a cytoplasmic dynein (Pazour et al. 1998; Porter et al. 1999; Scholey 2008). Thus, we now know most or all of the components of the IFT complex (Table 4) and that the IFT movement is driven by kinesin-2 in the anterograde direction and cytoplasmic dynein in the retrograde direction.

While significant advances have been made in understanding the IFT machinery, we know little about the interactions that exist between cargoes (e.g. ciliary precursors) and IFT complexes. In theory, any ciliary protein precursor is a candidate IFT cargo. This could include both axonemal complexes and ciliary membrane components. Powerful approaches to the problem of IFT-cargo interaction include live-cell imaging of sensory cilia in *C. elegans* showing that tubulin, for example, is a cargo for IFT (Scholey 2013a). Supporting these data, recent biochemical approaches have revealed a direct interaction of tubulin with specific IFT components (Bhogaraju et al. 2013a; Bhogaraju et al. 2013b; Bhogaraju et al. 2014). In an outstanding study by Wren et al. (Wren et al. 2013), a large axonemal structure known as the Nexin-Dynein Regulatory Complex (N-DRC) was used as a model axonemal cargo to test the hypothesis that axonemal complexes are transported by IFT. In this case, live-cell imaging using Total Internal Reflection Fluorescence Microscopy (TIRF-M) was used to demonstrate that the N-DRC is a bona

fide cargo of IFT. Critical to this study was the recognition that the cilium is ideally suited for study by TIRF microscopy (Engel et al. 2009a; Lechtreck 2013). In addition, the *Chlamydomonas* cells have a natural tendency to stick to glass cover slips without the need of special adhesives (Bloodgood 1977; Bloodgood 1995). Moreover, since the diameter of the flagella is ~200 nm, they fit perfectly within the restricted evanescent field of the TIRF, allowing for visualization of fluorescently labeled proteins such as IFT complexes and associated cargo. Due to the exceptionally high signal to noise ratio achieved by TIRF, it is possible to visualize proteins that are otherwise difficult to visualize by wide-field or confocal microscopy.

Wren et al. (2013) performed imaging of single complexes and could show the entire transport cycle of IFT and attached N-DRC complexes within the cilium and during ciliary assembly. This included clear observations and detailed analysis of the processive movement of N-DRC complexes that were coincident with IFT complexes. This observation indicated that N-DRC is associated with IFT during transport in the cilium. Other important advances included that IFT is required for N-DRC entry to the ciliary compartment. They also observed "unloading" of the N-DRC from the IFT complex, and upon unloading from IFT, the N-DRC began diffusion until either docked to the axoneme in an empty N-DRC site or re-associating another IFT complex for further processive transport. Unloading from IFT and diffusion always occurred before the N-DRC became docked in the axoneme consistent with a combination of IFT transport and diffusion for assembly (See also Ye et al., 2013 e Life for discussion of diffusion of membrane proteins in cilia). These outstanding studies provide the model for future live cell imaging of IFT mediated transport of other cargoes, such as the axonemal

dyneins, and ciliary assembly. In Chapter 4, I will discuss my own preliminary studies using TIRF microscopy to observe movement of I1 dynein in live cells.

Although these new studies by Wren et al. (2013) indicate that IFT is required for axonemal precursor entry to the ciliary compartment, it is not known how axonemal complexes such as the N-DRC are targeted to the base of the cilium. One idea is that axonemal precursor complexes such as the dyneins, radial spokes or the N-DRC are loaded onto and carried on membrane vesicles destined to the cilium (Wood and Rosenbaum 2014). In this study, axonemal cargoes were localized to a subset of membrane vesicles near the basal body. In addition, the authors isolated the vesicles and demonstrated that the vesicles contained axonemal proteins associated with the vesicle surfaces. Another important, related question is the nature of the barriers that separate the cytoplasm from the ciliary compartment (Nachury et al. 2010). Evidence indicates that barriers exist at the ciliary transition zone that regulates the composition of the ciliary membrane and is also critical for control the entry of soluble, axonemal complexes into the cilium (Craige et al. 2010; Dishinger et al. 2010a; Hu et al. 2010; Kee et al. 2012; Awata et al. 2014; Takao et al. 2014). The questions include, how do large axonemal complexes such as dyneins pass a ciliary barrier? Below, I provide a rationale for using I1 dynein as a model to study dynein assembly and I will define the hypotheses tested in this dissertation.

I1 dynein Assembly: Hypotheses and Experimental Predictions

The studies included in my dissertation are the first to examine the mechanisms of assembly of the inner dynein arms (IDAs). As discussed above, failure in the assembly of

axonemal dyneins result in severe impairment of ciliary motility and can adversely affect the developmental processes and function of organ systems that rely on normal functioning of motile cilia. Using I1 dynein as a model to study axonemal dynein assembly, the questions I have investigated include: Where is the I1 dynein complex assembled? That is, do the individual I1 dynein subunits enter the cilium independently and then assemble *in situ* into a complex on the outer doublet microtubules? Alternatively, does the I1 complex assemble into an intact complex in the cytoplasm before being transported to the cilium? How is I1 dynein trafficked to the base of the cilium? This difficult question of trafficking to the ciliary base has not been adequately addressed (for discussion, see Wood and Rosenbaum, 2014). However, recent studies have provided insight for how membrane proteins are targeted to the cilium (Follit et al. 2010; Kim et al. 2014; Malicki and Avidor-Reiss 2014; Mourao et al. 2014). How do large axonemal complexes such as I1 dynein enter the cilium? This is a timely question since several labs are focused on an understanding of the ciliary barrier (Hu and Nelson 2011; Reiter et al. 2012) that controls the entry of both "soluble" complexes, such as axonemal precursors, as well as membrane proteins. While there is evidence indicating that IFT is involved in the entry of soluble axonemal precursors (Wren et al. 2013), the movement of membrane proteins into and within the cilia may be independent of IFT (Belzile et al. 2013; Ye et al. 2013). Also, there is no data addressing how extremely large axonemal dynein complexes such as the ODAs or the IDAs enter the cilium. Based on studies of the N-DRC (Wren et al., 2013), it is reasonable to postulate that the entry of ODAs or IDAs relies on IFT. Thus, future studies in several labs will focus upon testing

this hypothesis. Following entry, how is I1 dynein transported within the cilium? This question is addressed in Chapter 3.

Why was I1 dynein selected as a model to study axonemal dynein assembly? Firstly, I1 dynein is highly conserved (Wickstead and Gull 2007; Song et al. 2015) and is required for normal ciliary motility (reviewed in Wirschell, 2007). Thus, understanding the mechanisms of I1 dynein assembly may provide general principles of axonemal dynein assembly and reveal new, conserved genes required for assembly. This in turn may be crucial for additional understanding the basis for PCD. The I1 dynein complex can be purified from the axoneme as an intact 20S complex containing all the 11 subunits and can be used for biochemical assays. Notably, the 20S I1 dynein complex can restore I1 dynein structure and function *in vitro* reconstitution studies (Smith and Sale 1992; Yamamoto et al. 2006). Thus, the axonemal 20S I1 complex is the functionally active form of the I1 dynein complex. While the 20S complex extracted from the axoneme is functionally active, it is possible that this 20S complex isolated lacks at least one or more subunits.

The genes encoding I1-dynein subunits have been cloned, and, in most cases, the subunits have been biochemically characterized (reviewed in Wirschell et al., 2007, Alford et al., 2012 Dynein book). In addition, the Sale lab has either made or obtained antibodies to each of the I1 dynein subunits. In particular, antibodies to intermediate chain subunits, IC140, IC138 and IC97 have been valuable for a range of biochemical analyses and have worked for immunofluorescence localization (Yang and Sale, 1998; Hendrickson et al., 2004; Wirschell et al., 2009). As demonstrated in Chapters 2-4 below, the antibody to the intermediate chain subunit IC140 has been used as a marker of I1

dynein and has been tremendously useful in localizing I1 dynein at various steps during the assembly process. Antibodies to the heavy chains and light chains have also been employed for biochemical analyses of I1 assembly as detailed in Chapter 2 below. Thus, all of the reagents to test ideas for I1 dynein assembly were available for my immediate experimentation.

The I1 dynein structural mutants have also been instructive in providing detailed information on the roles of individual subunits in assembly of the I1 complex and/or function of I1 dynein in ciliary motility (Bower et al. 2009a; Wirschell et al. 2009; Toba et al. 2011; VanderWaal et al. 2011; Heuser et al. 2012). For instance, most mutations in genes that encode 1α and 1β heavy chains or the intermediate chain subunit IC140 result in a complete failure in I1 dynein assembly, leaving a gap in every 96 nm repeat (Fig. 1.4b and (Piperno et al. 1990; Kamiya et al. 1991; Porter et al. 1992; Myster et al. 1997; Perrone et al. 1998; Myster et al. 1999; Perrone et al. 2000). Notably, loss of the I1 dynein does not affect the assembly of other inner dynein arms, radial spokes, outer arm dyneins, N-DRC or the MIA complex, indicating that the targeting and assembly of I1 dynein is independent of other axonemal components (Piperno et al. 1990; Kamiya et al. 1991; Porter et al. 1992; Perrone et al. 1998; Bui et al. 2012; Heuser et al. 2012; Yamamoto et al. 2013). Therefore, interpretation of motility and assembly phenotypes in I1 mutants (Brokaw and Kamiya 1987; Bayly et al. 2010; VanderWaal et al. 2011) is not further complicated by failure of assembly of additional axonemal components. The mutants used this study are listed in Table 3.

In addition to mutants that completely lack I1 dynein in the axoneme, a number of mutations in other I1 dynein genes result in partial assemblies of the I1 dynein complex

in the axoneme (Perrone et al. 1998; Hendrickson et al. 2004b; Bower et al. 2009a; Wirschell et al. 2009). For example, phenotypic analysis of the *bop5* mutant has revealed that the IC138 complex regulates I1 dynein activity and controls axonemal bending (VanderWaal et al. 2011). In the *bop5* mutant, mutation in the gene that encodes the IC138 intermediate chain subunit, assembles a partial I1 dynein complex in the axoneme containing only the heavy chains and IC140, but fails to assemble IC138 and associated proteins (Hendrickson et al. 2004b; Bower et al. 2009b; VanderWaal et al. 2011). The mutant has revealed that the IC138 regulatory complex also contains IC97, FAP120 and LC7b subunits. This and other partial assembly mutants have been valuable in revealing protein interactions within the I1 dynein complex (Heuser et al. 2012) as well as with neighboring axonemal structures such as the MIA complex (Yamamoto et al. 2013). An interaction map of I1 dynein is illustrated in Fig. 1.5.

Based on the observation that I1 dynein isolated from the axoneme sediments as a 20S complex and contains a full complement of known subunits, an important question is where the assembly of the 20S complex occurs. I hypothesized that 20S I1 dynein complex assembles in the cytoplasm before being transported to the ciliary compartment. In order to test this hypothesis, and as described in Chapter 2, I fractionated cytoplasmic extracts from wild type and select I1-dynein mutant cells. I found that I1 dynein assembles as a 20S complex in the cytoplasm. Upon entry into the ciliary compartment, I hypothesized that the I1 complex, first assembled as a 20S precursor in the cytoplasm, is transported to the distal tip of the cilium before docking in the axoneme. To test this hypothesis, I examined the site of rescue of I1 assembly in dikaryons formed between wild-type and mutant cells lacking I1 dynein (Chapter 3). As postulated, I found that I1

dynein first appears at the distal tip of the axoneme during dikaryon rescue. I then postulated that I1 dynein is transported to the distal end of the cilium by IFT. To test this hypothesis, once again, I took advantage of dikaryon rescue. In this case, I generated dikaryons between a kinesin-II mutant, *fla10* and an I1 dynein mutant, to test whether kinesin-2 is required for transport (Chapter 3). As predicted, I1 dynein transport requires kinesin-2 activity and IFT. I will also discuss the identification of a new gene, *IDA3*, required for I1 dynein assembly (Chapter 4). Although we do not yet know the exact function of IDA3, one idea is that IDA3 is an adapter that selectively links I1 dynein, as a cargo, to the IFT machinery. Others in the Sale lab are currently testing this hypothesis (Fig. 1.9). This is an important project testing the general idea that each large axonemal complex (i.e. dyneins, radial spokes, N-DRC) is associated with a specific-adapter that is required for IFT-cargo interaction.

Figures for Chapter 1

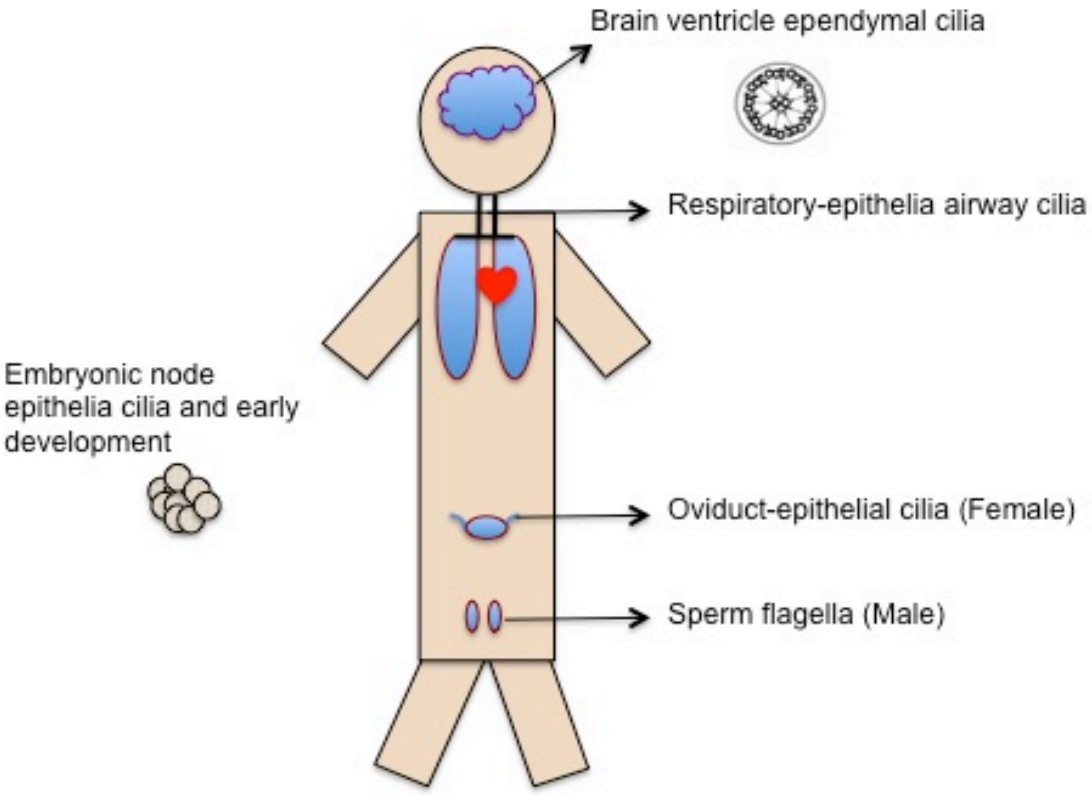
Brain ventricle ependymal cilia
Respiratory-epithelia airway cilia
Embryonic node epithelia cilia and early development
Oviduct-epithelial cilia (Female)
Sperm flagella (Male)

Figure 1.1. Locations of motile cilia in the human. Motile cilia play diverse roles during development and organ homeostasis in the adult. Motile cilia are present on the embryonic node epithelia and are responsible for generating fluid flow critical for establishing asymmetry during early development. Motile cilia are also required for heart morphogenesis. Functions of motile cilia in the adult include the movement of cerebrospinal fluid in the brain ventricles, fluid movement in the oviducts and mucus in the respiratory tract. In the male, the sperm flagellum (a long cilium) is required for propelling the sperm cell and fertilization. Defects in the assembly or function of the motile cilia can result in development diseases, particularly congenital heart abnormalities and in some cases, hydrocephaly, infertility and Primary Ciliary Dyskinesia (PCD).

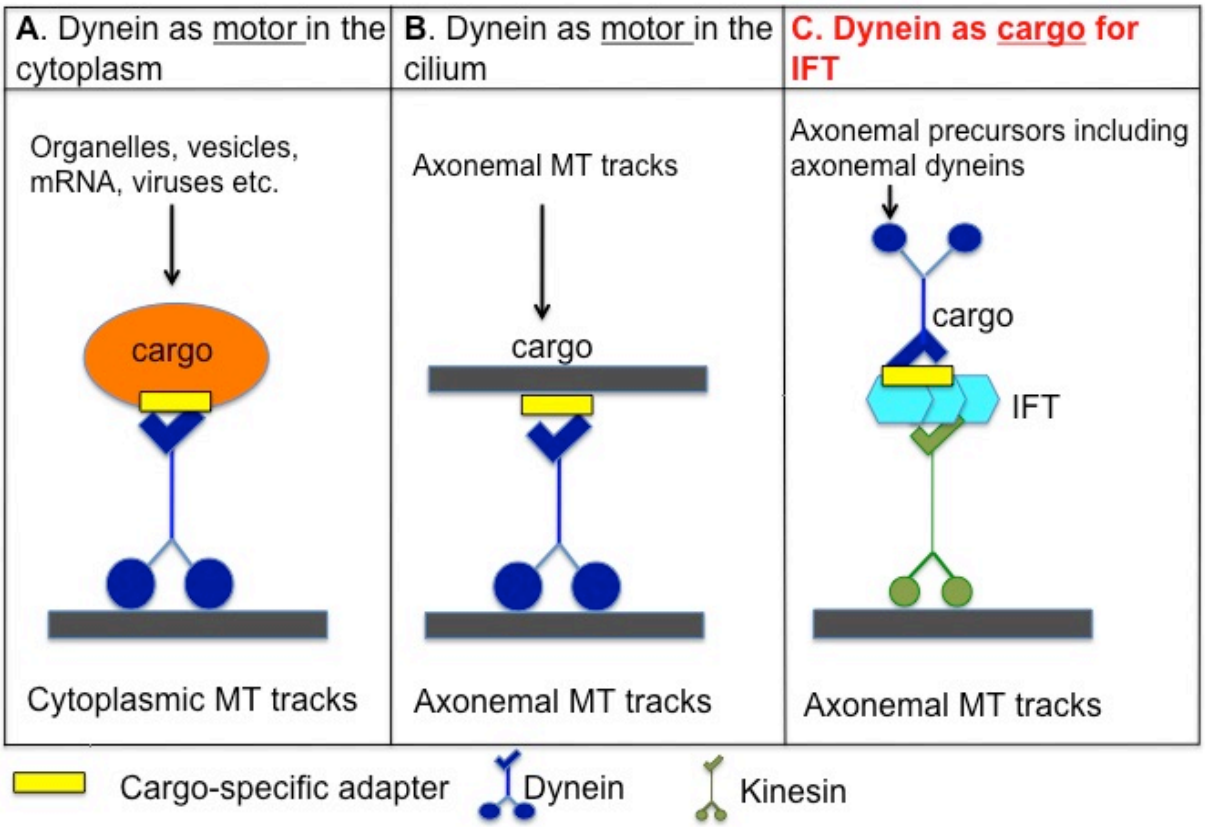
A. Dynein as motor in the cytoplasm
B. Dynein as motor in the cilium
C. Dynein as cargo for IFT
Organelles, vesicles, mRNA, viruses etc.
cargo
Cytoplasmic MT tracks
Axonemal MT tracks
cargo
Axonemal MT tracks
Axonemal precursors including axonemal dyneins
cargo
IFT
Axonemal MT tracks
Cargo-specific adapter
Dynein
Kinesin

Figure 1.2. Role of dyneins in three cellular contexts. Common features of all motors include large motor domains that contain the ATPase activity (shown here as blue and green circles), and several light and intermediate chain subunits mainly responsible for associating with cargo, presumably through adapters (yellow). The dynein motors shown in navy blue can be broadly categorized into two types: cytoplasmic dyneins and axonemal dyneins. (**A**) The cytoplasmic dyneins are responsible for transporting a variety of cargo including organelles, vesicles, mRNA, viruses etc. on microtubules tracks within the cell. (**B**) The axonemal dyneins are anchored to the axonemal microtubule cargo, and the motor domains cause the translocation of the adjacent outer doublet microtubules during sliding. (**C**) In this dissertation, I focus on studying the axonemal dyneins as a cargo, and I do not focus on I1 dynein motor activity. I tested the hypothesis that one of the axonemal dyneins, I1 dynein is transported in the cilium by IFT and kinesin (green) as a cargo. I further postulate that a specific adapter protein (yellow) mediates the interaction between I1 dynein and IFT.

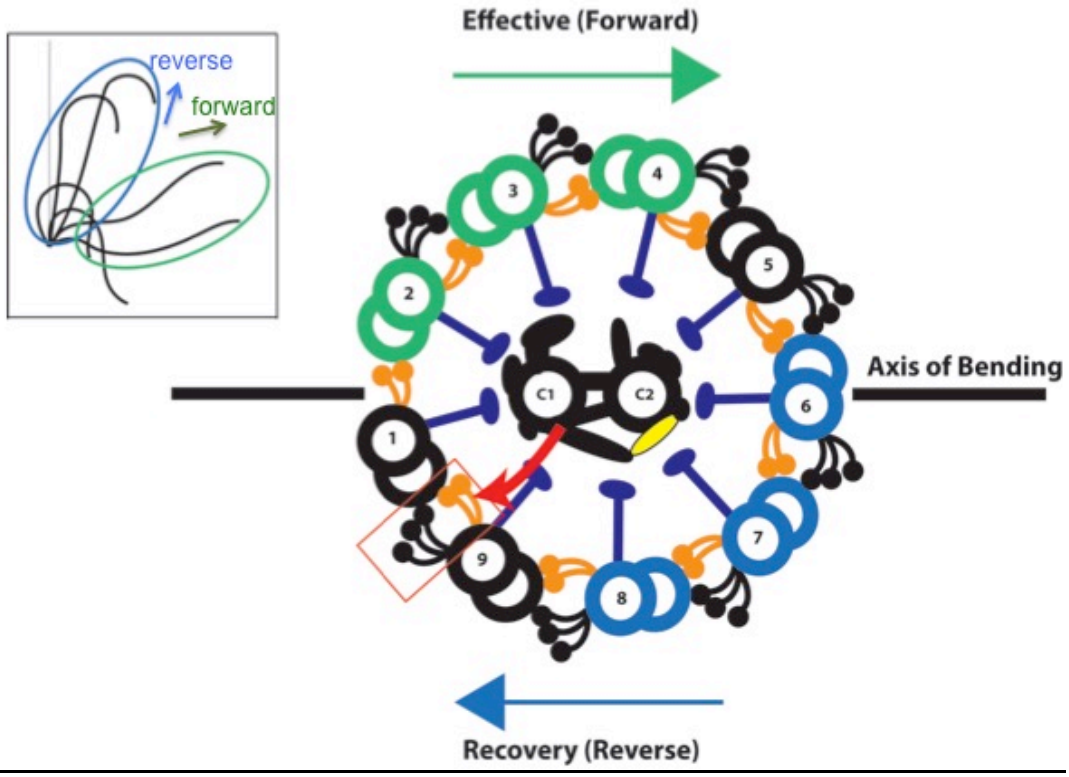
reverse
forward
Effective (Forward)
Axis of Bending
Recovery (Reverse)
1
2
3
4
5
6
7
8
9
C1
C2

Figure 1.3. Cross-section of an axoneme from *Chlamydomonas*. Illustrated in the inset is the forward (green) and reverse (blue) bends. In the cross section, doublet #1 is defined as the doublet lacking the ODAs. The other doublets are numbered in the direction the dyneins point. The ODAs are shown in black and the IDAs are shown in orange. Other features illustrated and required for normal movement include the radial spokes, central pair apparatus and the projections of the central pair. Signals from the central pair are transmitted by the radial spokes to the dynein arms (red arrow). The black line passing through doublet #1 and between doublets #5 and #6 represents the plane/axis of bending. According to the switching model, when dyneins on one side of the axis are active (i.e. on doublets #2,3 and 4), microtubule sliding can occur and generate the bend in the effective or forward direction (green in inset). When the direction of bending reverses, the dyneins on blue doublets #2,3 and 4 are inactivated and dyneins on doublets #6,7 and 8 are switched on to generate the recovery or reverse bend (blue in inset). Detailed discussion of the sliding microtubule/switching model can be found in (Satir et al. 2014).

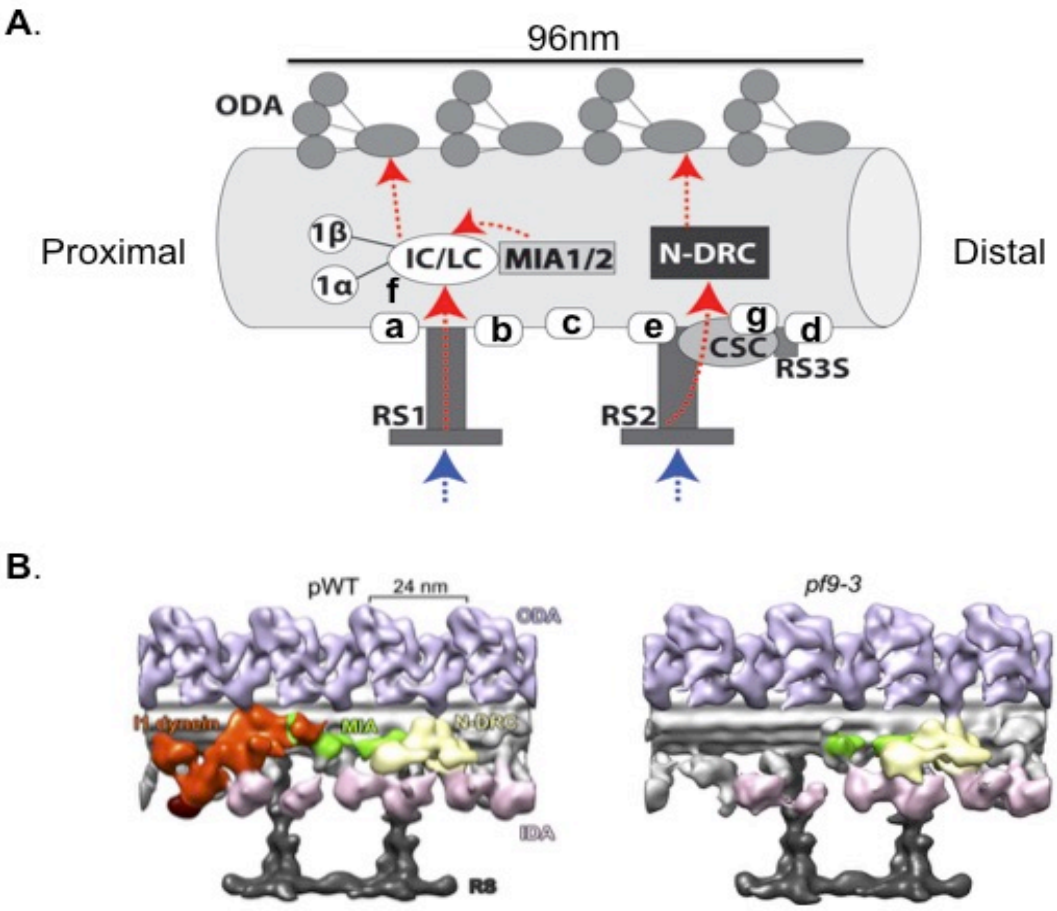
A.
96nm
ODA
Proximal
Distal
1β
1α
IC/LC
MIA1/2
N-DRC
f
a
b
c
e
g
d
CSC
RS3S
RS1
RS2
B.
pWT
24 nm
ODA
I1 dynein
MIA
N-DRC
IDA
R8
pf9-3

Figure 1.4. Longitudinal section of a single outer doublet microtubule illustrating the 96 nm repeat. (A) Schematic of the 96 nm repeat comprising of 4 copies of the ODA, single copy of each of the IDAs (a-g), a pair of radial spokes (RS1 and RS2) and several other regulatory protein complexes including the MIA complex, Nexin-Dynein Regulatory Complex (N-DRC) and the Calmodulin and Spoke-Associated complex (CSC). The I1 dynein complex, also known as dynein f is the only IDA with two motor head domains. For simplicity, the individual subunits of all the other single headed IDAs are not shown. The blue and red arrows indicate the parallel signaling pathways associated with the RS1 and I1 dynein-MIA complex and the RS2, CSC and N-DRC. Although we do not fully understand the regulatory mechanisms, genetic and functional analysis indicate signals from the central pair are transduced to the outer doublets for control of dyneins. (**B**) Cryo ET renderings of the 96 nm repeat from WT (pWT) and *pf9-1/ida1* (I1 dynein-deficient) mutant axonemes. The I1 dynein complex (shown here in red) is precisely localized at the proximal end of the 96 nm repeat. The absence of I1 dynein in the *pf9-1* axonemes leaves a gap in the structure (Adapted from (Yamamoto et al. 2013).

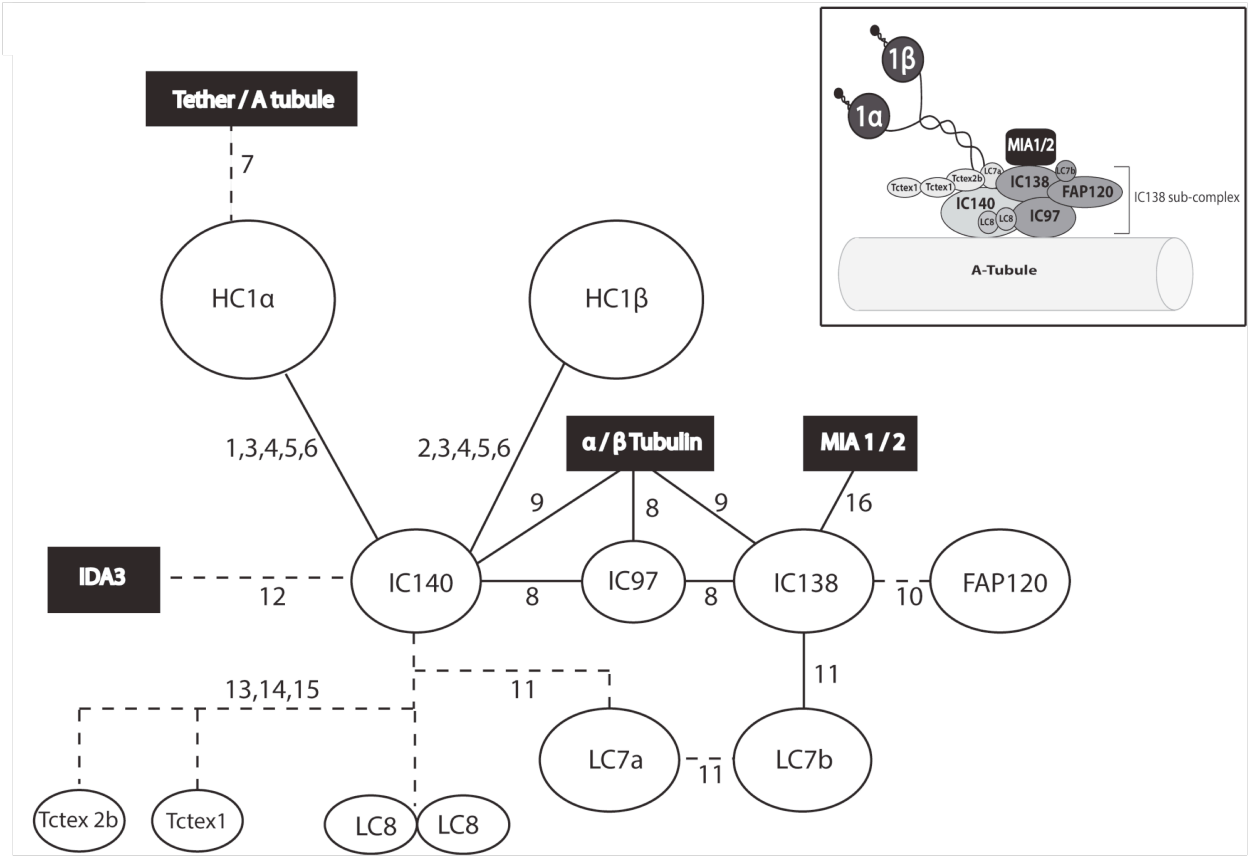
Tether / A tubule
7
HC1α
HC1β
1,3,4,5,6
2,3,4,5,6
α / β Tubulin
MIA 1 / 2
9
8
9
16
IDA3
12
IC140
8
IC97
8
IC138
10
FAP120
11
13,14,15
11
LC7a
11
LC7b
Tctex 2b
Tctex1
LC8
LC8
1β
1α
MIA1/2
IC138
FAP120
IC140
IC97
IC138 sub-complex
A-Tubule

Figure 1.5. Protein associations within I1 dynein and with non-I1 dynein components. The inset illustrates the structure of I1 dynein and arrangement of subunits (Wirschell et al., 2009, Bower et al., 2009). In the interaction map, the solid lines represent experimentally determined protein-protein interactions based on biochemical and/or structural analysis of I1 dynein assembly mutants. The dashed lines indicate predicted interactions based on the analysis of I1 assembly mutants. I1 dynein contains two distinct heavy chain domains (HC1α and HC1β), a cargo-binding region composed of three intermediate chains (IC140, IC97 and IC138), and five light chains (Tctex1, Tctex 2b, LC8, LC7a and LC7b). The stem regions of the heavy chains interact with IC140 (#1, Myster et al., 1997, #2, Perrone et al. 2000, #3, Bower et al, 2009, #4, Toba et al., 2010, #5, Vanderwaal et al. 2011 and #6, Perrone et al., 1998). Cryo-ET analysis identified a structure tethering the 1α to the A-tubule (#7, Heuser et al., 2012). Crosslinking evidence indicates that IC97 directly interacts with IC140, IC138 and α/β tubulin (#8, Wirschell et al., 2009); and that IC140 and IC138 bind tubulin (#9, Hendrickson et al. 2013). IC138 in complex with IC97, FAP120 and LC7b forms the IC138-regulatory subcomplex and is the key regulator of I1 dynein activity (#3, Bower et al, 2009, #5, Vanderwaal et al. 2011, #10, Ikeda et al., 2009; #11, Dibella et al., 2004). LC7a appears to mediate a stable interaction between LC7b and I1 dynein components (#11, Dibella et al., 2004). The IC140 subunit, required for the assembly of the I1 complex (#6, Perrone et al., 1998), may interact with a predicted adapter protein, IDA3 for transport by IFT (#12, Viswanadha et al., 2014). The light chains, Tctex1, Tctex 2b and LC8 are part of the I1 complex (#13, Wu et al., 2005; #14, Harrison et al., 1998 and

15. Yang et al., 2009). The MIA complex has shown to directly interact with the IC138 subunit to regulate I1 dynein activity (#16, Yamamoto et al., 2013).

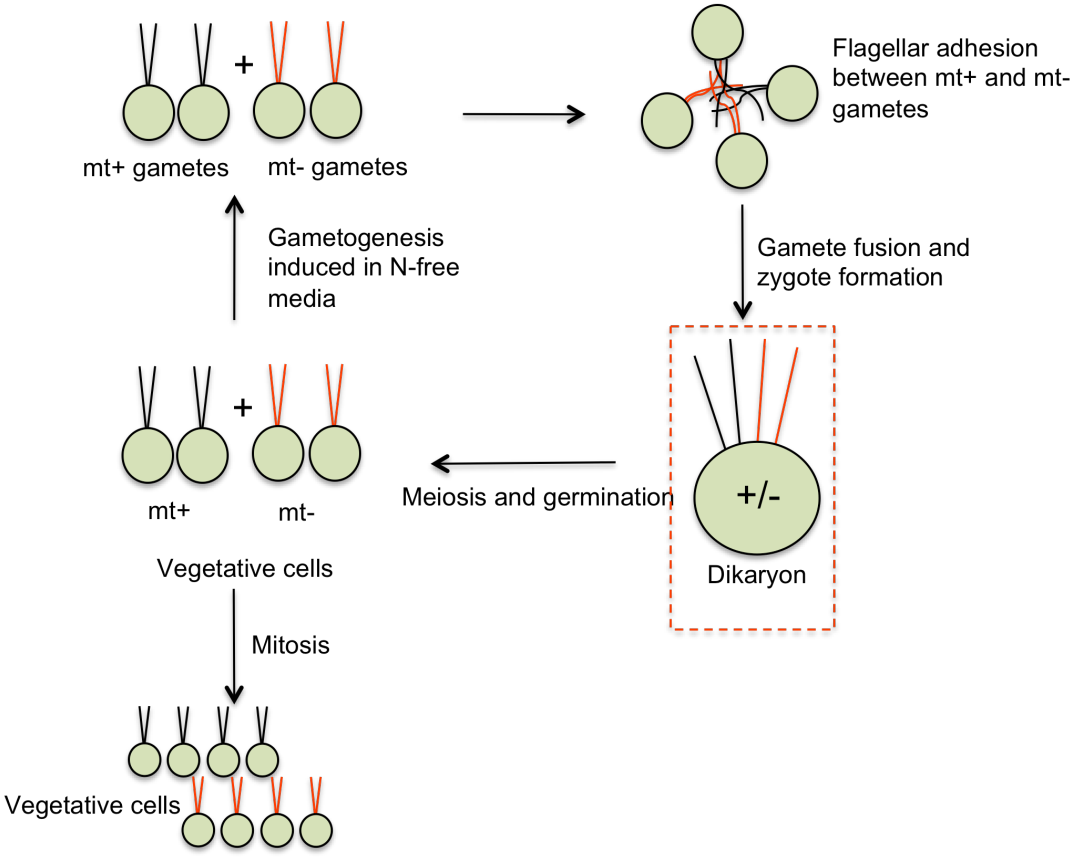
+
mt+ gametes
mt- gametes
Flagellar adhesion between mt+ and mt- gametes
Gametogenesis induced in N-free media
Gamete fusion and zygote formation
+
mt+
mt-
Vegetative cells
Meiosis and germination
+/-
Dikaryon
Mitosis
Vegetative cells

Figure 1.6. Overview of *Chlamydomonas* life cycle and quadraflagellate dikaryon zygote. *Chlamydomonas* cells are haploid and can reproduce sexually or asexually. In the sexual reproduction cycle, vegetative cells (that are either + or – mating types) can be differentiated into gametes by culturing in nitrogen-deficient media. Upon mixing the gametes of opposite mating types, the agglutinins present on the flagella cause flagellar adhesion followed by a series of defined steps and fusion of the cytoplasm. The resulting zygote is called the dikaryon and contains a shared cytoplasm with two nuclei and four flagella (two of which belong to each parent). The dikaryon is a temporary stage that lasts for 2.5 hours. During this time period, the dikaryons formed between wild-type and mutant cells can reveal valuable information regarding ciliary assembly and function. As discussed in Chapter 3, I have taken advantage of dikaryons to rescue I1 dynein assembly. The dikaryon cell then undergoes meiosis, giving rise to four haploid progeny that can either proliferate asexually (i.e. mitosis) or can enter the sexual lifecycle.

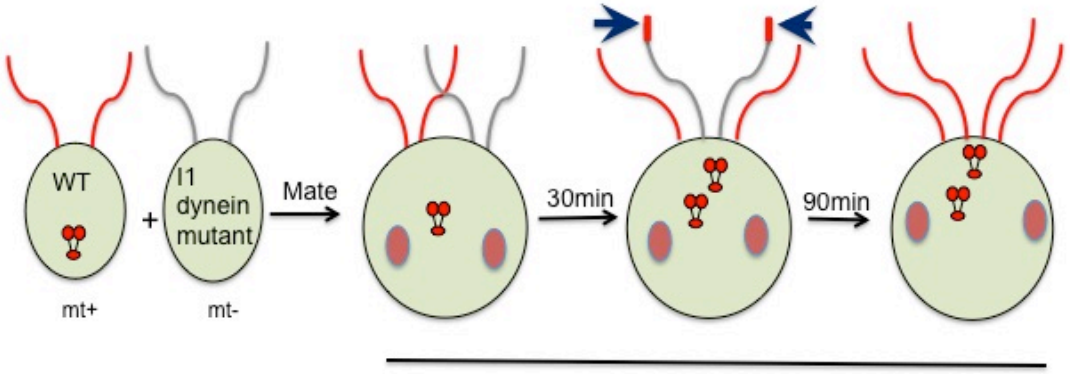

"Dikaryon Rescue"

Figure 1.7. Diagram illustrating the rescue of ciliary precursors in *Chlamydomonas* dikaryons formed between WT and an I1 dynein mutant cell. In certain cases, dikaryons can be used to restore (rescue) structures missing on the otherwise fully assembly axoneme. In the case illustrated here, wild type cells (mating type +) were mated with a mutant that fails to assemble I1 dynein (mating type -). The prediction was that wild type copy of the mutant I1 dynein component would complement and restore I1 dynein (shown in red). Using antibodies to I1 dynein subunits (e.g. IC140), and as predicted, I1 dynein was restored to the mutant axoneme. The surprise was that I1 dynein first appeared at the distal tip of the mutant axoneme. This result is discussed in Chapter 3 and is part of the foundation of my dissertation work. Evidently, the I1 dynein precursors (Chapter 2) are targeted to the distal end of the cilium (Chapter 3) before docking in the axoneme. Similar dikaryon experiments also determined that other axonemal precursors are targeted to the distal end of the cilium prior incorporation in the axoneme (Johnson and Rosenbaum 1992; Piperno et al. 1996; Wren et al. 2013).

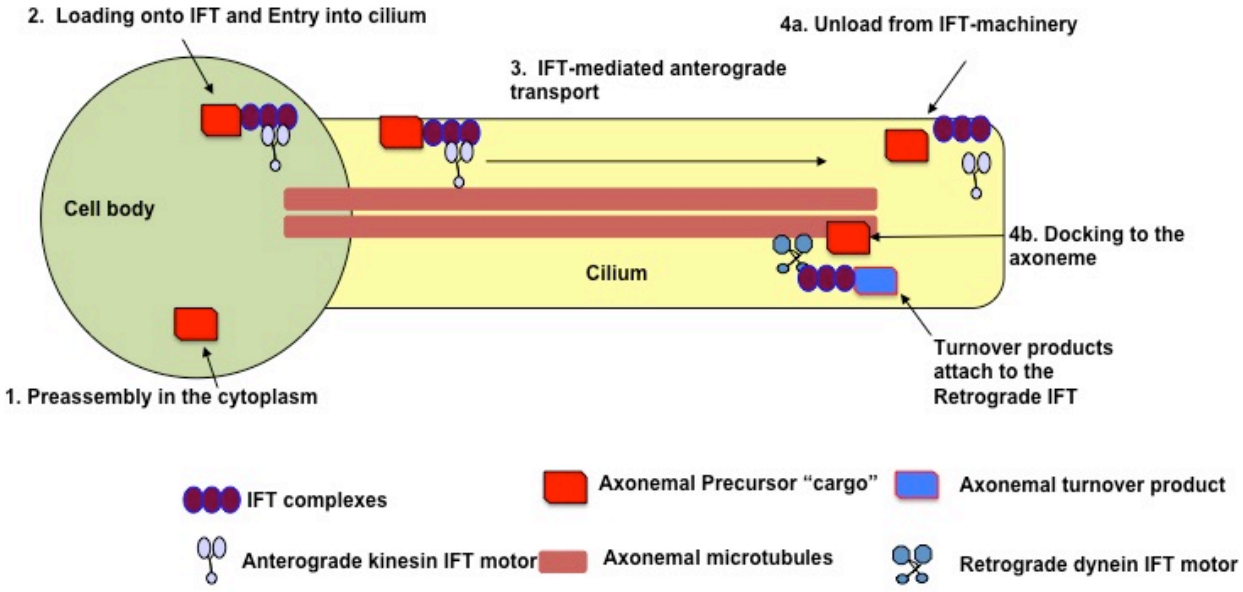
2. Loading onto IFT and Entry into cilium
4a. Unload from IFT-machinery
3. IFT-mediated anterograde transport
Cell body
4b. Docking to the axoneme
Cilium
Turnover products attach to the Retrograde IFT
1. Preassembly in the cytoplasm
IFT complexes
Axonemal Precursor "cargo"
Axonemal turnover product
Anterograde kinesin IFT motor
Axonemal microtubules
Retrograde dynein IFT motor

Figure 1.8. Diagram illustrating the IFT-mediated assembly of ciliary precursor complexes. In this dissertation, I propose that the assembly of axonemal precursors such as the dynein motors or the radial spokes occurs in a step-wise manner, starting with the preassembly in the cytoplasm (Step **1**). After preassembly (Step **2**), the axonemal precursor cargo is loading on IFT and enters the ciliary compartment (Step **2**). Upon entry, I then propose that the cargo is transported to the distal tip of the cilium by IFT (Step **3**). At the tip, the cargo is unloaded from the IFT machinery (Step **4a**) followed by diffusion and docking to the axoneme (Step **4b**). Although not addressed in this study, axonemal turnover products maybe recycled to the cytoplasm by retrograde IFT mediated by a cytoplasmic dynein.

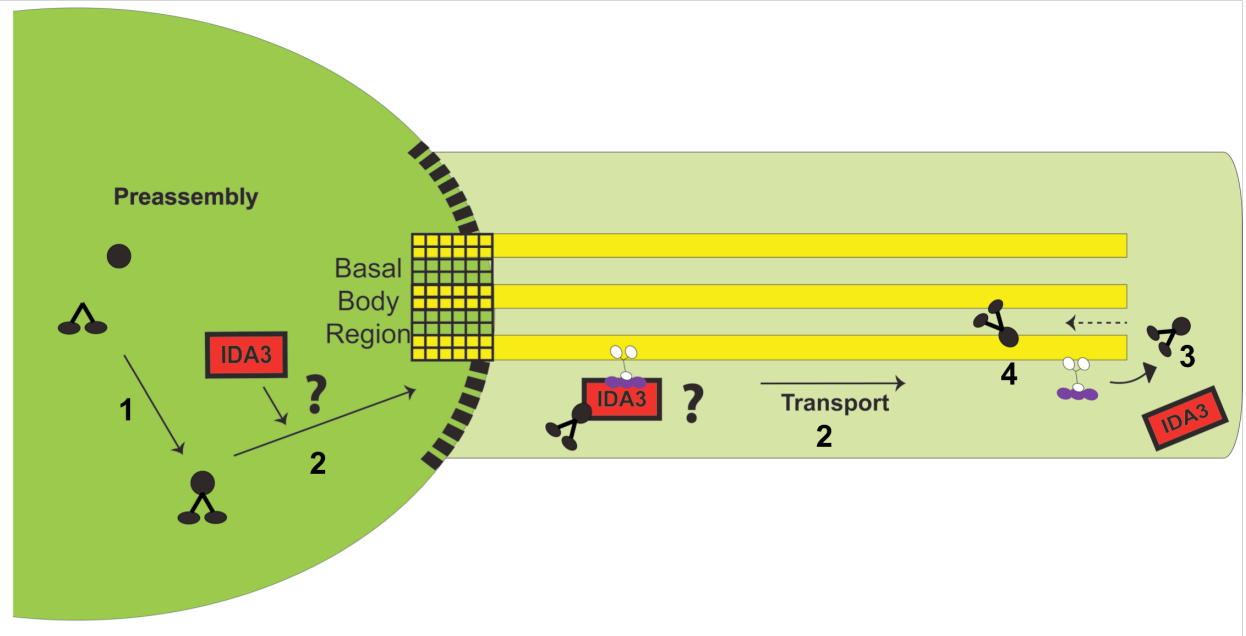
Preassembly
Basal
Body
Region
IDA3
1
?
2
IDA3
?
Transport
2
4
3
IDA3

Figure 1.9. Hypothetical steps leading to I1 dynein assembly in the axoneme. In my dissertation, I tested the hypotheses that I1 dynein: (**1**) preassembles in the cytoplasm; (**2**) the preassembled I1 complex is transported to the distal tip of the cilium by IFT; (**3**) I1 dynein is unloaded at the tip and (**4**) I1 dynein is docked in the axoneme. In the *ida3* mutant, I1 dynein fails to enter the ciliary compartment. I also indicate that IDA3 is an adapter required for I1 dynein entry and transport by IFT. As discussed in Chapter 4, the exact function of IDA3 is not known. The postulated barrier between the cytoplasm and the ciliary compartment is shown as black boxes.

Chapter 2: I1 dynein is assembled in the cytoplasm as a 20S precursor complex

Introduction:

To date we know little about the mechanisms of assembly of the inner dynein arms (IDAs). Understanding the mechanisms of assembly and discovery of the genes involved in assembly is an important goal because the IDAs are essential for normal ciliary motility. Predictably, the genes involved in the IDA assembly are conserved, and when defective, can lead to PCD. I address how I1 dynein is assembled and discuss the genes involved in the assembly process.

Early studies revealed that a pool of axonemal precursor protein complexes exist in the cytoplasm that can be mobilized to rapidly build new cilia (Rosenbaum et al. 1969; Stephens 1994). In *Chlamydomonas,* the cytoplasmic precursor pool is sufficient to build two half-length flagella even in the presence of a protein synthesis inhibitor (Rosenbaum et al. 1969). Thus, key questions include: What is the state of these cytoplasmic precursors? For example, are large structures fully formed in the cytoplasm for immediate delivery to and incorporation in the axoneme? Or, are the individual subunits transported separately to the cilium for assembly *in situ,* subunit by subunit? Two large axonemal complexes, the radial spokes (RS) and the outer dynein arms (ODAs) have been shown to be partially or completely assemble in precursor form in the cytoplasm before transport to the ciliary compartment (Qin et al. 2004; Ahmed and Mitchell 2005; Ahmed et al. 2008; Diener et al. 2011). To date, the ODAs and the RSs are the only axonemal complexes that have been examined for precursor assembly in the cytoplasm before transport to the cilium and docking in the axoneme.

The mechanism of assembly of the RSs and the ODAs differ in important ways. The radial spokes (RS) are “T” shaped structures composed of 23 proteins (Yang et al.

2006; Pigino et al. 2011; Lin et al. 2012; Pigino and Ishikawa 2012; Nakazawa et al. 2014; Oda et al. 2014b). When extracted from the axoneme, the radial spoke proteins sediment together as a 20S complex (Yang et al. 2001; Smith and Yang 2004; Yang et al. 2006; Kelekar et al. 2009). *In vitro* reconstitution analysis revealed that the 20S RS complex, derived from the axoneme, is competent to form radial spoke structures on the axoneme following reconstitution (Yang et al. 2001; Diener et al. 2011). This result indicated that the 20S RS complexes are the functional form of the radial spoke. However, examination of the radial spoke proteins from the cytoplasm revealed that the RSs exist as partial precursor complexes containing a subset of RS subunits that sediment at 12S (Qin et al. 2004; Diener et al. 2011). The 12S radial spoke precursor complex enters the cilium, is transported to the distal tip by IFT (Qin et al. 2004) and associates with other RS proteins to form the mature 20S complex prior to docking in the axonemes. The mature 20S radial spoke is then localized very precisely in the 96 nm repeat (Smith and Yang 2004; Yang et al. 2005; Diener et al. 2011; Gopal et al. 2012; Gupta et al. 2012). Furthermore, final steps of RS assembly appear to occur at the distal tip of axoneme (Johnson and Rosenbaum 1992; Yang et al. 2005; Diener et al. 2011). In contrast to the 20S complex, the 10-12S sub-complexes from the cytoplasm are incompetent to bind axonemes *in vitro* (Diener et al. 2011; Alford et al. 2013). Thus, the radial spoke is partially assembled in the cell body and assembly is completed in the ciliary compartment prior to docking in the axoneme.

In contrast to the RSs, the ODAs appear to assemble in the cytoplasm as a complete 23S that are then transported to the ciliary compartment and axoneme as intact structures. The ODAs can be extracted from the axoneme and purified as a 23S complex

by ion-exchange chromatography or by velocity sedimentation on sucrose gradients (King and Kamiya 2009; King 2013). The 23S complex is composed of 16 subunits in *Chlamydomonas*. These subunits include three heavy chains, two intermediate chains and several light chains (King and Kamiya 2009; Hom et al. 2011; King 2013). Fractionation of the cytoplasmic extracts revealed that 23S ODA complex is assembled and contains all the known subunits before entering the cilium (Fowkes and Mitchell 1998; Ahmed and Mitchell 2005). The cytoplasmic assembly of the ODA also requires a number of additional conserved proteins, not part of the ODA complex, which when defective result in a failure in ODA assembly in the axoneme and in many cases results in PCD (Hornef et al. 2006; Zariwala et al. 2006; Loges et al. 2008; Omran et al. 2008; Loges et al. 2009; Horani et al. 2012; Kobayashi and Takeda 2012; Mitchison et al. 2012; Panizzi et al. 2012; Austin-Tse et al. 2013; Horani et al. 2013; Knowles et al. 2013b; Knowles et al. 2013c; Moore et al. 2013; Onoufriadis et al. 2014). For example, the mutant *pf13*/*ktu* is defective in ODA cytoplasmic assembly, and defects in PF13/KTU in humans' results in PCD (Omran et al. 2008). PF13/KTU is one of the several factors required for ODA assembly (see also (Mitchison et al. 2012; Panizzi et al. 2012). Notably, the assembled 23S complex can rebind ODA deficient axonemes *in vitro* (Dean and Mitchell 2013) and is capable of rescuing function (Takada et al. 1992).

These data demonstrate that the 23S ODA complex in the cytoplasm is likely that complete ODA complex found in the axoneme. Since the 23S ODA is first assembled in the cytoplasmic compartment, there must be a transport mechanism that delivers ODA complexes to and within the cilium for docking to the axoneme. Additional studies have revealed that the ODA is transported as a cargo by IFT within the cilium. Phenotypic

analysis of a mutant deficient in the IFT46 subunit revealed an absence of ODA in the cilium, suggesting that IFT46 may be required for ODA assembly (Hou et al. 2007). IFT mediated transport of the ODA complex requires an additional factor, ODA16, thought to mediate the IFT-ODA interaction (Ahmed and Mitchell 2005; Ahmed et al. 2008). Consistent with the studies by Hou et al. on the role of IFT46 in ODA assembly, evidence from yeast two hybrid experiments showed a possible interaction between IFT46 and ODA16 (Ahmed et al. 2008). However, the evidence that the ODA is transported by IFT is still indirect. No live cell studies of ODA assembly have been published.

To date, there have been no studies investigating the steps of assembly of other large axonemal complexes including the inner dynein arms (IDAs). To address questions of assembly of the IDAs, I focused on the I1 dynein (Piperno et al. 1990; Kagami and Kamiya 1992; Wirschell et al. 2007a). When isolated from the axoneme, I1 dynein is a 20S complex that contains two distinct heavy chains, 1α and 1β (Myster et al. 1997; Myster et al. 1999; Perrone et al. 2000) that also differ in function (Kotani et al. 2007; Toba et al. 2011). Most relevant to this chapter, the axonemal 20S I1 dynein can be isolated and will rebind I1-deficient axonemes, restoring I1 dynein to its original position in the 96 nm repeat (Smith and Sale 1992) and also restoring I1 dynein function (Yamamoto et al. 2006). These important studies revealed that the 20S I1 dynein complex, derived from the axoneme, is the intact, functional form of I1 dynein. How is I1 dynein assembled? The 20S I1 dynein complex may fully assemble in the cytoplasm before entry to the cilium. Alternatively, the I1 dynein complex may assemble by a stepwise addition of subunits on the axoneme, or like the RS, I1 dynein may partially assemble in the cytoplasm with final steps of assembly occurring in the cilium.

To distinguish these possibilities, I fractionated cytoplasmic extracts from wild-type and I1 dynein mutant cells. The experimental strategy is shown in Fig. 2.1. As presented in Fig. 2.2, my observations include the following: [1] I1 dynein is assembled into a 20S complex in the cytoplasm; [2] the 20S I1 complex appears to have similar composition as the axonemal 20S I1 dynein; [3] the cytoplasmic assembly of I1 dynein is dependent upon the heavy chains and IC140. However, unlike the 20S I1 dynein derived from the axoneme, the cytoplasmic 20S I1 dynein fails to rebind isolated axonemes lacking I1 dynein (Fig. 2.6). [4] Analysis of the cytoplasmic extracts from *ida3*, a mutant that fails to assemble I1 dynein in the axoneme (Table 3), revealed that the 20S I1 dynein complex is assembled in the cytoplasm (Fig. 2.2B). This result appears to eliminate the possibility that *IDA3* encodes a factor required for the cytoplasmic assembly of the 20S I1 dynein complex. Instead, this result supports a hypothesis that *IDA3* encodes a protein required for the modification of I1 dynein before transport or an adapter for transport of I1 dynein to the ciliary compartment (Fig. 1.9, and Chapter 4 for additional discussion of *ida3*).

Results

I1 dynein assembles as a 20S complex in the cytoplasm

Axonemal I1 dynein is a multisubunit complex that, when fully assembled, sediments at 20S (Piperno et al. 1990; Smith and Sale 1991; Porter et al. 1992). To test the hypothesis that I1 dynein assembles as a 20S complex prior to transport to the cilia and axoneme, I fractionated cytoplasmic extracts from wild-type cells by velocity sedimentation on sucrose gradients (Fig. 2.1). Similar to the axonemal I1 dynein,

cytoplasmic I1 dynein sediments at 20S, suggesting the complex is assembled in the cytoplasm before entering the cilium (Fig. 2.2A). Axonemal and cytoplasmic fractions were probed with antibodies to various I1 subunits to determine the subunit composition in the 20S complexes. The 20S complex from the both the axoneme and cytoplasm contain the heavy chains (HC1α and HC1β) (Fig. 2.2A) and three intermediate chains (IC138, IC140 and IC97) (Fig. 2.2A). Immunoblots of the cytoplasmic 20S I1 dynein also revealed the presence of the light chains TcTex1, TcTex 2b, LC7a, LC7b and LC8 in the complex. However, since many of the light chains are also present in other axonemal structures, the presence of the light chains in the 20S fractions cannot be definitively assigned to the I1 dynein complex without further purification of the I1 complex.

Wild type cytoplasmic extracts contain both a 12S radial spoke (RS) precursor complex and an intact 20S radial spoke (Diener et al. 2011). Further studies revealed the 20S RS in the cytoplasm is a recycled component from the cilium (Qin et al. 2004; Diener et al. 2011). That is, the presence of the intact 20S RS in the cytoplasm is a result of retrograde movement of the intact RS from the cilium to the cytoplasm – "recycled" (See Fig. 1.8). Based on this observation, it was possible that the 20S I1 dynein complex observed in the cytoplasm is also a recycled ciliary product. To test this idea, an aflagellate mutant, *bld1* (stands for "bald") (Brazelton et al. 2001), which lacks cilia due to a mutation in IFT52, a component of the IFT complex B required for ciliary assembly was used (Deane et al. 2001). Cytoplasmic extracts from *bld1* were fractionated and examined for the presence of the 20S I1 complex. The prediction was that if the 20S I1 dynein complex was present in extracts from *bld1*, then the 20S I1 dynein complex is not a recycled "ciliary" product. The sedimentation profile from *bld1* extracts shows that the

20S I1 dynein complex forms as in wild-type extracts (Fig. 2.2B). This result indicated that the cytoplasmic 20S I1 dynein complex is not a recycled ciliary component, but rather is formed in the cytoplasm before transport to the cilium.

Studies of *Chlamydomonas* mutants *ida1* and *ida2,* lacking the heavy chains 1α and 1β, respectively, and the mutant *ida7*, lacking the intermediate chain, IC140 have revealed that the assembly of I1 dynein in the axoneme is dependent on the heavy chains (Myster et al. 1997; Myster et al. 1999; Perrone et al. 2000) and IC140 (Perrone et al. 1998) (See Table 3). Based on these results, I hypothesized that HC1α, HC1β and IC140 are also required for the cytoplasmic assembly of the 20S I1 dynein complex. To test this hypothesis, I examined I1 dynein assembly in cytoplasmic extract fractions from *ida1*, *ida2* and *ida7*. As predicted, the 20S I1 dynein complex failed to assemble in cytoplasmic extracts from *ida1, ida2* (Fig. 2.3) and *ida7* (lower panel, Fig. 2.2B). Therefore, both the heavy chains and IC140 are required for 20S I1 complex assembly in the cytoplasm. Smaller sub-complexes (~10-12S) appear in the extracts from *ida1*, *ida2* and *ida7*. These results indicate that I1 dynein preassembly occurs in a stepwise manner and begins with a single heavy chain and one of the intermediate chains (See Fig. 2.9 and discussion). However, definitive tests of the steps of I1 complex assembly will require purification of sub-complexes by higher resolution fractionation.

Similar to the *ida1*, *ida2* and *ida7* mutants, the *ida3* mutant is also defective in the assembly of I1 dynein in the axoneme (Kamiya et al. 1991). I reasoned that failure in assembly in the *ida3* axoneme is a consequence of defective 20S I1 dynein complex assembly in the cytoplasm. To test this idea, I compared wild-type and *ida3* cytoplasmic fractions for the presence of the 20S I1 complex. Immunoblot analysis indicated that I1

dynein from *ida3* cytoplasmic extracts forms a 20S complex that co-sediments with the I1 dynein complex from wild-type extracts (Fig. 2.2B). Thus, the *ida3* mutant does not appear to be defective in assembly of the 20S I1 complex in the cytoplasm. The assembled I1 complex in the *ida3* cytoplasm appears to have the same subunit composition as wild-type. However, since fractionation on sucrose gradients by velocity sedimentation is a relatively low-resolution method of fractionation, it is possible that the 20S complex in the *ida3* cytoplasm differs from that in the wild type cytoplasm. A higher resolution fractionation method such as ion-exchange chromatography will be required to accurately compare the composition of the 20S I1 complex in the *ida3* and wild-type extracts.

Previous structural and biochemical studies of axonemes from mutants defective in the light chain, LC8 and intermediate chain IC138 revealed the presence of partial assemblies of I1 dynein in the axoneme (Fig. 2.3A and (Bower et al. 2009a; Wirschell et al. 2009). That is, in the absence of LC8 and IC138 components, I1 dynein still assembles the I1 structure in the axoneme, but as partial complexes. Furthermore, these partial assemblies of I1 dynein derived from the axoneme, sedimented in the 15-18S range. The question was whether the partially assembled I1 dynein complexes are also assembled as partial I1 complexes in the cytoplasm. I predicted that fractionation of cytoplasmic extracts derived from the LC8 mutant, *fla14-3* and IC138-null mutant, *bop5-3*, would reveal I1 dynein complexes similar in size (~15-18S) to the I1 dynein complex derived from the *fla14-3* and *bop5-3* axonemes. As predicted, the fractionation profiles of the cytoplasmic extracts showed the presence of I1 dynein complexes sedimenting in the 15-18S range (Fig. 2.3B). Therefore, as long as the heavy chains and IC140 were present, I1

dynein complexes were able to assemble as partial precursor complexes in the cytoplasm before transport to the cilium and docking in the axoneme.

The cytoplasmic 20S I1 dynein complex is incompetent to bind I1-deficient axonemes *in vitro*.

Previous studies carried out by demonstrated that the 20S I1 dynein isolated from the axoneme could rebind I1-deficient axonemes *in vitro* and restore function in the presence of ATP (Smith and Sale 1992; Yamamoto et al. 2006). Since I1 dynein assembles as a 20S complex in the cytoplasm (Fig. 2.2A), I hypothesized that the 20S I1 dynein from the cytoplasm assembles in a form competent to bind axonemes lacking I1 dynein. To test this possibility, I first repeated the *in vitro* reconstitution assays performed in Smith and Sale (1992) (Fig. 2.5). As shown in Fig. 2.6A, I1 dynein isolated from the axoneme reconstituted I1-deficient *ida7* and *ida3* axonemes. To determine if the cytoplasmic I1 dynein complex can bind axonemes, I isolated cytoplasmic extracts from *oda2* that contains wild-type 20S I1 dynein, but does not contain the intact ODA complexes that have been previously shown to interfere with I1 dynein rebinding to the axoneme (Smith and Sale 1992). I combined the cytoplasmic extracts with a fixed amount of *ida3* or *ida7* axonemes in the presence of ATP (See illustration in Fig. 2.5A and Toba et al. 2011; Yamamoto et al. 2006). In contrast to isolated axonemal I1 dynein (Fig. 2.7A), cytoplasmic I1 dynein, from the *oda2* cytoplasm, failed to reconstitute I1 dynein with either *ida3* or *ida7* axonemes (Fig. 2.7B). In addition, I1 dynein complexes derived from *ida3* cytoplasmic extracts also failed to rebind isolated axonemes. The same results were

obtained using the antibody to IC138 to assess *in vitro* reconstitution (Fig. 2.7C). Thus, the cytoplasmic 20S I1 dynein is not competent to bind the axoneme.

In vitro reconstitution analysis revealed that the *ida3* mutant is not defective in an I1 dynein docking mechanism.

Given that *ida3* assembles the 20S I1 dynein in the cytoplasm (Fig. 2.2B) but fails to assemble it in the axoneme (Kamiya et al. 1991), I tested the possibility that *ida3* is defective in docking I1 dynein in the axoneme. For example, although a docking complex for I1 dynein has not yet been identified, docking of the ODA complex in the axoneme requires a complex of proteins called the ODA-docking complex (ODA-DC) (Takada and Kamiya 1994; Casey et al. 2003a; Casey et al. 2003b). Mutations in the ODA-DC results in failure of ODA docking in the axoneme. As illustrated in Fig. 2.7A, immunoblot analysis revealed that I1 dynein from *oda2* axonemal high salt extracts (HSE) is capable of rebinding equally to *ida3* and *ida7* (control) mutant axonemes (Fig. 2.7A, P). In both cases, I1 bound the axonemes to saturation (Fig. 2.5), indicating that I1 is binding to specific sites along the axoneme. Therefore, *ida3* axonemes are able to support I1 dynein docking in the axoneme, and IDA3 is not likely an axonemal docking component.

The cytoplasmic 20S I1 dynein complex is absent in the *ida3* ciliary compartment

Since *ida3* is neither deficient in cytoplasmic assembly of 20S I1 dynein (Fig. 2.2B) nor in *in vitro* docking of axonemal I1 dynein (Fig. 2.7A), I tested whether I1 dynein is capable of entry into the ciliary compartment in *ida3*. I first confirmed that the cytoplasmic 20S I1 complexes were present at a similar concentration in *ida3* and wild-

type cytoplasmic extracts (Fig. 2.8A). Next, as expected, I1 dynein was significantly reduced in *ida3* cilia and axonemes compared to wild type (Fig. 2.8B). I then examined the membrane plus matrix fractions, the ciliary fraction that can be obtained by solubilizing isolated cilia with non-ionic detergents such as Nonidet (See Methods). The membrane plus matrix fraction contains IFT complexes and associated cargoes (Piperno and Mead 1997; Cole et al. 1998; Qin et al. 2004). Thus, the membrane plus matrix fractions from WT and *ida3* cilia were compared and analyzed by immunoblots for the presence of I1 dynein (Fig. 2.8B). I1 dynein is present in the wild-type membrane plus matrix fraction, indicating that the cytoplasmic I1 dynein complex is able to enter the ciliary compartment (Fig. 2.8A). In contrast, at the same protein concentration, I1 dynein is missing in membrane plus matrix fraction from *ida3* (Fig. 2.8, top right panels). The same results were obtained using a freeze-thaw method (See Methods), and as an alternative to using detergent, to generate the membrane plus matrix fraction (Behal and Cole 2013). Thus, compared to wild-type, the 20S I1 dynein complex does not appear to enter the ciliary compartment in *ida3* mutant cells.

Discussion

The overall goal of this work is to study the mechanisms of assembly and transport of I1 dynein by exploiting the considerable experimental advantages of I1 dynein and *Chlamydomonas*. From the axoneme, the I1 dynein complex is found as a 20S complex (Fig. 2.2A and (Piperno et al. 1990; Smith and Sale 1991). However, until this study very little was known about the process of 20S I1 dynein complex assembly. In this chapter, I addressed questions regarding I1 dynein assembly in the cytoplasm. I also used a mutant,

ida3 to understand various steps of I1 dynein assembly. The *ida3* mutant fails to assemble I1 dynein in the axoneme, but assembles the 20S I1 complex in the cytoplasm.

The conclusions from the data presented in this chapter include: the 20S I1 complex is assembled in the cytoplasm; assembly of the cytoplasmic 20S I1 complex requires the heavy chains and intermediate chain IC140; the 20S I1 dynein complex in the cytoplasm is not a recycled product of the axoneme. I also determined that the cytoplasmic 20S I1 dynein complex is not competent to bind I1-deficient axonemes in *in vitro* reconstitution assays. Moreover, the *ida3* mutant is not defective in the cytoplasmic assembly and docking of the 20S I1 dynein complex. The data presented in this chapter, and Chapters 3 and 4, support the hypothesis that the *ida3* mutant is most likely defective in the entry and/or transport of I1 dynein into the cilium (See Fig. 1.9, Chapters 3 and 4 for further discussion).

The steps of cytoplasmic assembly of I1 dynein

Examination of the sedimentation profiles of cytoplasmic extracts derived from wild type and I1 dynein mutant cells revealed the presence of 10-12S I1 dynein sub-complexes (Fig. 2.2A). While the cytoplasmic 20S I1 dynein complex represents the nearly complete complex, the 12S fractions contain smaller sub-complexes are postulated to be intermediates in the preassembly process (Fig. 2.4). The detailed molecular composition of the smaller I1 dynein sub-complexes remains undefined. One idea is that 10-12S fractions contain an assortment of different 12S I1 dynein precursors, each composed of a heavy chain and an intermediate chain and any of the several light chains (illustrated in Fig. 2.4). Based on the presence of the 12S sub-complexes in mutants

lacking the heavy chains and IC140, and along with the presence of partial complexes in the range of 15-18S in the *fla14-3* and *bop5* mutants (Fig. 2.3), the simplest model is that the assembly of I1 dynein takes place in a step-wise manner. The first step involves the association of one of the heavy chains with either or both IC140. Presumably, the next step is the association of two 12S complexes and addition of the remaining I1 dynein subunits to eventually form the intact "two headed" 20S I1 dynein complex (See Fig. 2.9).

Tests of the I1 dynein assembly process require alternate, higher resolution biochemical fractionation. Approaches will include tagging the intermediate chains, IC140 and IC138 and resolution of the 10-12S and 15-18S sub-complexes by ion-exchange chromatography, and blue native gels. These approaches will reveal the exact I1 dynein subunit composition in the sub-complexes and the sequence of the steps of preassembly. As a bonus, identifying the specific I1 dynein subunit composition in the 12S sub-complexes will define key protein interactions within the I1 dynein complex. These biochemical results would complement and extend high-resolution structural analysis by cryo-ET (see (Heuser et al. 2012) and biochemical analysis by chemical cross linking (Hendrickson et al. 2004b; Wirschell et al. 2009). With the recent success of coupling cryo-ET with tagged proteins (Oda and Kikkawa 2013; Oda et al. 2014a; Oda et al. 2014b; Song et al. 2015), it is possible that this approach can be used to define domains within the I1 dynein complex.

The LC8 subunit may play an important role in I1 dynein assembly

Examination of the sedimentation profile of the LC8 mutant allele, *fla14-3* (Fig. 2.3) shows a slight shift in sedimentation of the I1 dynein complex derived from the cytoplasm. Based on this result, and previous studies of LC8, dimerization of 10-12S sub-complexes (Fig. 2.4), to form the two-headed 20S I1 dynein complex may require the light chain, LC8. LC8 is a particularly interesting protein required for the assembly of a range of large protein complexes including cytoplasmic dynein (Barbar 2008), ODA (DiBella et al. 2001; Tanner et al. 2008), I1 dynein (Wirschell et al. 2009; Yang et al. 2009), RS (Gupta et al. 2012), etc. The idea proposed by Barbar (2008) is that the LC8 dimer forms a platform essential for the assembly of large, dimeric complexes such as the dyneins and radial spokes. For instance, Gupta et al., (2012) showed that the LC8 dimer plays a critical role in the assembly of the mature 20S RS complex in the cilium, bringing together the two 12S sub-complexes. In the case of I1 dynein, the LC8 dimer may be responsible in bringing together the heavy chain-containing sub-complexes to form the dimeric 20S I1 dynein complex (Fig. 2.9). Further studies of the LC8 mutant alleles are required to test this hypothesis.

The cytoplasmic and axonemal 20S I1 dyneins differ in their ability to bind axonemes

One of the surprising observations in this study is the failure of the 20S I1 dynein from the cytoplasm to reconstitute I1-deficient axonemes (Figs. 2.6 and 2.7). All of the *in vitro* reconstitutions were carried out in the presence of ATP, to ensure that rebinding of I1 dynein was occurring by the docking domains and not the motor domains. In the absence of ATP, I1 dynein from the cytoplasm rebound axonemes, most likely by the

motor domains (Fig. 2.6 and see Toba et al. 2011). However, in the presence of ATP, I1 dynein complex from the cytoplasm did not bind axoneme. In contrast, I1 dynein derived from the axoneme specifically restores I1 dynein to I1 dynein-depleted axonemes (Fig. 2.7A and (Smith and Sale 1992; Yamamoto et al. 2006). One possible explanation for the failure in binding is that the cytoplasmic 20S I1 complex lacks one of the light chains necessary for docking in the axoneme. Refined purification of the cytoplasmic I1 dynein (e.g. (Toba et al. 2011) is required to test this idea and to definitively determine the light chain composition of the cytoplasmic complex.

It is equally possible that the I1 complex must be modified for docking onto the axoneme. For example, before docking on the axoneme, the radial spokes undergo additional assembly and modification in the ciliary compartment involving additional protein assembly and altered phosphorylation of key radial spoke assembly proteins, LC8 and RSP3 (Yang et al. 2005; Diener et al. 2011; Gupta et al. 2012). Similarly, modification of I1 dynein may occur in the ciliary compartment before the complex is competent to dock to the axoneme. For example, as a starting point, I would focus on the IC140 subunit as a candidate. The IC140 subunit is required for the assembly of I1 dynein in the cytoplasm and the C-terminal WD-repeat domain of IC140 is required for assembly of the I1 dynein complex in the axoneme (Perrone et al. 1998; Yang and Sale 1998). In addition, 2D gel analysis published by Lin et al. (Lin et al. 2011) revealed multiple isoforms of IC140 in the axonemes, suggesting that IC140 is modified. However, the nature of this modification that leads to multiple isoforms is not currently known, but could include different phosphorylation states that are important for docking to the axoneme. One approach to test the idea that modification of IC140 involves

phosphorylation, is to treat the cytoplasmic and ciliary extracts with kinase or phosphatase inhibitors and examine whether I1 dynein can bind to axonemes by the *in vitro* reconstitution assay illustrated in Fig. 2.5.

The *ida3* mutant maybe defective in entry and/or transport of the I1 dynein complex

Despite not knowing the function of IDA3, the *ida3* mutant has proven to be informative in understanding the process of I1 dynein assembly. The key observation is that the 20S I1 complex assembles in the *ida3* cytoplasm (Fig. 2.2B). The simplest interpretation of this result is that IDA3 is not required for I1 dynein cytoplasmic assembly. However, higher resolution biochemical analysis of the 20S I1 dynein complex in *ida3* is necessary to definitively determine whether minor subunits are missing. Another possibility is that *IDA3* encodes an axonemal protein required for docking I1 dynein, analogous to ODA-DC proteins (Takada et al. 2002; Casey et al. 2003a; Wirschell et al. 2004; Dean and Mitchell 2013; Ide et al. 2013; Owa et al. 2014). However, our *in vitro* reconstitution analysis (Fig. 2.7A) does not support this model and indicates that the *ida3* axoneme is not defective in I1 dynein docking.

Based on our observation that I1 dynein assembles in the *ida3* mutant cytoplasm but not in the axoneme, the simplest model is that IDA3 is required for the entry/transport of I1 dynein into the ciliary compartment (Fig. 1.9). Consistent with this model, the I1 dynein complex does not appear in the membrane plus matrix fraction of *ida3* cilia (Fig. 2.8B). While the absence of I1 dynein in the *ida3* ciliary compartment supports my hypothesis that IDA3 encodes a protein required for entry and transport of I1 dynein in the ciliary compartment, alternate hypotheses for the function of IDA3 exist. As

illustrated in my model (Fig. 1.9), one hypothesis is that IDA3 may be an adapter that selectively links I1 dynein to IFT for entry and transport within the ciliary compartment. The adapter model is founded on studies of ODA16 as an adapter that mediates interaction between the ODA and IFT46 (Hou et al. 2007; Ahmed et al. 2008). Additionally, new evidence indicates IFT, and associated axonemal cargoes (such as the I1 dynein), are carried with membrane vesicles destined to the cilium (Wood and Rosenbaum 2014). A novel idea, consistent with the model proposed by Wood and Rosenbaum, is that IDA3 links the 20S I1 complex onto the membrane vesicles destined to the base of the cilium. Tests of this model would include identification of IDA3, localization of IDA3 by microscopic approaches and biochemical approaches to isolate or enrich IDA3/I1 dynein-bound vesicles. Based on studies of N-DRC (nexin-dynein regulatory complex) transport (Wren et al. 2013), IFT is required for both entry into and transport within the ciliary compartment (Fig. 2.9).

An alternative to the adapter model is that the IDA3 protein is a modifier, such as a protein kinase, that is required for selectively controlling the interaction between the I1 complex and IFT and entry into the cilium. Definitive tests of these ideas require the identification of *IDA3* and characterization of the IDA3 protein. The Sale lab members are testing the idea that IDA3 is a cytoplasmic protein required for I1 dynein entry to the cilium. Notably, the function of IDA3 is specific to I1 dynein. In *ida3*, the cilia are normal length and with the sole exception of I1 dynein, remaining axonemal components are assembled at wild-type levels.

Figures for Chapter 2

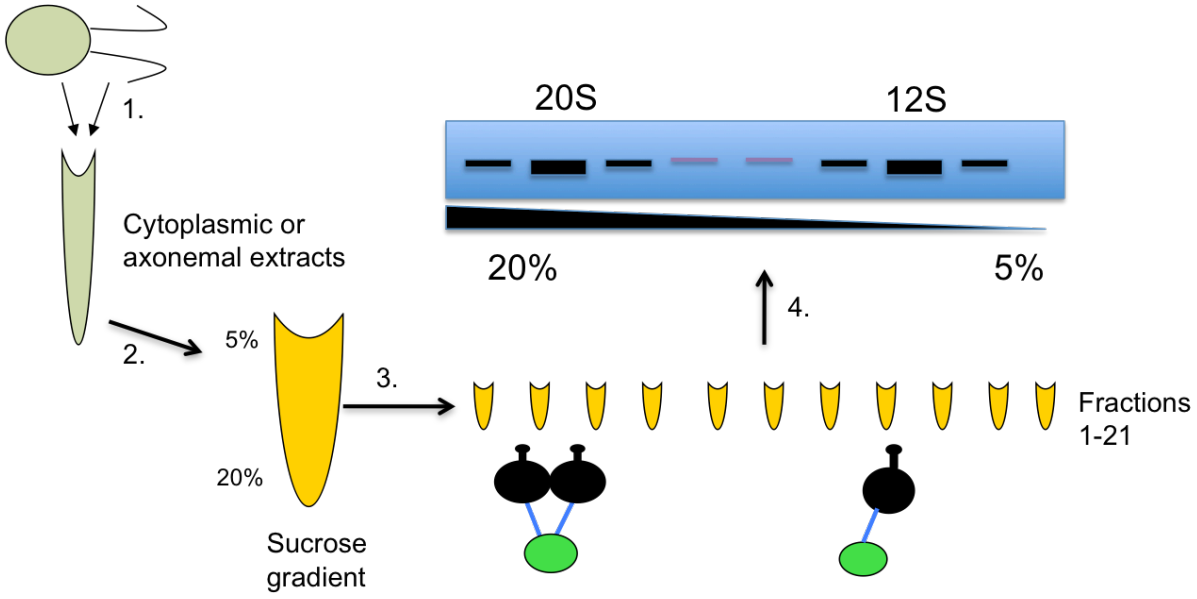
1.
Cytoplasmic or
axonemal extracts
2.
5%
20%
Sucrose
gradient
3.
20S
12S
20%
5%
4.
Fractions
1-21

Figure 2.1. Illustration of the fractionation method used to isolate I1 dynein in this study. Fractionation of cytoplasmic or axonemal extracts by velocity sedimentation on sucrose gradients is a very effective method to study large axonemal complexes such as the I1 dynein (King 2009, Inaba and Mizuno 2009). In order to determine the assembly state of the I1 dynein in the cytoplasm, I isolated the cytoplasmic extracts from wild-type and I1 mutant cells (**1**), fractionated by velocity sedimentation and examined each fraction by immunoblots. As a positive control, I prepared axonemal extracts (See Methods) from wild-type cells (**1**). The general method is: Application of cytoplasmic and axonemal extracts to a 5-20% sucrose gradient followed by a high-speed (36,000 rpm, 16 hour) spin; (**2**) Twenty-one 0.5mL fractions were collected (**3**); the fractions analyzed by western blots (**4**). The S-values of the complexes were established using standard proteins and method (Smith and Sale 1991). The fully assembled I1 dynein complex derived from the axoneme sediments at 20S (Piperno et al. 1990; Smith and Sale 1991). I predicted that a "preassembled" I1 dynein complex would also sediment at 20S.

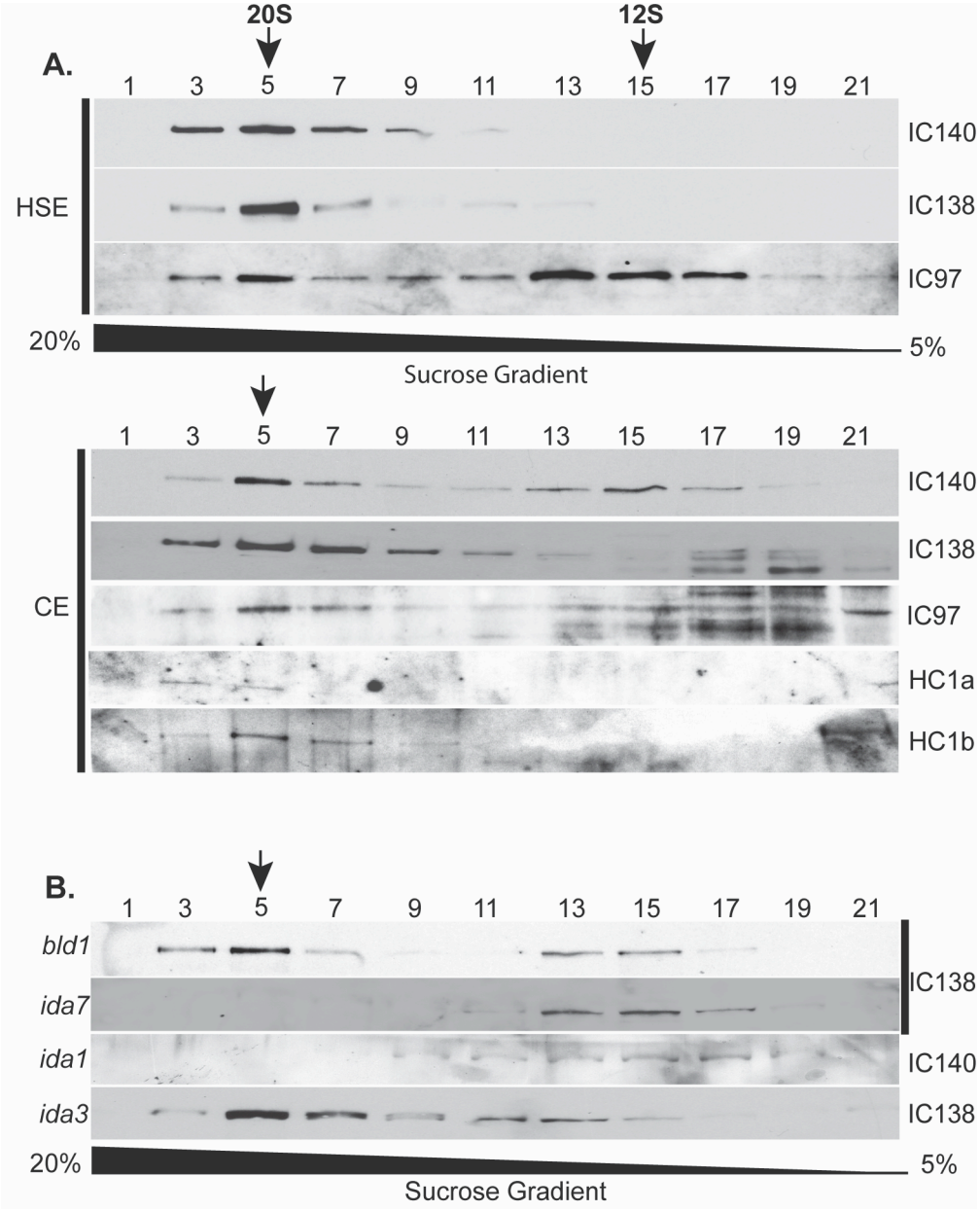
A.
20S
12S
1 3 5 7 9 11 13 15 17 19 21
HSE
IC140
IC138
IC97
20%
5%
Sucrose Gradient
1 3 5 7 9 11 13 15 17 19 21
CE
IC140
IC138
IC97
HC1a
HC1b
B.
1 3 5 7 9 11 13 15 17 19 21
bld1
ida7
ida1
ida3
IC138
IC140
IC138
20%
5%
Sucrose Gradient

Figure 2.2. I1 dynein assembles in the cytoplasm as a 20S complex. (A) Immunoblots of fractions from velocity sedimentation of axonemal high salt extracts (HSE) and cytoplasmic extracts (CE) were analyzed. The I1 dynein subunits IC140, IC138 and IC97 co-sediment at fraction 5 (arrows) in both axonemal high salt extracts and cytoplasmic extracts from wild-type cells. Similar to the 20S complex from the axoneme (Piperno et al. 1990), the 20S complex in the cytoplasm contains both heavy chains (HC 1 α and HC 1 β). **(B)** Cytoplasmic extracts derived from *bld1, ida1, ida3* and *ida7* were fractionated by velocity sedimentation and analyzed by immunoblots using IC138 or IC140 as a marker of I1 dynein. Cytoplasmic I1 dynein from *bld1* and *ida3* cosediment with wild-type 20S I1 complex. The 20S I1 complex is missing in the I1 dynein heavy chain mutant *ida1* and *ida2* (Fig. 2.3) and in the IC140-null mutant *ida7*. Relevant to the study of *ida3* (Chapter 4), the 20S I1 dynein preassembly is intact. This indicates that in *ida3*, I1 dynein entry or transport to the cilium is defective (see Fig. 2.8 below).

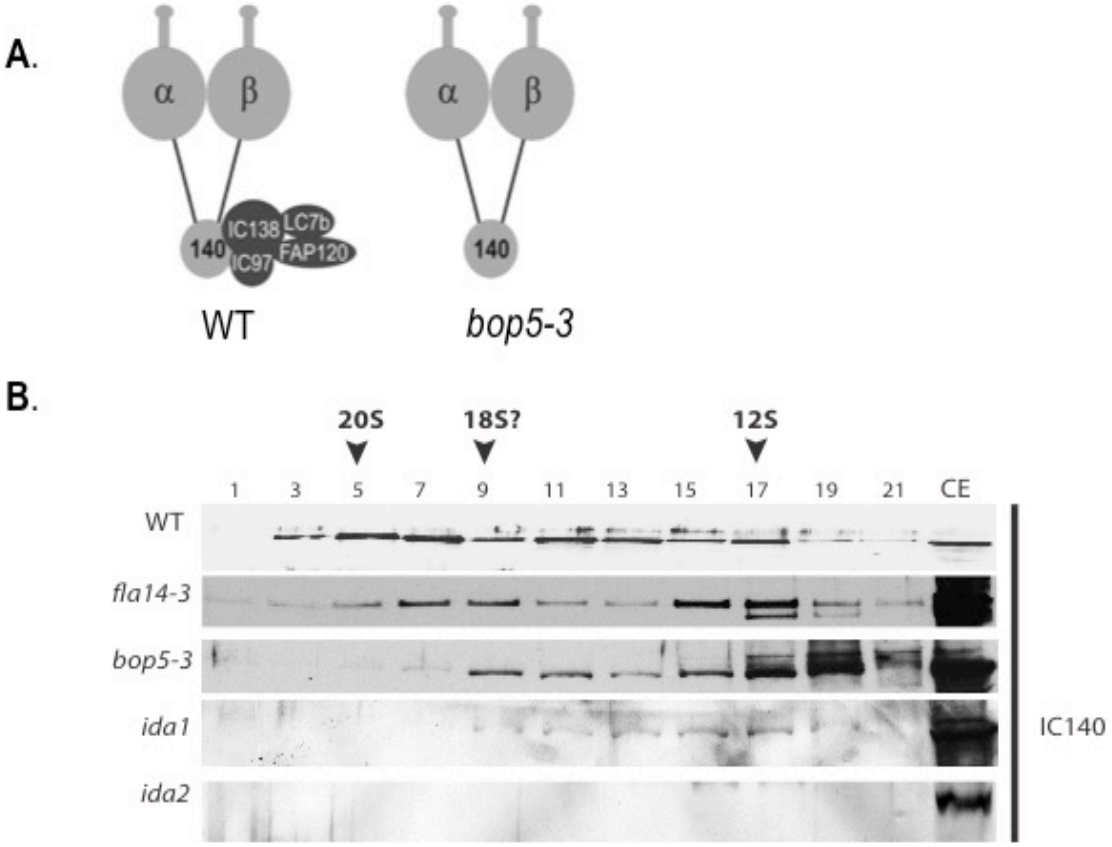
A.
α
β
α
β
140
IC138
LC7b
IC97
FAP120
140
WT
bop5-3
B.
20S
18S?
12S
1
3
5
7
9
11
13
15
17
19
21
CE
WT
fla14-3
bop5-3
ida1
ida2
IC140

Figure 2.3. Mutations in specific I1 dynein subunits result in either the absence or partial assembly of the I1 dynein complex in the cytoplasm. (A) Axonemal I1 dynein is partially assembled in an allelic LC8 mutant, *fla14-3* and IC138 null allele, *bop5-3*. **(B)** In order to determine whether these partial I1 dynein complexes also preassemble, I fractionated cytoplasmic extracts from the *fla14-3* and *bop5-3* mutants. As shown in Figure 2.2, I1 dynein fully assembles as a 20S complex in the wild-type cytoplasm. However, in the *fla14-3* and *bop5-3* mutants' cytoplasm, partial complexes in the 15-18S range can form. Since the heavy chains are required for preassembly, their absence in the *ida1* (HC1α-null) or *ida2* (HC1β-null) results in the complete absence of the 20S complex. Here, I used an antibody to the IC140 subunit as a marker of I1 dynein. The 12S fractions may contain subcomplexes of I1 dynein predicted to contain an assortment of I1 dynein subunits and be intermediates in the preassembly process (See Fig. 2.4).

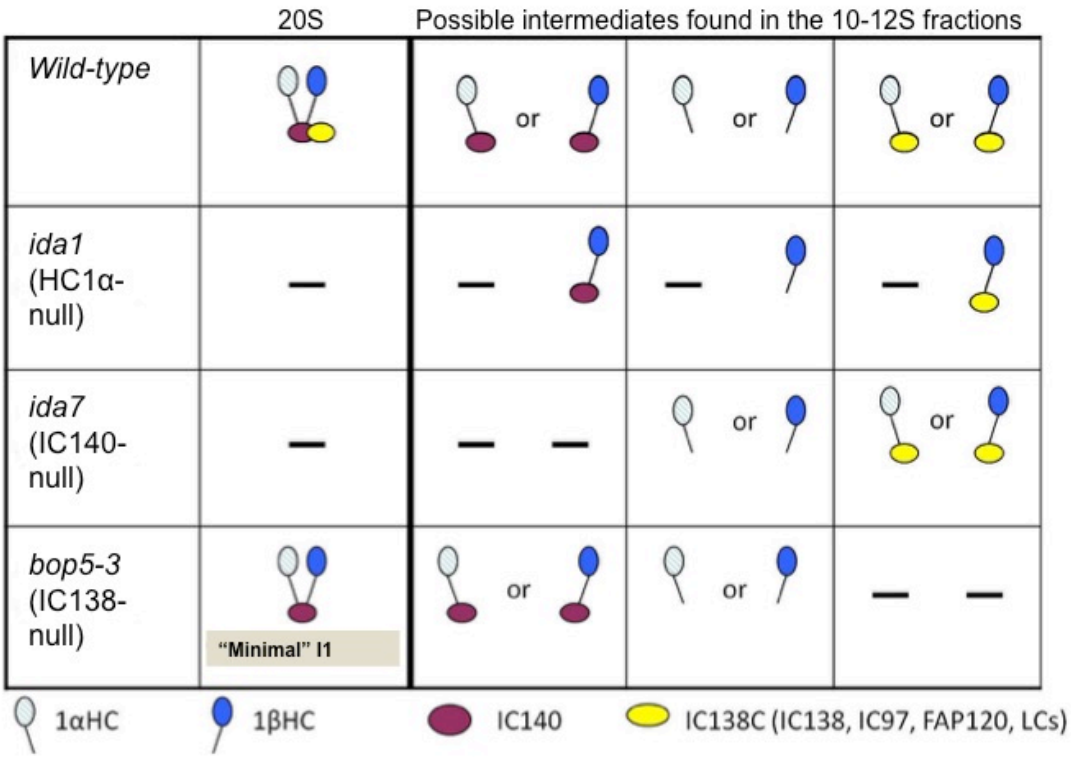
20S
Possible intermediates found in the 10-12S fractions
Wild-type
or
or
or
ida1 (HC1α-null)
ida7 (IC140-null)
or
or
bop5-3 (IC138-null)
or
or
"Minimal" I1
1αHC
1βHC
IC140
IC138C (IC138, IC97, FAP120, LCs)

Figure 2.4. Summary of preassembly of I1 dynein: 20S complex and 12S subcomplexes. In WT, the 20S complex preassembles in the cytoplasm and contains the heavy (HC1α and HC1β), intermediate (IC140, IC138 and IC97), and the light chains (LCs). The 12S fractions are predicted to contain several intermediate complexes shown in the last three columns. The I1-dynein structural mutants provide valuable tools for assessing the sub-complexes—*e.g.* possible 12S complexes are shown for three I1-dynein mutants (*ida1*, *ida7* and *bop5-3*) and for probing protein interactions between the I1 dynein subunits. The preassembled subcomplexes indicate that cytoplasmic assembly of I1 dynein occurs in a stepwise manner. The "minimal" I1 dynein (that is the dynein subcomplex that assembles in the axoneme) in *bop5-3* contains both heavy chains and IC140. This partial preassembled I1 dynein complex is competent of pre-assembly, transport to the cilium and docking in the axoneme, thus supporting our hypothesis that the heavy chains and IC140 is required for all three steps of I1 dynein assembly.

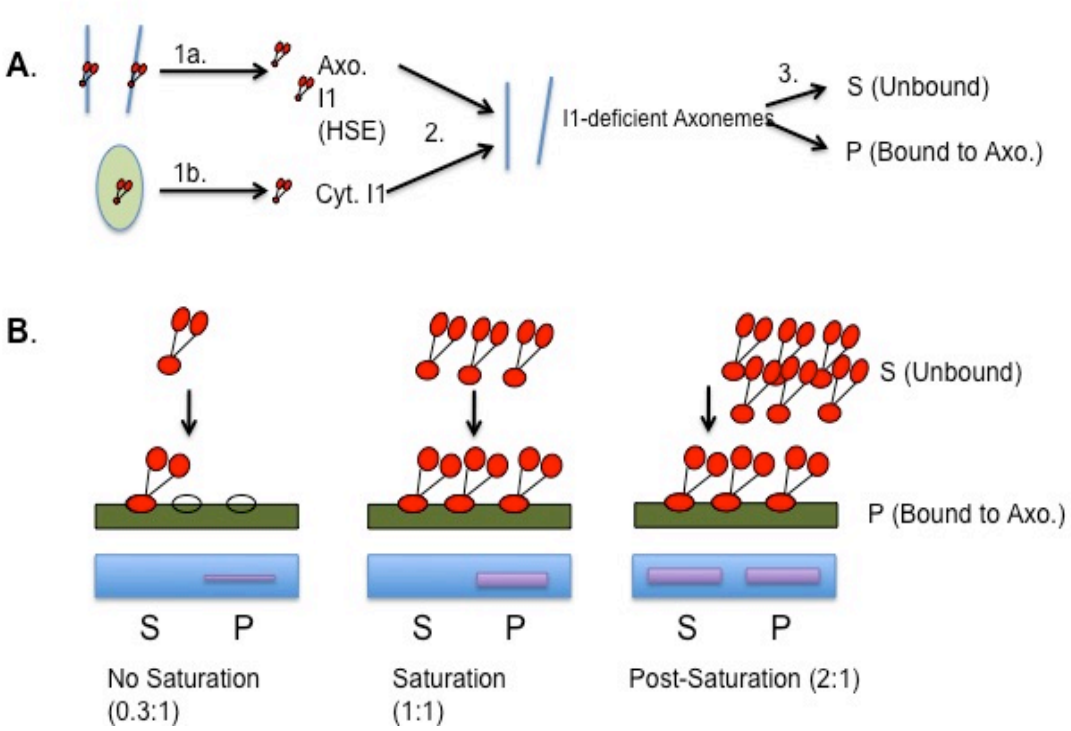
A.
1a.
Axo. I1 (HSE)
1b.
Cyt. I1
2.
I1-deficient Axonemes
3.
S (Unbound)
P (Bound to Axo.)
B.
S (Unbound)
P (Bound to Axo.)
S
P
No Saturation (0.3:1)
Saturation (1:1)
Post-Saturation (2:1)

Figure 2.5. Strategy for *in vitro* reconstitution of I1 dynein onto I1-deficient axonemes. The questions addressed in this experiment include: (**1**) Whether the 20S I1 dynein complex from the cytoplasm will bind axonemes and (**2**) and if so, whether rebinding is specific, and (3) whether the *ida3* mutant is defective in docking I1 dynein in the axoneme. **(A)** Axonemal high-salt extracts (HSE) or cytoplasmic extracts (cyt.) containing I1 dynein were prepared (**1a** and **1b**). Then varying ratios of extracts were mixed with a fixed amount of I1 dynein-deficient axonemes in the presence of 1mM ATP (**2**). Next, each combination is spun to separate the supernatant (S) containing unbound I1, and pellet (P) fractions containing I1 dynein bound to the axonemes (3). The S and P fractions can be analyzed by western blots to examine I1 dynein binding to the axoneme. **(B)** To test for specificity of I1 dynein binding, saturation of binding was examined. For example, when the number of I1 dynein complexes added are less than the available binding sites (e.g. 0.3:1 ratio), predictably all I1 dynein binds to the axoneme and can be found exclusively in the pellet (P) fractions. In contrast, when the number of I1 molecules added exceeds the number of available binding sites, the unbound I1 can be detected in supernatant fractions. Predictably, if cytoplasmic I1 dynein binds axonemes and saturates, then that would indicate a specificity of binding. As shown in Fig. 2.6, cytoplasmic I1 dynein does not bind axonemes. In addition, the reconstitution experiment can also be used to assess whether I1 dynein mutant cells are defective in an I1 dynein docking mechanism. In this case, this reconstitution experiment was used to test the hypothesis that *ida3* is defective in an I1 dynein-specific docking protein.

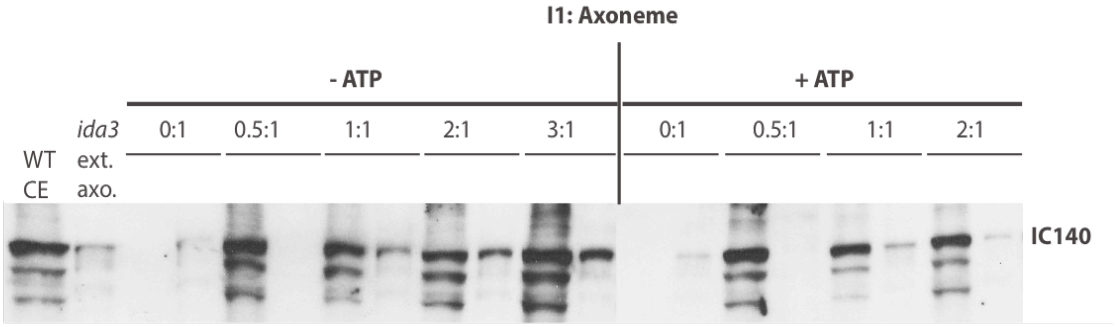
I1: Axoneme
- ATP
+ ATP
ida3
0:1
0.5:1
1:1
2:1
3:1
0:1
0.5:1
1:1
2:1
WT
CE
ext.
axo.
IC140

Figure 2.6. Immunoblot showing *in vitro* reconstitution of cytoplasmic extracts (CE) containing I1 dynein onto salt-extracted I1 dynein-deficient *ida3* axonemes in the presence and absence of ATP. Varying ratios of cytoplasmic extracts containing I1 (CE) to extracted axonemes (I1: Axonemes) were combined in an ATP-containing buffer, incubated on ice for 30 min and probed with IC140 as a marker for I1 dynein in immunoblots analysis. Each mixture was centrifuged to separate the supernatant (S = unbound I1 dynein) and pellet (P = bound I1 dynein) fractions. I1 dynein derived from the cytoplasm binds I1-deficient axonemes in the absence of 1mM ATP as indicated by the presence of I1 dynein in the pellet (P) fractions. However, in the presence of ATP, I1 dynein from the cytoplasm is not found in the P fractions in the ratios examined, indicating that cytoplasmic I1 dynein (cyt.) does not bind to the axoneme as indicated by I1 presence in the supernatant (S) only. A small amount of IC140 is present in the *ida3* axonemes most likely due to the incomplete extraction of the *ida3* axonemes.

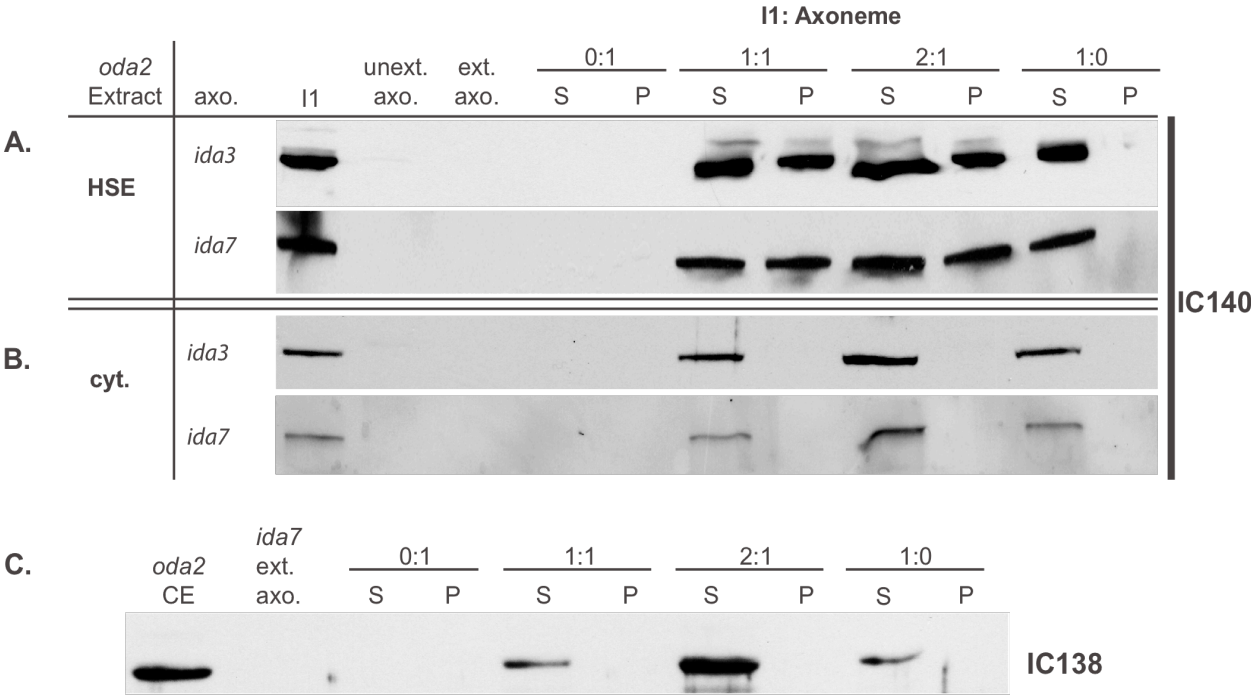
I1: Axoneme
oda2 Extract
axo.
I1
unext. axo.
ext. axo.
0:1
1:1
2:1
1:0
S
P
A.
HSE
ida3
ida7
IC140
B.
cyt.
ida3
ida7
C.
oda2 CE
ida7 ext. axo.
0:1
1:1
2:1
1:0
S
P
IC138

Figure 2.7. Immunoblot showing the *in vitro* reconstitution results: (1) I1 dynein derived from the cytoplasm does not bind I1-deficient axonemes; (2) The *ida3* mutant is not defective in docking of I1 dynein to the axonemes *in vitro*. **(A)** High salt extracts (HSE) containing I1 dynein from *oda2* axonemes were reconstituted onto salt-extracted I1-deficient *ida3* and *ida7* axonemes in the presence of 1mM ATP. Varying ratios of axonemal I1 (HSE) to extracted axonemes (I1: Axonemes) were combined in an ATP-containing buffer, incubated on ice for 30 min and probed with IC140 as a marker for I1 dynein in immunoblots analysis. Each mixture was centrifuged to separate the supernatant (S = unbound I1 dynein) and pellet (P = bound I1 dynein) fractions. Axonemal I1 (HSE) reconstituted onto both *ida3* and *ida7* axonemes results in I1 dynein binding to the axonemes to saturation (P = pellet/bound I1). This result indicated that the *ida3* mutant is not defective in a docking mechanism. **(B)** I1 dynein-containing cytoplasmic extracts (cyt.) from *oda2* were added to *ida3* and *ida7* axonemes in the presence of ATP. Notably, cytoplasmic I1 dynein (cyt.) does not bind to the axoneme as indicated by I1 presence in the supernatant (S) only. **(C)** The same results were obtained using the IC138 antibody.

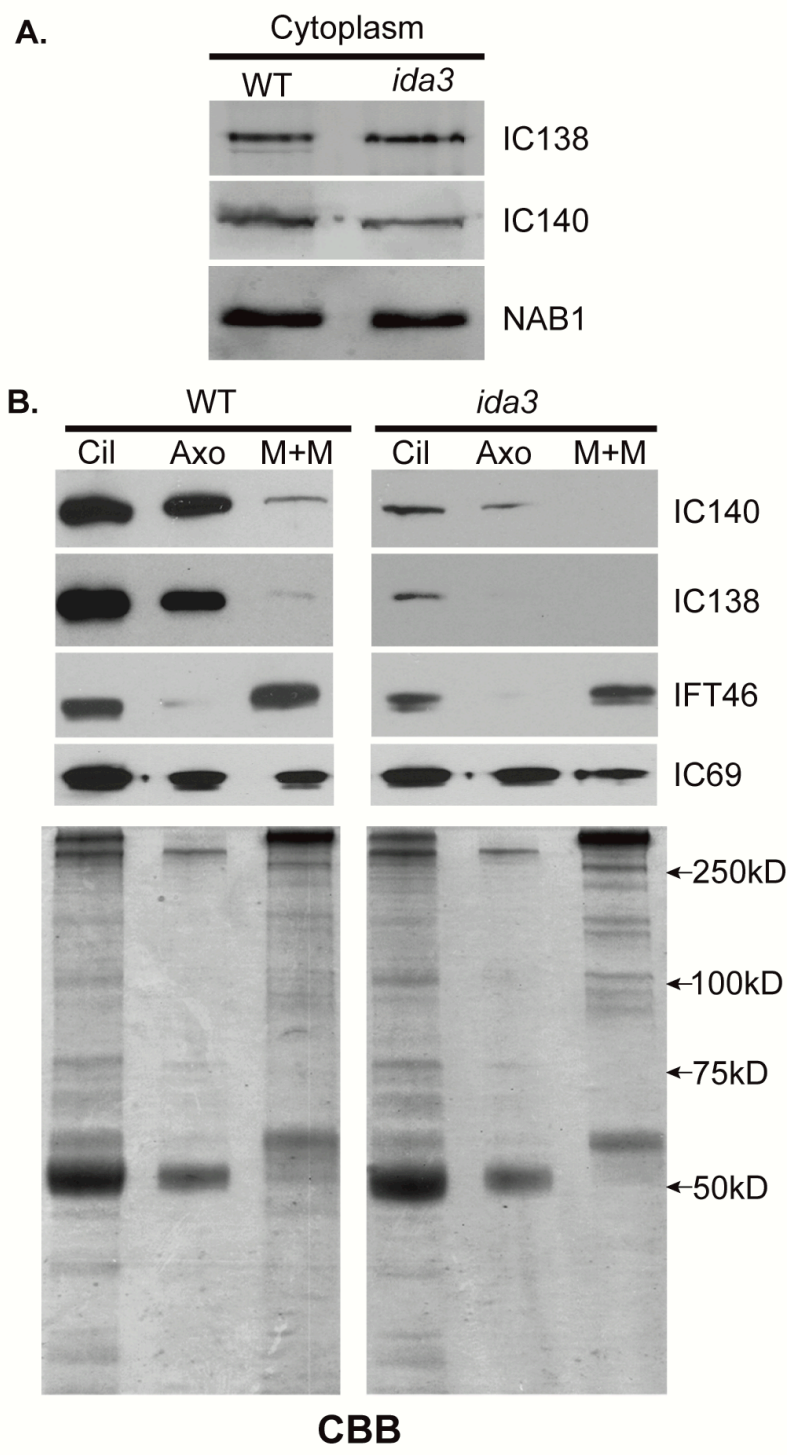
A.
Cytoplasm
WT
ida3
IC138
IC140
NAB1
B.
WT
ida3
Cil
Axo
M+M
Cil
Axo
M+M
IC140
IC138
IFT46
IC69
250kD
100kD
75kD
50kD
CBB

Figure 2.8. The 20S I1 dynein assembled in the *ida3* mutant cytoplasm is defective in entry to the ciliary compartment. (**A**) Immunoblots comparing I1 intermediate chains, IC138 and IC140, in wild-type and *ida3* cytoplasmic extracts. NAB1 was used as a marker and loading control [Mussgnug et al.,2005] (**B**) Immunoblots of ciliary (Cil), axonemal (Axo) and membrane + matrix (M+M) fractions were analyzed using antibodies to the IC138 and IC140 subunits of I1 dynein. For detection of axonemal subunits (IC69, IC140, IC138), the M+M was loaded at five times the relative amount of cilia and axonemes. Analysis showed a significant reduction in ciliary and axonemal I1 dynein in *ida3* compared to wild-type. In addition, M+M fractions show that I1 dynein is absent in *ida3* compared to wild-type indicating inefficient entry into the ciliary compartment. The M+M samples from WT and *ida3* were also examined by immunoblots at twice the protein load (data not shown), and I1 dynein subunits were never present in *ida3*. The outer arm component, IC69, is present in equivalent amounts in WT and *ida3* M+M and serves as a control for IFT cargo. The IC69 immunoblot also validates that the defect in *ida3* is specific to I1 dynein. IFT46 serves as a positive control for M+M fractionation. CBB = Coomassie Brilliant Blue loading control.

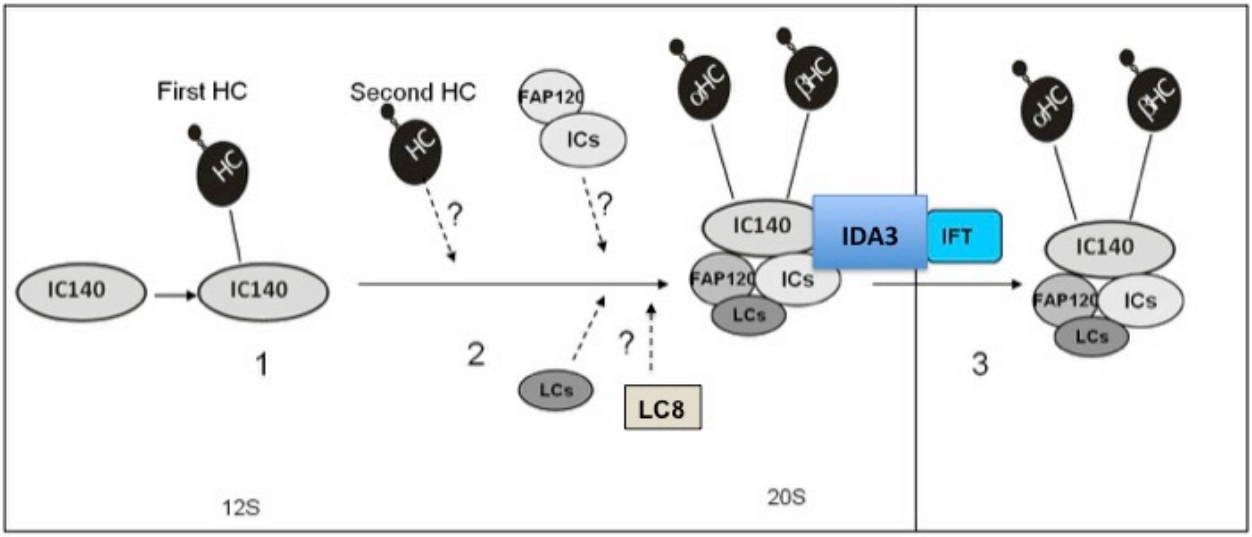
First HC
Second HC
FAP120
ICs
αHC
βHC
HC
IC140
IC140
IC140
IDA3
IFT
FAP120
ICs
LCs
1
2
3
LCs
LC8
12S
20S
Cytoplasm
Cilia

Figure 2.9. Schematic showing steps of I1 dynein preassembly prior to transport to the ciliary compartment. In this model, the preassembly of I1 dynein in the cytoplasm is dependent on IC140 and the heavy chains that recruit other subunits to eventually form the 20S subcomplex. Predictably, IC140 first recruits one of the heavy chains (HCs) to form a 12S subcomplex **(1).** In an order that is unknown, indicated by "?" and dashed arrows, the second HC, and the intermediate chains (IC138, IC97 and FAP120) and light chains (LC8, LC7a, LC7b, Tctex1 and Tctex2) get recruited to form the 20S I1 dynein complex **(2).** Once I1 dynein is preassembled, the predicted adapter, IDA3, mediates the interaction between I1 and IFT for entry into and transport within the cilium **(3).**

Chapter 3: I1 dynein is transported to the distal tip by IFT

Introduction

Fractionation of cytoplasmic extracts from wild-type cells revealed that the I1 dynein assembles as a 20S complex prior to entry and transport to the ciliary compartment (Fig. 2.2). Upon entry into the cilium, where does the 20S I1 dynein complex begin assembly in the axoneme? One possibility is that assembly begins at the proximal end of the axoneme immediately after entry into the ciliary compartment and then proceeds towards the distal tip. However, diverse evidence has indicated that the assembly of ciliary precursors begins at the distal end of the growing axoneme (Lefebvre et al. 1978; Lefebvre and Rosenbaum 1986). For example, original studies by Witman and colleagues using pulse labeling with [^{3}H]-acetate followed by autoradiography, showed that majority of silver grains, (representative of newly synthesized proteins), appeared at the distal tip of the regenerating cilium (Witman 1975). More recently, Johnson and Rosenbaum (Johnson and Rosenbaum 1992) examined the incorporation of tubulin in regenerating cilia and observed that new addition of tubulin subunits occurred exclusively at the distal end of cilia during ciliogenesis. Thus, I predicted that the addition of cytoplasmic 20S I1 dynein, like tubulin and the radial spoke, also occurs at the distal end of axoneme during ciliogenesis.

Based on the successful use of dikaryon rescue to study axonemal protein assembly by (Johnson and Rosenbaum 1992), (Alford et al. 2013) and (Wren et al. 2013), I took advantage of dikaryon rescue (Fig. 3.1) to test the hypothesis that assembly of I1 dynein begins at the distal tip of the cilium before docking in the axoneme. While the quadraflagellate dikaryon stage lasts for only 2.5 hours before cilia are resorbed, the 2.5-hour time period is sufficient to observe the rescue of mutant ciliary phenotypes in certain

cases (reviewed in Dutcher, 2014; Fig. 3.1). For example, in dikaryons formed by mating of wild-type cells with a paralyzed, radial spoke-deficient mutant such as *pf14*, cytoplasmic complementation resulted in the rescue of both motility and radial spoke assembly in the formerly paralyzed, *pf14* cilia (Fig. 1.7 and (Luck et al. 1977)). In another example, Johnson and Rosenbaum (Johnson and Rosenbaum 1992) used dikaryon rescue to show that radial spoke proteins, like tubulin, were added to the distal tip of mutant axonemes in dikaryons formed between WT and a RS-deficient mutant, *pf14*. Most recently, Wren et al. (Wren et al. 2013), used live cell imaging and directly observed that the N-DRC complex is also transported to the distal tip of the axoneme prior to unloading from IFT, diffusion and docking in the axoneme.

Together, these results indicated that axonemal proteins must first be transported to the distal end of the cilium before assembly in the axoneme. Thus, the dikaryon rescue approach provides important and unique means to examine the site of assembly of axonemal precursors in an otherwise fully assembled axoneme. Based on past successes, the question I first addressed whether dikaryon rescue be used to examine I1 dynein assembly in the cilium. In particular, can cytoplasmic complementation of the preassembled I1 dynein precursors restore I1 dynein assembly in the full-length mutant cilium? In the event rescue occurs in the dikaryon, I asked where I1 dynein begins to incorporate in the axoneme. I have illustrated all the possible outcomes in Fig. 3.2.

In this chapter, I also explored how the large I1 dynein complex is transported within the ciliary compartment. Studies focused on the transport of the N-DRC, ODA and radial spoke revealed that IFT is responsible for transporting these axonemal protein complexes in the cilium (Bhogaraju et al. 2013b). For instance, one of the IFT

components, IFT46 and a predicted IFT adapter, ODA16, are necessary for transporting the ODA complexes into and within the ciliary compartment (Ahmed and Mitchell 2005; Hou et al. 2007; Ahmed et al. 2008). In the case of the radial spoke complexes, anterograde IFT is directly involved with the transport of the preassembled complexes to the site of assembly at the distal tip of the cilium (Qin et al. 2004). In addition, live cell imaging has also revealed that tubulin is transported by IFT (Craft et al. 2015). Consistent with this idea, Bhogaraju et al. demonstrated that tubulin forms a complex with IFT proteins indicating that tubulin is a cargo for IFT (Bhogaraju et al. 2013a; Bhogaraju et al. 2013b; Bhogaraju et al. 2014). Based on these studies, I hypothesized that transport of the I1 dynein complex to the distal tip requires IFT.

In order to test the hypothesis that I1 dynein is transported to the distal tip by IFT, I took advantage of dikaryon rescue involving an I1 dynein assembly mutant, *ida3* (Table 3) and the *fla10*^{ts} mutant. The *fla10*^{ts} mutant contains a temperature-sensitive allele of the *FLA10* locus that encodes the motor subunit of the heterotrimeric kinesin, kinesin-2 (Walther et al. 1994). In the *fla10*^{ts} mutant, kinesin motor activity is abolished at restrictive temperature (32ºC), resulting in the cessation of anterograde IFT (Kozminski et al. 1995). I predicted that when the kinesin motor and IFT are functional at permissive temperature, the transport of I1 dynein to the distal tip of the *ida3*; *fla10-1*^{ts} axoneme would occur normally in dikaryons formed between *fla10*^{ts} and *ida3*; *fla10-1*^{ts}. However, upon switching these dikaryons to restrictive temperature, I1 dynein transport to the distal tip would be completely inhibited, indicative of IFT-dependent transport of I1 dynein transport. The experimental design is illustrated in Fig. 3.5.

In this chapter, I present the following results: In dikaryons formed between WT

and I1 dynein mutant cells, the addition of I1 dynein complexes first occurs at the distal tip of the cilia. The assembly of I1 dynein then proceeds towards the proximal end of the axoneme. This result is consistent with the transport of I1 dynein to the distal tip for assembly during ciliary generation. In dikaryons generated from *fla10-1^{ts}* and *ida3*; *fla10-1^{ts}* gametes, IFT-dependent transport of I1 dynein is completely inhibited at restrictive temperature (Fig. 3.6). This result strongly indicates that IFT is required for the transport of the I1 dynein complex as a cargo before assembly in the axoneme. An additional and important observation from this data is that a functional copy of IDA3 is required for transporting I1 dynein into or within the cilium. One possibility is that IDA3 is an adapter required to link I1 dynein to IFT. I provide further discussion of IDA3 in Chapter 4.

Results

I1 dynein is transported to the distal tip of the cilium prior to docking onto the axoneme

Since IFT typically transports cargo to the distal tip of the cilium prior to docking onto the axoneme (Wren et al. 2013), we performed dikaryon rescue experiments to determine the pattern of I1 dynein assembly (Johnson and Rosenbaum 1992; Piperno et al. 1996; Bower et al. 2013); reviewed in (Dutcher 2014). Wild-type and I1-deficient (*ida1, ida3* and *ida7;* Table 3, Chapter 1*)* cells were mated to allow for cytoplasmic complementation in temporary dikaryons. Resulting dikaryons were fixed at 30, 60 and 90 minutes for immunofluorescence with an antibody to IC140 as a marker for I1 dynein (Fig. 3.3). By 30 minutes, I1 dynein assembly began at the distal tip of the *ida7* axoneme

and proceeded toward the proximal end (Fig. 3.3A, yellow arrows). I1 dynein assembled along the entire length of the axoneme in less than 90 minutes (Fig. 3.3A, bottom panels).

To estimate the rate of assembly, I measured I1 dynein assembly along the axoneme from tip to base by generating fluorescence intensity profiles of individual cilia undergoing I1 dynein rescued-assembly at each time point (Fig. 3.3B). The length of I1 dynein assembly along the axoneme was measured from the distal tip to a point defined when the normalized fluorescence intensity dropped below the established threshold of 0.2 AU (Fig. 3.3B, dashed lines; see Methods in (Alford et al. 2013). Quantification of I1 dynein staining from the tip revealed that assembly occurred progressively starting at the distal tip and proceeding to proximal end of the axoneme (Fig. 3.3C, blue line). Therefore, I1 dynein is transported to the distal tip of the mutant cilium before incorporation into the axoneme, and then proceeds towards the proximal axoneme.

I also tested whether cytoplasmic complementation could rescue the assembly of I1 dynein in *ida3* axonemes. Dikaryons between wild-type and *ida3* were generated and fixed for immunofluorescence to determine the site of assembly of I1 dynein. The wild-type x *ida3* dikaryons illustrated rescue in the same tip to base assembly pattern compared to wild-type x *ida7* dikaryons (Fig. 3.3C, compare black circle and triangle line). Similar to wild-type x *ida7* and wild-type x *ida3* dikaryons, rescue of axonemal I1 dynein assembly was seen in *ida3* x *ida1* dikaryons (Fig. 3.3C, black triangle line). In addition, in *ida3* x *ida1* and *ida3* x *ida7* dikaryons, the rate of rescue of I1 dynein assembly was synchronous in all four mutant cilia. However, in contrast to other combinations, the rate of I1 axonemal assembly is delayed in *ida3* x *ida7* dikaryons relative to other dikaryon combinations examined (Fig. 3.3 C, red line).

I hypothesized that the delay in rescued assembly of I1 dynein in the *ida7* x *ida3* dikaryon required new protein synthesis. To test the hypothesis that the delay is due to the requirement of new protein synthesis, I repeated dikaryon rescue in the presence of the protein synthesis inhibitor cycloheximide (CHX) (Fig. 3.4). In wild-type x *ida3*, wild-type x *ida7*, and *ida3* x *ida1* dikaryons, axonemal I1 dynein assembly occurred at the same rate and in the same tip to base assembly pattern irrespective of the presence (Fig. 3.4A, lower panel and Fig. 3.4B) or absence (Fig. 3.4A, upper panel and Fig. 3.4B) of cyclohexamide. In contrast to other dikaryon combinations tested in the presence of cycloheximide, rescue of I1 dynein assembly was blocked in *ida3* x *ida7* dikaryons (Fig. 3.4A, yellow circles in bottom panel; 3.2B, red line and boxes). Thus, the delay in rescue of I1 dynein assembly is due to a requirement for new protein synthesis in the *ida3* x *ida7* dikaryon. One interpretation of these results is that IC140 and IDA3 form a complex that requires the presence of one or both proteins for complex formation, stability and entry and/or within the ciliary compartment (Fig. 3.5 and see Discussion).

Transport of I1 dynein requires the IFT anterograde motor, kinesin-2

Based on our observations that I1 dynein is transported to the distal tip before docking to the axoneme in dikaryons, and recent evidence showing axonemal components such as the N-DRC are transported by IFT (Wren et al. 2013), I proposed that I1 dynein transport to the distal tip is mediated by IFT. To test this idea, I took advantage of the conditional mutant, *fla10-1*^{ts}, a temperature-sensitive allele of the *KHP1* locus encoding the heterotrimeric kinesin-2 motor required for anterograde IFT (Walther et al. 1994; Kozminski et al. 1995). An *ida3; fla10-1*^{ts} double mutant was recovered from

non-parental tetrads and was used for cytoplasmic complementation in dikaryons. The design of the experiment and potential outcomes are illustrated in Fig. 3.5.

I analyzed *fla10-1^{ts}* x *ida3; fla10-1^{ts}* dikaryons at permissive (21°C) and restrictive (32°C) temperatures for rescue of axonemal I1 dynein assembly from the distal tip. Dikaryons were fixed at two time-points post-mixing for immunofluorescence with the IC140 antibody. As described before (Piperno et al. 1996; Pan and Snell 2002), the number of zygotes formed at restrictive temperature (32°C) was reduced. At restrictive temperature, IFT is inactivated and cilia begin to resorb. Since cilia are required to initiate the mating process, resorption of cilia at restrictive temperature may result in the reduction in mating and zygote formation. However, sufficient numbers of *fla10-1^{ts}* x *ida3; fla10-1^{ts}* dikaryons were formed for analysis. At permissive temperature (21°C), I1 dynein assembly was observed at the distal tip of *ida3; fla10-1* mutant cilia in the dikaryon (Fig. 3.6A, arrows) and progressed towards the proximal end of the axoneme (Fig. 3.6B, blue line). Complete rescue of I1 assembly along the length of *ida3; fla10-1^{ts}* cilia was seen within 90 minutes. In contrast, at restrictive temperature (32°C) rescue of I1 assembly did not occur in the *ida3; fla10-1^{ts}* mutant cilia (Fig. 3.6A, dashed circles; Fig. 3.6B, red line). This result provides strong evidence that I1 dynein transport to the distal tip of the cilium requires functional kinesin-2 and IFT.

To control for secondary effects of temperature variation on dikaryon rescue, *fla10-1^{ts}* x *ida3* and wild-type x *ida3* dikaryons were also analyzed by immunofluorescence for rescued I1 dynein assembly at permissive and restrictive temperatures. Similar to the dikaryons observed in Fig. 3.3 and as expected, I observed rescue of I1 dynein in the dikaryons formed between *fla10-1^{ts}* x *ida3* and WT x *ida3* at both temperatures. Rescue

of I1 dynein assembly occurred at comparable rates from tip to base, indicating that increase in temperature had no effect on the function of the wild type proteins, FLA10 and IDA3 (Fig. 3.6B). As an additional essential control, *ida3* x *ida3; fla10-1^{ts}* dikaryons (lacking IDA3) were analyzed. I predicted that in this combination of control dikaryons, rescue of I1 dynein assembly will not occur at either temperature. Consistent with this prediction, *ida3* x *ida3; fla10-1^{ts}* dikaryons do not rescue I1 dynein assembly in any of the four ciliary axonemes at either temperature (Fig. 3.6B, black dashed lines). Together, these results indicate that that kinesin-2/IFT is required for I1 dynein transport to the distal tip of the axonemes.

Discussion

The main objectives of the experiments presented in this chapter were to determine the site of incorporation of the 20S I1 dynein in the ciliary axoneme and to test the hypothesis that I1 dynein is transported in the cilium by IFT. In order to achieve these goals, I took advantage of the zygote or the dikaryon stage in the *Chlamydomonas* life cycle with the idea that assembly in a fully established axoneme is representative of the transport and distal assembly of axonemal precursors in a growing cilium. I determined that I1 dynein transport to the tip can be rescued in a dikaryon. I present evidence showing that I1 dynein is transported to the distal tip before incorporated in the mutant axoneme. I also show that I1 dynein transport to the distal tip is dependent on IFT, and that rescue of I1 dynein assembly requires IDA3.

I1 dynein is transported to the distal tip by IFT

Cilia assemble by addition of tubulin and protein complexes at the distal end of the growing axoneme (Witman 1975; Johnson and Rosenbaum 1992). Analysis of rescued assembly of I1 dynein in the cilia of *Chlamydomonas* quadraflagellate dikaryons has been a powerful approach demonstrating many proteins are transported to the distal tip of the cilium for incorporation in the axoneme (Johnson and Rosenbaum 1992; Piperno et al. 1996; Bower et al. 2013; Wren et al. 2013); reviewed in (Dutcher 2014). Consistently, analysis of dikaryons, generated using I1 dynein assembly mutants such as *ida1*, *ida3* or *ida7*, revealed that the I1 dynein complex is transported to the ciliary distal tip before incorporation in the axoneme (Fig. 3.3). Furthermore, quantification of assembly as a function of time demonstrated that assembly begins at the distal axoneme and then proceeds progressively toward the proximal axoneme until rescue is complete (Fig. 3.3C). With the exception of one dikaryon combination, *ida3* x *ida7*, which displayed a delayed rescue of I1 dynein assembly, the relative rate of tip to base rescue was uniform across several different dikaryon combinations (Fig. 3.3C, wild-type x *ida3*; wild-type x *ida7*; *ida1* x *ida3*). Furthermore, the rate of rescue of I1 dynein was synchronous for both cilia in dikaryons made from complementary I1 dynein assembly mutants (e.g. *ida1* x *ida3; ida1* x *ida7*). This result indicated that there is no difference in the rate of rescue of I1 dynein assembly between the *ida* mutants (in complementing dikaryon combinations such as *ida1* x *ida7* or *ida3* x *ida7*), suggesting that the mechanism of rescued assembly is the same in each of the *ida* mutants.

My data also resolved a delay in rescue in I1 dynein assembly in the *ida3* x *ida7* dikaryons (Fig. 3.5B, red boxes). I determined that the delay in I1 dynein assembly in the axonemes from the *ida3* x *ida7* dikaryon combination is due to a requirement of new

protein synthesis (Fig. 3.5). In contrast, in the time course examined, new protein synthesis was not required for I1 dynein assembly in axonemes from the *ida3* x *ida1* dikaryon (Fig. 3.4B). Therefore, the delay in rescue appeared to be unique to the *ida3* x *ida7* dikaryon combination. One interpretation of these results is that IC140, the gene product of *IDA7*, and the IDA3 protein form a complex, and that this interaction cannot be complemented in the *ida3* x *ida7* dikaryon without new protein synthesis. I have illustrated one model to explain this result in Fig. 3.5. In this model, I propose that the stability of IDA3 depends on the presence of IC140 in the cytoplasm. This idea is consistent with a hypothesis that IDA3 interacts with IC140 as an adapter required for I1 dynein transport into the ciliary compartment (Fig. 1.9). However, to test these ideas, the identification and characterization of IDA3 is necessary and is the highest priority in the Sale lab (see Chapter 4).

Upon entry into the cilium, the 20S I1 dynein is transported to the ciliary tip by IFT. This conclusion is based on the failure of rescue of I1 dynein assembly upon inactivation of the IFT anterograde motor kinesin-2 at restrictive temperature (see Methods and (Kozminski et al. 1995; Piperno et al. 1996). Additionally, failure of I1 dynein rescue in the *ida3* and *ida3; fla10-1* dikaryons (Fig. 3.7) revealed that a functional copy of IDA3 is essential for I1 assembly in the axoneme. Once I1 is unloaded from the transport complex, I postulate that I1 dynein may diffuse towards the base (dashed arrow, Fig. 1.9), in a manner similar to DRC4, before incorporation into the axoneme at unoccupied I1 dynein docking sites (Wren et al. 2013). This result also indicates that the majority of the I1 dynein complex remains associated with IFT until reaching the distal tip where unloading of cargo presumably occurs. This interpretation is consistent with

the live cell imaging study of Wren et al., (Wren et al. 2013) in which the majority of the N-DRC is transported as a cargo to the distal tip of the axoneme prior to release and diffusion towards the base for incorporation in the axoneme. However, diffusion of I1 dynein, prior to docking in the axoneme, cannot be assessed by the assays I employed in this paper. Live cell imaging will be required for further tests of how I1 dynein enters the ciliary compartment and to determine the sites of loading, rate of assembly and diffusion after unloading from IFT. In Chapter 4, I have elaborated on progress using live cell imaging to observe IFT-dependent movement of GFP-tagged I1 dynein.

Figures for Chapter 3

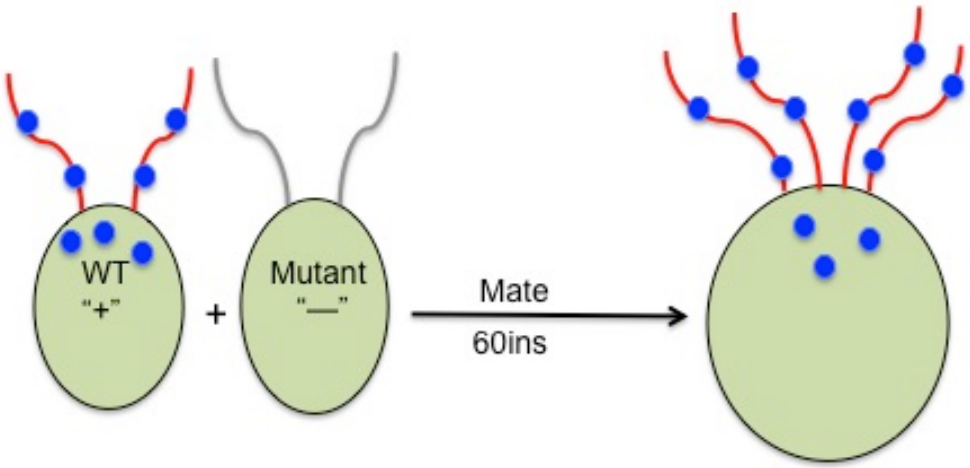
WT
"+"
+
Mutant
"—"
Mate
60ins

Figure 3.1. During dikaryon rescue, cytoplasmic complementation can lead to the rescue of the mutant phenotype. A dikaryon resulting from the fusion of the WT and mutant cell has a shared cytoplasm and four flagella, each of which is derived from the parental cells. The quadraflagellate dikaryon stage lasts for ~2.5hours before the cilia are resorbed and meiosis proceeds. Axonemal precursor components (blue spheres) from WT cytoplasm can enter the mutant ciliary compartment, resulting in the rescue of the mutant phenotype (structure and function). I used dikaryon to test whether I1 dynein could be restored by mating WT and mutant cells defective in I1 dynein (e.g. *ida1*, *ida2*, *ida3*, *ida7* and *bop5-3*). I have illustrated the potential outcomes of this experiment in Figure 3.2.

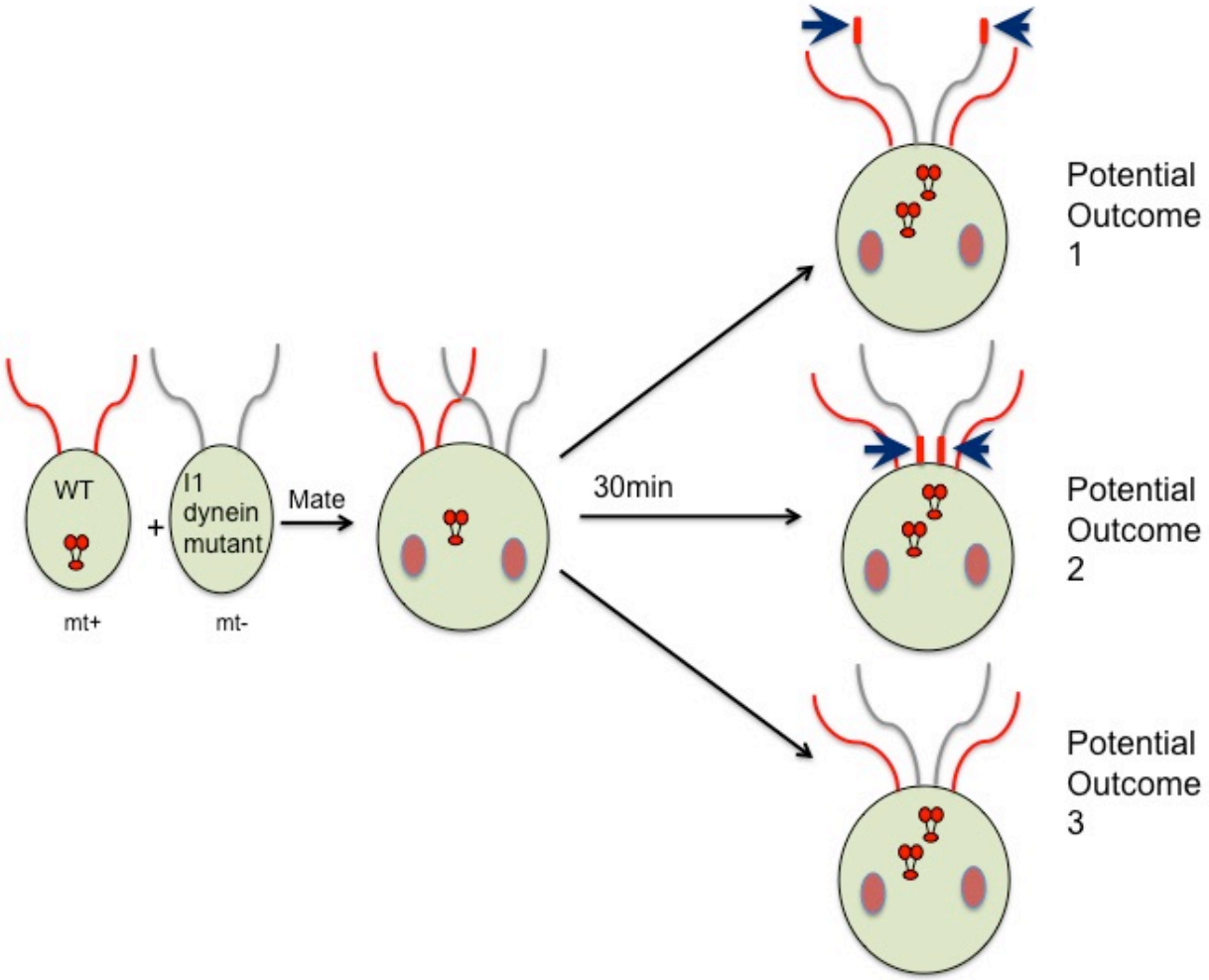
WT
+
I1
dynein
mutant
Mate
mt+
mt-
30min
Potential
Outcome
1
Potential
Outcome
2
Potential
Outcome
3

Figure 3.2. Complementation of cytoplasmic I1 dynein precursors in dikaryons generated between WT and I1 dynein mutants. At the start of these studies, I envisioned three possible outcomes of rescue of I1 dynein assembly in dikaryons formed between WT and I1 dynein mutant cells. The first potential outcome in which I1 dynein assembly begins at the distal tip of the mutant cilium. This was the expected outcome since cilia grow by addition of subunits at the distal end. The second potential outcome was that I1 dynein begins to incorporate in the axoneme at the proximal end immediately after entry into the ciliary compartment. Lastly, it was possible that cytoplasmic complementation in the dikaryon will not result in the rescue of I1 dynein assembly in the mutant cilium. Such cases have been reported, and in these cases, ciliary regeneration in the dikaryon is required for rescue to occur (Dutcher 2014). The data from this experiment is presented in Figure 3.3.

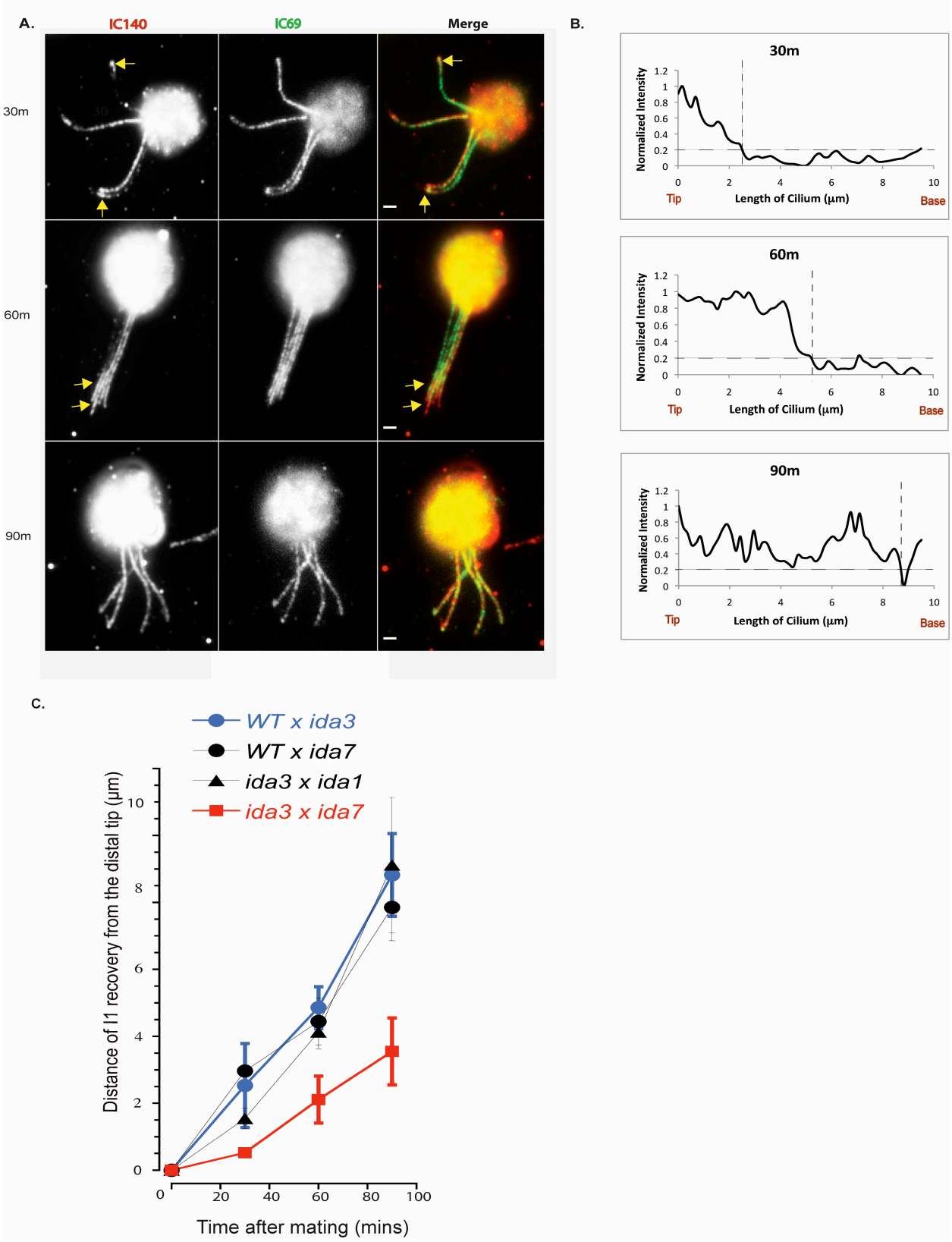
A.
IC140
IC69
Merge
30m
60m
90m
B.
30m
60m
90m
Normalized Intensity
Tip
Length of Cilium (µm)
Base
C.
WT x ida3
WT x ida7
ida3 x ida1
ida3 x ida7
Distance of I1 recovery from the distal tip (µm)
Time after mating (mins)

Figure 3.3. Dikaryon rescue of I1 dynein assembly occurs from the distal tip.

(A) Immunofluorescence of IC140 in *ida7* x wild-type (WT) dikaryons. Cytoplasmic complementation in WT and I1-deficient dikaryons results in the rescue of I1 dynein assembly (arrows) and rescue began from the distal tip and then proceeded towards the base in the *ida7* mutant cilia. Scale bar = 2μm. **(B)** Quantification of I1 dynein staining along the cilia of I1 mutants at various time points post mating. Normalized fluorescence intensity is plotted against the distance of rescue from the tip for one rescuing mutant cilium of the WT x *ida7* dikaryon shown in part A (See Methods, Appendix I). The length of I1 assembly at the ciliary tip (vertical dotted line) increased progressively over time: 2.5 μm at 30m, 5.25 μm at 60m, and 8.75 μm at 90m. **(C)** Comparison of dikaryon rescue rates of I1 assembly in various mutant combinations. The length of IC140 staining at the distal end of the cilium is plotted versus time. WT x *ida3* (blue circles, n = 83) and WT x *ida7* (black circles, n = 29) dikaryons demonstrate progressive rescue of axonemal I1 dynein assembly with complete recovery at 90m. Dikaryons between *ida3* and *ida1* show this same pattern of rescue along all four cilia (black triangles, n = 59). However, rescue of axonemal I1 dynein assembly is delayed in *ida3* x *ida7* dikaryons (red squares, n = 30), but occurs from the distal tip like other dikaryon combinations. Thus, the delay in rescue only occurred in a single combination of I1 dynein mutants.

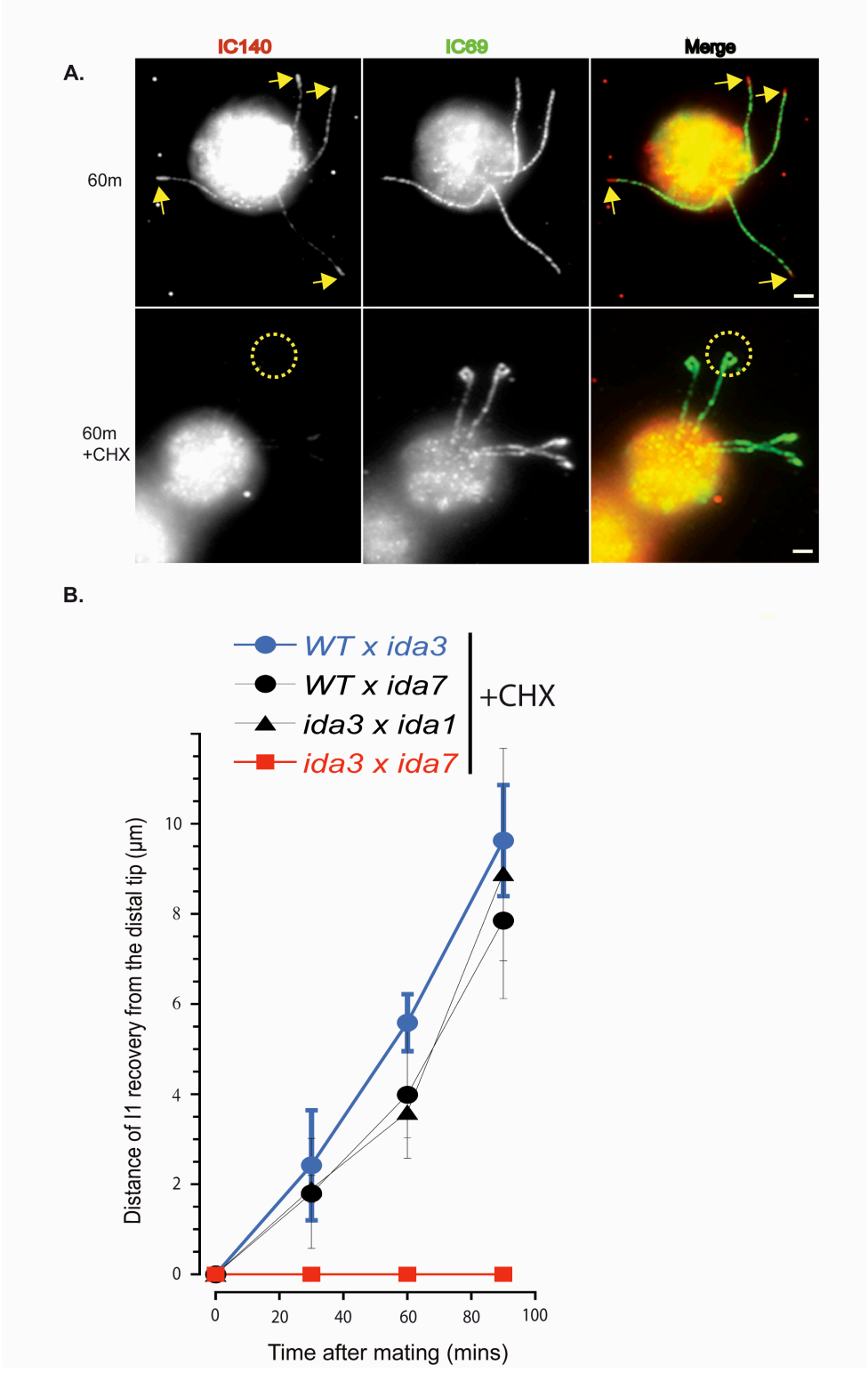
A.
IC140
IC69
Merge
60m
60m
+CHX
B.
WT x ida3
WT x ida7
ida3 x ida1
ida3 x ida7
+CHX
Distance of I1 recovery from the distal tip (µm)
0
2
4
6
8
10
0
20
40
60
80
100
Time after mating (mins)

Figure 3.4. Dikaryon rescue of axonemal I1 assembly requires protein synthesis of IC140 and/or IDA3. I tested the hypothesis that delay in I1 dynein rescue in the *ida3* x *ida7* dikaryons was due to a requirement for new protein synthesis. **(A)** Immunofluorescence of IC140 in *ida3* x *ida7* dikaryons 60 minutes after mixing gametes. Rescue of axonemal I1 dynein assembly is seen at the distal end as in Figure 3.3A (arrows, top panel). In contrast, in the presence of the protein synthesis inhibitor, cyclohexamide (CHX), the recovery of I1 dynein is not seen in the cilia (dotted circle, bottom panel). Scale bar = 2μm. **(B)** Quantification of IC140 staining from the distal tip of I1-deficient cilia as in Fig. 3.3B in the presence of CHX. Axonemal I1 dynein assembly occurs progressively from the distal tip to base in WT x *ida3* (blue circles, n = 25), wild-type x *ida7* (black circles, n = 25) and *ida3* x *ida1* (black triangles, n = 22) dikaryons. In contrast, I1 dynein is not assembled on the axoneme in *ida3* x *ida7* dikaryons (red squares, n = 29).

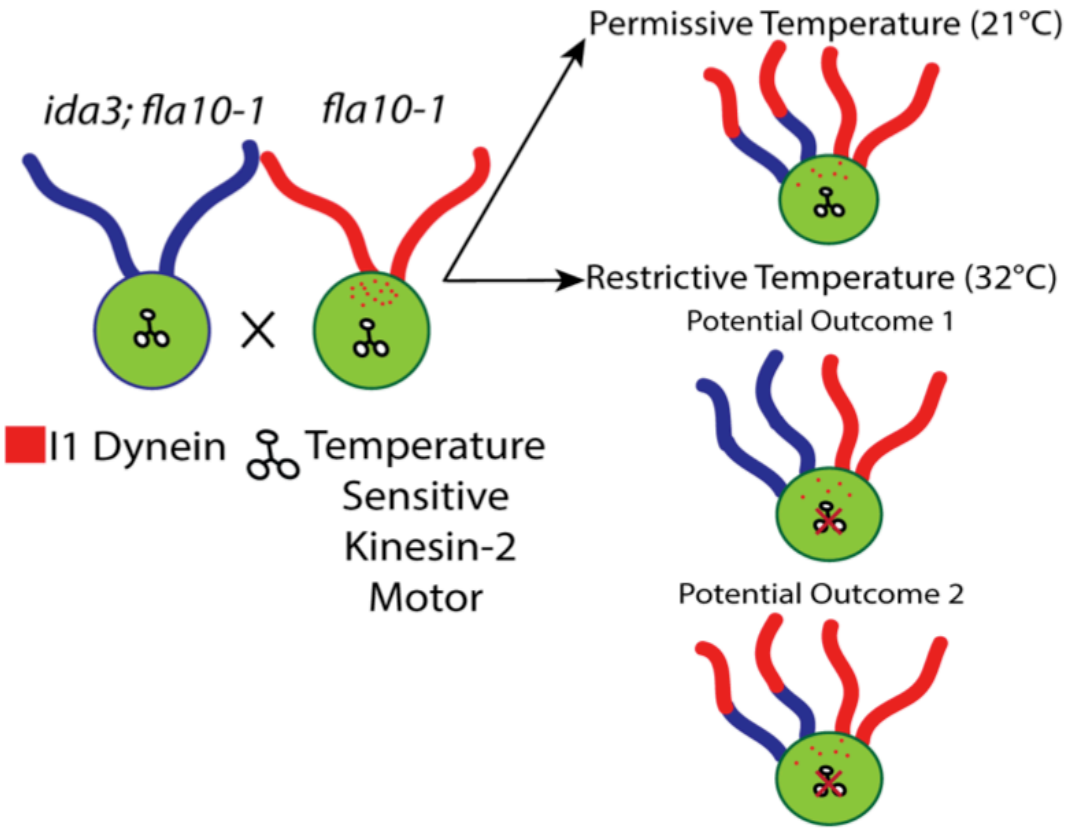
Permissive Temperature (21°C)
ida3; fla10-1
fla10-1
Restrictive Temperature (32°C)
Potential Outcome 1
I1 Dynein
Temperature Sensitive Kinesin-2 Motor
Potential Outcome 2

Figure 3.5. Design of dikaryon rescue experiments to examine whether IFT is required for I1 dynein assembly using the temperature sensitive mutant, *fla10-1^{ts}*. Since I1 dynein is transported to the distal cilium before assembly in the axoneme, I tested the hypothesis that IFT is required for transport of I1 dynein. The details of the time and temperature controls are described in the Methods. Critical features of this experiment included recovery of the double mutant, *ida3*; *fla10-1* (from a non-parental tetrad), exact regulation of temperature and timing of the temperature shift to maximize mating efficiency for dikaryon formation. Predicted outcomes at permissive and restrictive temperatures are illustrated. In *ida3*; *fla10-1 ^{ts}* x *fla10-1 ^{ts}* dikaryons generated at permissive temperature (21ºC), the kinesin-2 motor is functional and assembly of I1 dynein is predicted to occur at the distal tip of the *ida3*; *fla10-1 ^{ts}* mutant axoneme. In contrast, at the restrictive temperature (32ºC), the lack of functional kinesin-2 will block the rescue of I1 dynein assembly in the mutant cilia (Potential Outcome 1). This outcome would be consistent with my hypothesis that I1 dynein (red dots) is transported to the distal tip by IFT/kinesin-2 before docking in the axoneme. However, if rescue of I1 dynein assembly is observed at the restrictive temperature (Potential Outcome 2), then this result would support an alternate hypothesis that I1 dynein transport to the tip is independent of IFT/kinesin-2. The actual data from this experiment is presented in Fig. 3.6.

A.

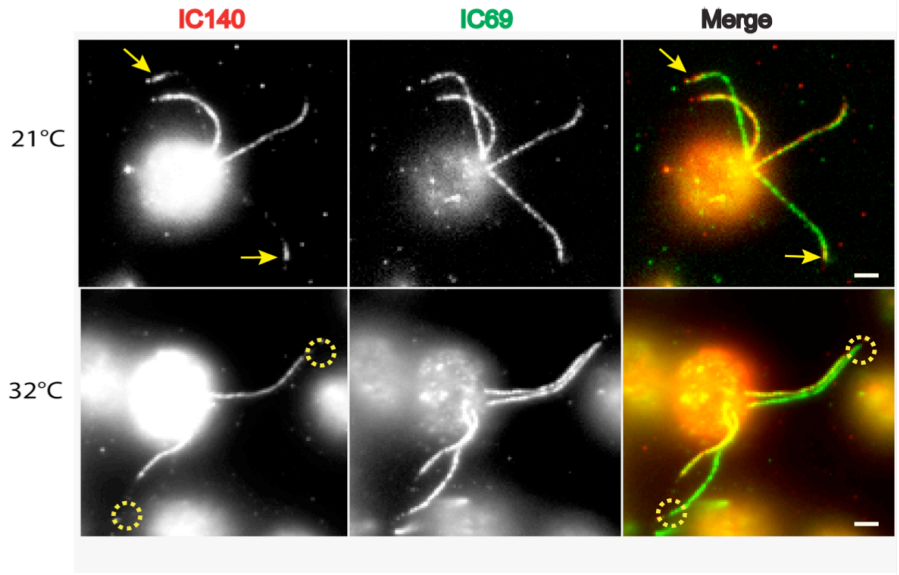
IC140
IC69
Merge
21°C
32°C

B.

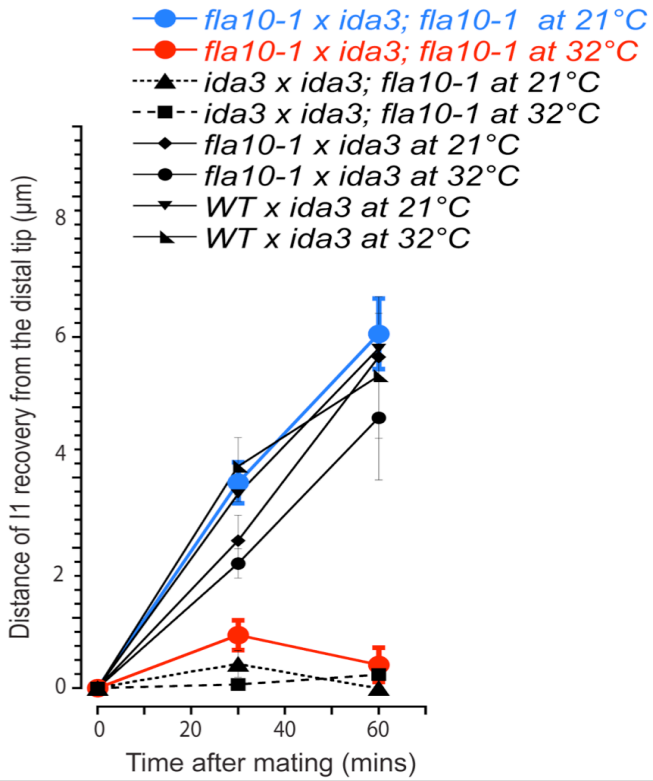
fla10-1 x ida3; fla10-1 at 21°C
fla10-1 x ida3; fla10-1 at 32°C
ida3 x ida3; fla10-1 at 21°C
ida3 x ida3; fla10-1 at 32°C
fla10-1 x ida3 at 21°C
fla10-1 x ida3 at 32°C
WT x ida3 at 21°C
WT x ida3 at 32°C
Distance of I1 recovery from the distal tip (µm)
0
2
4
6
8
0
20
40
60
Time after mating (mins)

Figure 3.6. I1 Transport of I1 to the tip of the cilium requires kinesin-2.

(A) Immunofluorescence of IC140 in *fla10-1* x *ida3; fla10-1* dikaryons 60 minutes after mixing gametes. At the permissive temperature (21°C), recovery of axonemal I1 dynein assembly occurs from the distal end of *ida3* cilia (arrows). At the restrictive temperature (32°C), I1 dynein assembly on the axoneme is not seen in *ida3; fla10-1* cilia (dotted circles). Scale bar = 2μm. **(B)** Quantification of IC140 staining at the distal end of I1-deficient cilia at permissive (21°C) and restrictive (32°C) temperatures. Axonemal I1 dynein assembly occurs progressively from the distal tip to base in wild-type x *ida3* (n = 19) and *fla10-1* x *ida3* (black diamonds and black circles, n = 39) dikaryons at both permissive and restrictive temperatures. While I1 assembly at the distal tip is seen at the permissive temperature in *fla10-1* x *ida3; fla10-1* dikaryons (blue circles, n = 52), I1 assembly at the tip does not occur at restrictive temperature (red circles, n = 19). As a control, *ida3*; *fla10-1* x *ida3* dikaryons were tested for a lack of I1 axonemal assembly at both temperatures (black dotted triangles and squares, n = 46). These data support a model in which I1 dynein is transported as a cargo, by IFT to the distal end of the cilium for docking in the axoneme.

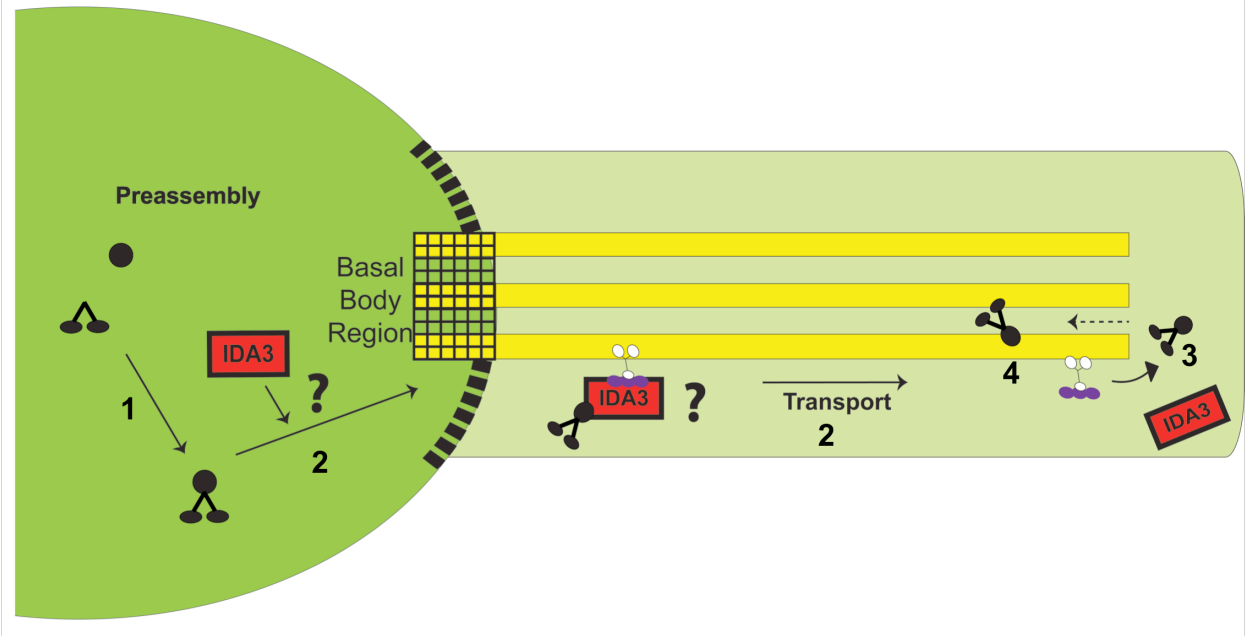
Preassembly
Basal
Body
Region
IDA3
1
?
2
IDA3
?
Transport
2
4
3
IDA3

Figure 3.7. Hypothetical steps leading to I1 dynein assembly in the axoneme. Based on the evidence presented in my dissertation, I1 dynein assembly in the axoneme appears to occur in a stepwise manner: (**1**) preassembly in the cytoplasm; (**2**) transport to the distal tip of the cilium in an IDA3 and IFT-dependent manner; (**3**) unloading from IFT at the tip and (**4**) docking in the axoneme. In the *ida3* mutant, I1 dynein fails to enter the ciliary compartment. I also indicate that IDA3 is an adapter required for I1 dynein entry and transport by IFT. As discussed in Chapter 4, the exact function of IDA3 is not known. The postulated barrier between the cytoplasm and the ciliary compartment is shown as black boxes.

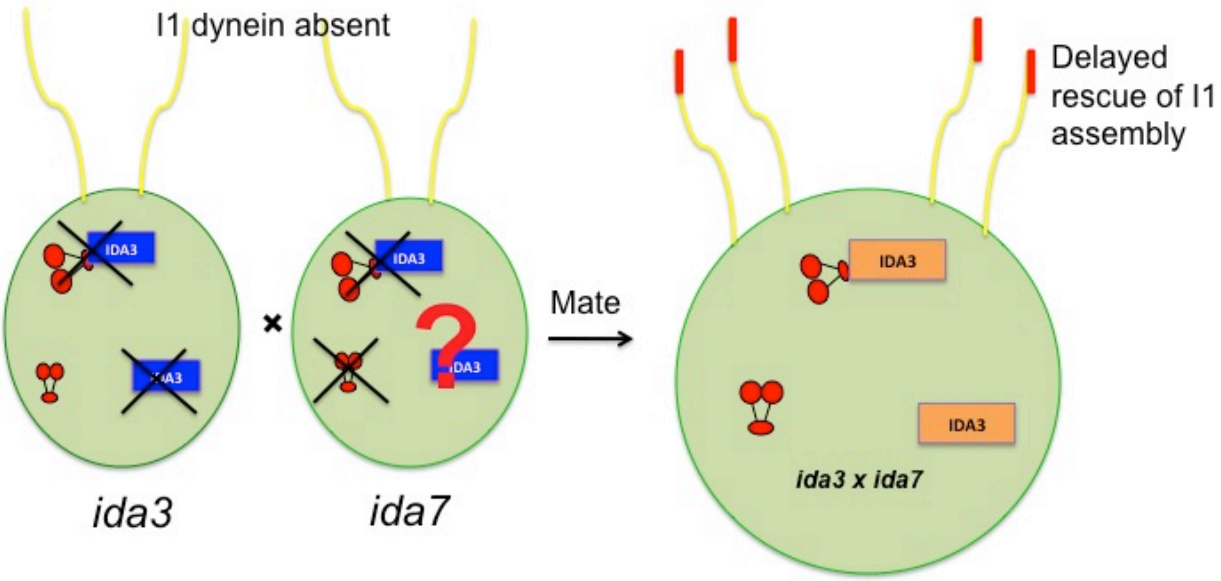
I1 dynein absent
IDA3
IDA3
IDA3
?
ida3
ida7
Mate
Delayed rescue of I1 assembly
IDA3
IDA3
ida3 x ida7

Figure 3.8. One model to explain the delayed rescue of I1 dynein assembly in *ida3* x *ida7* dikaryons. Since protein synthesis is required for rescue of I1 dynein in the *ida3* x *ida7* dikaryons, one hypothesis is that either of both gene products, IDA3 and IC140 (IDA7) must be synthesized before I1 dynein can be assembled. One possibility is that IC140 is required for the stability of IDA3. Thus, in the IC140-null mutant, *ida7*, the wild-type copy of IDA3 is unstable and degraded in the absence of IC140/I1 dynein complex. When the *ida3* x *ida7* dikaryon forms, the rescue of I1 dynein assembly in the mutant cilia fails to occur unless new copies of IDA3 (orange) are synthesized. The time required for new protein synthesis can justify the delay in rescue of I1 dynein assembly in the *ida3* x *ida7* dikaryon. In the presence of a protein synthesis inhibitor such as cycloheximide, since no new copies IDA3 can be produced, rescue of I1 dynein assembly in the cilia is blocked.

Chapter 4: Conclusions and new questions

Introduction

Studies using motility mutants in *Chlamydomonas,* along with biochemical and structural approaches, have revealed that the axoneme bears at least eight different types of dyneins that are distinct in composition and function (Kamiya and Yagi 2014). The axonemal dyneins are organized into the outer dynein arms and inner dynein arms (Porter and Sale 2000; Gokhale et al. 2009; King and Kamiya 2009). Each dynein is targeted to a specific position in the axoneme and contributes uniquely to the generation and control of ciliary motility (Kamiya and Yagi 2014). Despite the advances in understanding the structural organization and function of these dyneins, we know little about the molecular mechanisms by which dyneins and other large axonemal complexes are assembled, targeted and docked in the ciliary axoneme. Mutations in genes that encode dynein subunits, or components required for the assembly, transport or docking of the axonemal dyneins, result in a wide range of developmental defects and ciliopathies that are generally referred to as primary ciliary dyskinesia (PCD). In most cases, PCD results in defective assembly of axonemal dyneins (Zariwala et al. 2007; Horani et al. 2014). Thus, the major questions that motivated my dissertation work on axonemal dynein assembly included where are the dyneins assembled, how are the dyneins transported to and within the ciliary compartment and what is the mechanism by which the dyneins are docked in the axoneme.

In an attempt to answer these questions, I selected I1 dynein as a model (Fig. 1.5). I1 dynein was selected, in part, because the complex can be isolated, the genes encoding the structural proteins are known and informative mutants in *Chlamydomonas reinhardtii* that fail to assemble I1 dynein are available (Table 3*)*. As described in Chapters 2 and 3

of this dissertation, my work has made key contributions to the understanding I1 dynein assembly. Using a variety of biochemical approaches, I demonstrated that I1 dynein is assembled as a 20S precursor complex in the cytoplasm prior to transport to the ciliary compartment. This result provided the foundation for further questions. One major question I have not yet directly addressed is how a large complex such as I1 dynein can enter the ciliary compartment. Presumably, the process of entry requires IFT, but tests of this idea will require new studies using live cell imaging (see below and (Wren et al. 2013)).

Upon entry into the ciliary compartment, I1 dynein is transported to the distal tip of the cilium by IFT before docking to the axoneme. These conclusions are based on the study of dikaryon rescue in quadraflagellate zygote and the use of a conditional mutant in kinesin-2, called *fla10-1*. I determined that the IFT-dependent transport of I1 dynein to the cilium requires IDA3. In the novel I1 dynein mutant, *ida3*, the 20S I1 dynein is assembled in the cytoplasm and is similar in composition to the axonemal I1 dynein, but does not appear to enter the cilium. One potential explanation for this observation is that IDA3 is an adapter protein, analogous to ODA16, a predicted adapter protein that is required for ODA transport (Ahmed and Mitchell 2005; Ahmed et al. 2008). IDA3 may facilitate an interaction between the preassembled I1 dynein and IFT for transport in the ciliary compartment. While alternate hypotheses for the role of IDA3 exist, as a working model, I currently favor the idea that IDA3 is an adapter that mediates an interaction between the I1 dynein complex and the IFT. Based on this one hypothesis, the discovery of *IDA3* may define a new family of genes that are conserved and encode proteins

responsible for mediating an interaction and between specific cargos, such as I1 dynein, and IFT.

Several new questions arise from my dissertation work. What is the function of IDA3? Does IDA3 interact with the IC140 subunit of I1 dynein? Does the localization of IDA3 change during ciliogenesis or in a dikaryon during the rescue process? Does IDA3 interact with any of the IFT components? Members of the Sale lab are pursuing these questions. They have now successfully cloned *IDA3*, and confirmed the gene by transformation rescue of *ida3* mutant. As a first test, lab members are in the process of generating a rescue strain expressing an epitope-tagged IDA3 for localization and protein interaction studies. The lab is also in the process of generating an antibody to IDA3. With these tools, IDA3 can be localized and interacting proteins (e.g. IC140 or IFT proteins) can be identified.

I have also made progress on the construction of GFP-tagged I1 dynein for examination of IFT-dependent transport by live-cell imaging. Although my progress on live cell imaging was limited, continued focus on live cell imaging of I1 dynein transport may address the questions of how this large dynein complex enters the cilium. Live cell imaging may also reveal how I1 dynein is unloaded from IFT at the distal tip of the cilium, and reveal subsequent diffusion of I1 dynein until docking occurs in the axoneme. The final step in assembly of I1 dynein is docking in the axoneme. Although I did not directly address the questions of targeting and docking of I1 dynein, with discovery that CCDC39/CCDC40 (PF7/FAP172 and PF8/FAP59 in *Chlamydomonas*) complex that forms the 96 nm axonemal “ruler” (Oda et al. 2014a), it is possible to test the hypothesis

that the FAP172/FAP59 complex is also responsible for I1 dynein localization and docking within the axoneme.

What have I learned from the study of the *ida3* mutant?

The *ida3* mutant was originally discovered by Kamiya et al. in a screen to isolate mutants defective in the inner dynein arms (Kamiya 1991; Kamiya et al. 1991). This important screen involved mutagenesis of cells lacking the ODA and recovery of new mutants that: (1) lack cilia (bald mutant), (2) bear paralyzed cilia or (3) swim more slowly than ODA cells. Following backcross to restore the ODA, the cells were further examined for slow swimming revealing among other mutations, *ida3*. Compared to WT, *ida3* has a reduced swimming velocity with defective ciliary waveform, similar to other *ida* mutants (Fig. 4.1 and (Brokaw and Kamiya 1987; Bayly et al. 2010; Elam et al. 2011). In addition, like other I1 dynein mutants, *ida3* cells fail to perform phototaxis (Elam et al. 2009; Elam et al. 2011). The failure in phototaxis is due to defective regulation of ciliary waveform and control of the direction of swimming. Failure in phototaxis has also been used to successfully screen for mutants defective in I1 dynein (King and Dutcher 1997; Okita et al. 2005). The *ida3* mutant lacks I1 dynein in the axoneme, but the genetic defect does not reside in any known I1 dynein structural genes (Kamiya et al. 1991); Fig. 4.1B and C). However, it is critical to note that *ida3* cells bear full-length cilia and with the exception of I1 dynein, the *ida3* axonemes are fully assembled including assembly of all other dyneins, radial spokes, N-DRC and central pair structures. Thus, the *ida3* mutant appears to have a mutation that specifically affects I1 dynein assembly. Based on these observations, I reasoned that the defect in the *ida3* mutant lies in a gene required for cytoplasmic assembly of I1 dynein, transport of I1

dynein by IFT, or for docking I1 dynein in the axoneme. In Chapter 2, using biochemical approaches, I presented evidence likely eliminating IDA3's role in precursor assembly and docking (Figs. 2.2 and 2.6). Like WT, the *ida3* mutant assembles the 20S I1 dynein complex in the cytoplasm indicating that that *ida3* is not defective in a assembly factor. However, at this stage we cannot rule out that the 20S I1 dynein complex in *ida3* is missing a small subunit. In addition, data from *in vitro* reconstitution experiments demonstrated that I1 dynein, derived from axonemes, bind *ida3* axonemes in a manner similar to other I1 dynein mutant axonemes (e.g. *ida1* and *ida7*). This result indicated that *IDA3* is not an axonemal I1 dynein-docking factor. Therefore, the defect in *ida3* most likely resides in the transport of I1 dynein from the cytoplasm to and/or within the ciliary compartment. Consistent with this hypothesis, compared to WT, the membrane-matrix fraction of *ida3* lacked I1 dynein. This result demonstrated that *ida3* may be defective in the entry of I1 dynein to the ciliary compartment. To test this idea more directly, it is necessary to identify *IDA3* and characterize IDA3.

Mapping by the Kamiya lab (University of Tokyo) revealed that *IDA3* is located close to the centromere on chromosome 3 (Fig. 4.3). IDA3 was independently mapped to the same region of chromosome 3 by the Dutcher lab (Wash University, St. Louis). This region is ~300,000 bp in size and contains a number of predicted genes that could correspond to *IDA3*. Due to close proximity to the centromere, the candidate region in Chromosome 3 was not accurately assembled in recent genomic maps. Thus, identification of the mutation in *ida3* by whole genome sequencing had proved to be challenging. My approach for identifying *IDA3* was to use transformation-rescue of *ida3* using overlapping BAC clones that were predicted to span the mapped region predicted

to contain the *IDA3* gene (Fig. 4.3). Thus, the strategy was to identify the *IDA3* gene by transforming the *ida3* mutant with BAC clones with the goal of rescuing motility and I1 dynein assembly in the *ida3* mutant cells.

To facilitate screening of rescued (i.e. swimming) cells, I used a paralyzed double mutant, *ida3;oda1*, that was isolated in a non-parental tetrad from a cross between *ida3* and *oda1*. The idea was that successful DNA-mediated transformation would restore swimming to the double mutant. For example, if BAC16C10 contains the *IDA3* gene, the paralyzed *ida3;oda1* mutant that had been transformed successfully would display an *oda1* swimming phenotype. Rescued clones (i.e. swimmers) would then be assessed for I1 dynein assembly by immunoblots of isolated axonemes. Sub-cloning and transformation-rescue could then identify the *IDA3* gene. However, I was not successful in using the BACs that map to the *IDA3* locus for transformation and rescue of the *ida3* mutant. My method of transformation was not a problem since positive controls for transformation-rescue of a paralyzed radial spoke deficient mutant, *pf14* with the *RSP3* gene was successful.

While the BAC transformations were underway, the assembly of the genome was improved based on additional sequencing and specialized algorithms for sequence assembly (http://genome.jgi-psf.org/chlamy/chlamy.home.html). Thus, the release of the newer version of the genome database permitted a more accurate assignment of *ida3* candidate region. Consequently, Dr. Susan Dutcher (Washington University, St. Louis) used whole genome sequencing to successfully identify the mutation in *ida3*. The mutation has since been confirmed in the Sale laboratory, and analysis of IDA3 has become the focus of the lab. This is a major advance for the Sale laboratory since we can

now potentially define the role of IDA3 in I1 dynein assembly. Lab members have confirmed that I1 dynein is fully assembled in the rescued *ida3;oda1* cells. In addition, discovery of *IDA3* revealed why I was unsuccessful with my BAC transformation strategy. Due to the inaccurate assembly of the genome in chromosome 3, the BACs used in my earlier study were mapped to regions that did not contain *IDA3*.

Despite my not knowing the *IDA3* gene, the *ida3* mutant has proven to be informative in revealing important aspects of I1 dynein assembly. For instance, the presence of the 20S I1 dynein in the cytoplasm, but the absence of I1 dynein in the membrane-matrix strongly indicated that I1 dynein requires the gene product of *IDA3* for entry to the cilium (Fig. 2.7, Chapter 2). Furthermore, in control dikaryons formed between *ida3* and *ida3;fla10-1*, I did not observe rescue of I1 dynein assembly in the cilia (Fig. 3.6, Chapter 3). Thus, the lack of rescue of I1 dynein assembly in the control dikaryon (formed between *ida3* x *ida3;fla10-1*) further indicated that IDA3 is required for entry and transport of I1 dynein. The simplest hypothesis at this time is that IDA3 functions as an adapter to specifically link I1 dynein to IFT (Fig. 3.7, Chapter 3). The formation of the I1 dynein-IDA3-IFT complex would therefore be a prerequisite for entry and transport within the cilium. Consistent with IDA3 being an adapter, I presented indirect evidence that IDA3 may physically interact with the IC140 subunit of I1 dynein. With the discovery of the gene and successful transformation with the HA-tagged IDA3, further biochemical analysis can now test the idea that IDA3 and IC140 interact. As an additional benefit, these biochemical studies may reveal protein-protein interactions between I1-dynein subunits as well as with non-dynein proteins; possibly including IFT

subunits. Predictably, *IDA3* as well as additional genes discovered by these studies will be conserved, and thus when defective in the human, will result in PCD.

Live Cell Imaging of I1 dynein transport using TIRF-M

The main goal of the experiments described in this final section is to directly test and visualize IFT-dependent transport and diffusion of I1 dynein. One approach is to image fluorescently tagged I1 dynein in live cells using Total Internal Reflection Fluorescence Microscopy (TIRF-M) (Engel et al. 2009a; Engel et al. 2009b; Lechtreck et al. 2009; Lechtreck 2013; Wren et al. 2013). For example, Wren et al. used live-cell imaging to demonstrate that the N-DRC is a bona fide cargo of IFT. This work was founded upon the demonstration that the N-DRC assembly can be rescued in dikaryons formed between WT and N-DRC mutants and that N-DRC mutants can be rescued by DRC4-GFP (Bower et al. 2013). Subsequently, Wren et al. (Wren et al. 2013) showed that the entry of DRC4 into the ciliary compartment requires IFT. To my knowledge, this was the first evidence that that entry of axonemal precursors from the cytoplasm to the ciliary compartment is IFT dependent.

Another highlight of the Wren et al. (2013) study is that while the majority of DRC4 is transported to the distal tip of the cilium for unloading, a minor fraction of DRC4 unloads from IFT before reaching the distal tip (i.e. unloading from IFT can occur while in transit). After unloading, DRC4 appears to diffuse to the available axonemal N-DRC docking sites for incorporation in the axoneme or reloaded on IFT for further processive movement to the distal tip of the cilium. These are the first data that distinguish IFT dependent processive movement from diffusion of axonemal cargoes.

Thus, with the successful use of TIRF-M to examine DRC entry and transport, Wren et al. established the groundwork for live cell imaging of any tagged protein destined to the ciliary axoneme.

For live cell imaging of I1 dynein transport, two experimental strategies were designed that attempt to avoid background fluorescence signal from GFP-IC140 incorporated into the axoneme. The first approach was to examine the transport of I1 dynein in full-length cilia that have been photo bleached. The diffusion and/or transport of newly synthesized I1 dynein, presumably in an IFT-dependent manner, could then be directly examined without interference from axonemal fluorescence. As discussed below, the same approach can be used during ciliary regeneration. Studies have shown that there is an increased occurrence of IFT-dependent transport of ciliary cargoes during the regeneration process due to increased cargo loading (Avasthi and Marshall 2012; Engel et al. 2012; Ludington et al. 2013; Wren et al. 2013; Avasthi et al. 2014; Craft et al. 2015). A complementary approach is to examine the transport of I1 dynein during the rescue process in a dikaryon formed between cells expressing a GFP tagged IC140 and an I1 dynein mutant cell (illustrated Fig. 4.8). My prediction was that during the rescue process, I1 dynein transport would be revealed as a processive, IFT-dependent transport combined with unloading at the distal tip, diffusive movement and docking in the axoneme.

The first step was to generate a fluorophore-tagged I1 dynein construct. Amongst the I1 dynein subunits, I chose the IC140 subunit to tag with a fluorophore for several reasons. First, the Sale lab cloned *IC140* (*IDA7*) and characterized the protein (Yang and Sale 1998). Thus, the clone was immediately ready to work with. Second, an IC140-null

mutant, *ida7*, is available for transformation with genes encoding tagged IC140 (Perrone et al. 1998). Third, Perrone et al. (1998) determined that the N-terminal region of IC140 is not required for the assembly of I1 dynein in the axoneme. The C-terminal WD-repeat region of IC140 is necessary and sufficient for I1 dynein assembly in the axoneme. Therefore, it was logical to insert the GFP (or other tags) at or in the N-terminus of IC140 (illustrated in Fig. 4.4). I used a modified GFP containing a specific mutation to enhance folding and fluorescence. The "superfolded"-GFP (sfGFP) was codon optimized for expression in *Chlamydomonas* and the clone was obtained from Karl Lechtreck (UGA). Lechtreck is an expert in live cell imaging of *Chlamydomonas* cells using TIRF-M (Lechtreck et al. 2009; Lechtreck 2013) and has successfully imaged a number of ciliary proteins including BBS proteins, N-DRC and tubulin in live cells. The coding region of sfGFP was sub-cloned in frame into exon 1 of the *IC140* gene located within a 11.5kb genomic fragment (containing all the necessary upstream regulatory elements required for expression in *Chlamydomonas*) using a specific combination of unique restriction enzymes (Kpn1 and EcoR1).

The next step was to transform the *ida7* cells with the GFP-IC140 construct and recover a transformant expressing GFP-IC140 that rescued of I1 dynein assembly and function. To facilitate the screening of positive transformants, the *ida7* mutant was crossed to *oda6* to recover an *ida7*;*oda6* double mutant that is paralyzed. Double mutants successfully transformed and rescued by IC140-GFP would regain motility and display an *oda6* swimming phenotype. Transformation of the *ida7*;*oda6* double mutant cells with the IC140-GFP construct yielded four independent clonal isolates (B10-1, B10-2, B10-3, B10-4) that displayed the *oda* swimming phenotype. Further biochemical analysis of

axonemes isolated from these transformants demonstrated that I1 dynein was restored in the axonemes and the GFP-IC140 fusion protein was migrating at the expected size (Fig. 4.5).

As a complementary test, I examined the rescue of I1 dynein assembly in the axoneme by immunofluorescence by using antibodies to IC140 and to GFP (Fig. 4.6). Thus, the IC140-GFP rescued I1 dynein assembly and motility. The most relevant test was to examine in live cells whether in the *ida7;oda6*::IC140-GFP transformants, the axonemal IC140-GFP was detectable by TIRF-M. As shown in Fig. 4.7, the B10-4 transformant expressed the IC140-GFP fusion protein and was detectable by TIRF-M indicating that IC140-GFP was stably incorporated in the axoneme and visible in live cells. The question was whether I could also view I1 dynein transport or diffusion in the *ida7;oda6*::IC140-GFP cells.

As a positive control, I observed IFT in cells expressing kinesin-GFP (Fig. 4.7 and (Mueller et al. 2005)). Using this positive control, I was successful in using TIRF-M in both the Lechtreck (UGA) and Zheng (Cell Biology, Emory) labs to observe IFT in live cells. However, despite extensive work with Karl Lechtreck and the members of the Zheng lab, I was not successful in observing IC140-GFP transport or diffusion in the *ida7oda6*::IC140-GFP transformants. From my discussions with Karl Lechtreck, it was possible, that either too little IC140-GFP is targeted to the fully assembled cilia or that an insufficient amount of properly folded IC140-GFP was present in this particular transformant. To address these issues, one approach is to repeat the imaging in regenerating cilia due to the increased amount of IFT-mediated cargo transport (Wren et al. 2013). In order to perform this experiment, the *ida7oda6*::IC140-GFP cells will be de-

flagellated by pH shock (Alford et al. 2013) followed by photobleaching of the entire regenerating cilium to eliminate background signal from the incorporated, axoneme-bound I1 dynein. The prediction is that IC140-GFP transport (i.e. I1 dynein transport) or diffusion could then be visualized, since, predictably, a greater amount of IFT and cargo are moved into the ciliary compartment during ciliary regeneration (Wren et al. 2013; Craft et al., 2015).

As an alternate approach, a brighter flourophore may be required to visualize IC140 in live cells. From my discussions with Karl Lechtreck and Pinfen Yang (Marquette University), they advised the use of a new and improved yellow-green florescent protein tag called the mNeonGreen (Shaner et al. 2013). While the experiments involving ciliary regeneration are underway, a new IC140 construct tagged with mNeonGreen will be generated for transformation of the *ida7;oda6* cells. Based on the success that Karl Lechtreck and Pinfen Yang have had with imaging the mNeonGreen tagged proteins (e.g. EB1, tubulin), I predict that the IC140-mNeonGreen will yield brighter fluorescence during the course of imaging.

In addition to examining I1 dynein transport in regenerating flagella, IFT-dependent transport or diffusion of I1 dynein may also be examined during the rescue process in a dikaryon formed between *ida7oda6*::IC140-GFP and *ida7* cells. As outlined in Fig. 4.8, the transformant expressing IC140-GFP will be mated to *ida7* cells of the opposite mating type to generate dikaryons for immediate imaging by TIRF. Similar to DRC4, I predict that IC140-GFP will move in a processive manner along the *ida7* mutant cilia during the rescue process. Additional critical questions about transport of axonemal precursor proteins could be answered. How does I1 dynein enter the ciliary

compartment? Is I1 dynein association with IFT required for entry into the ciliary compartment? Where along the cilium is I1 dynein unloaded from IFT? Thus, live cell imaging of I1 dynein addressing these unresolved questions is a high priority in the Sale lab.

Figures for Chapter 4

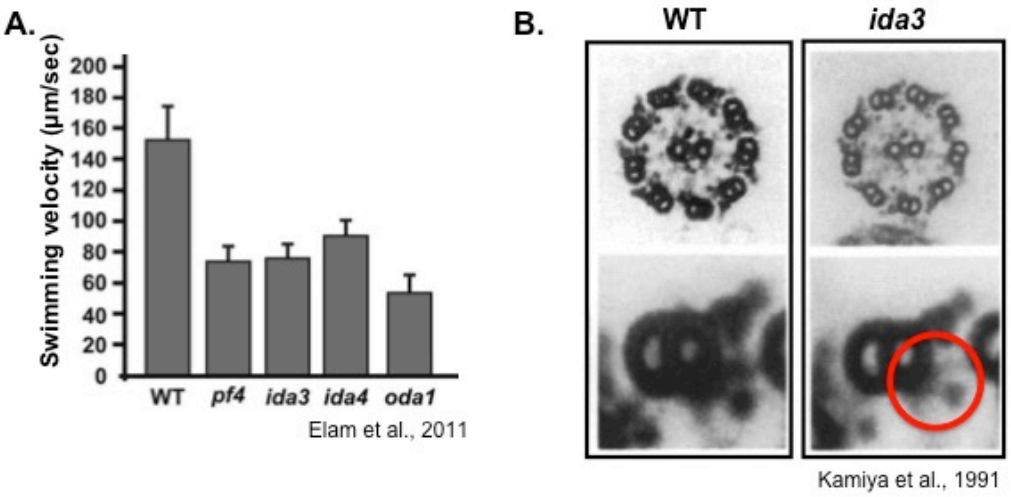
A.
Swimming velocity (µm/sec)
200
180
160
140
120
100
80
60
40
20
0
WT
pf4
ida3
ida4
oda1
Elam et al., 2011
B.
WT
ida3
Kamiya et al., 1991

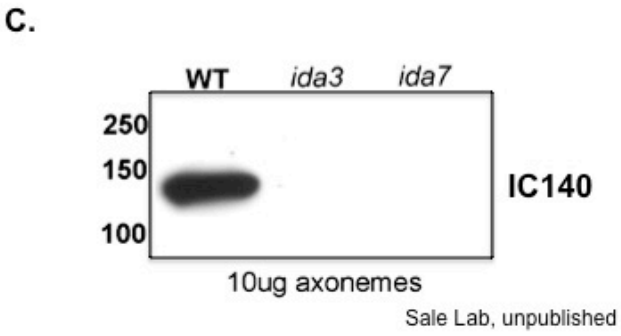
C.
WT
ida3
ida7
250
150
100
IC140
10ug axonemes
Sale Lab, unpublished

Figure 4.1. The *ida3* mutant is a slow swimmer and lacks I1 dynein in the axoneme. **(A)** Quantitative analysis of swimming velocities revealed that the *ida3* mutant swims at approximately half the velocity of wild-type cells. The slow swimming phenotype of *ida3* is similar to mutants that are defective in the regulation of I1 dynein activity, such as *pf4*. (**B**) Electron microscopy of axonemal cross sections from wild type and *ida3* reveal that compared to wild-type, inner arm density is decreased on every outer doublet microtubule of *ida3* axonemes (top panel). The bottom panel shows a single outer doublet microtubule and the red circle points to the missing density in *ida3* axonemes, due to the lack of I1 dynein. (**C**) Western blot of axonemes isolated from wild-type, *ida3* and *ida7* probed with an antibody to the IC140 subunit of I1 dynein. In contrast to wild-type, I1 dynein is absent in *ida3* and *ida7* (negative control) axonemes.

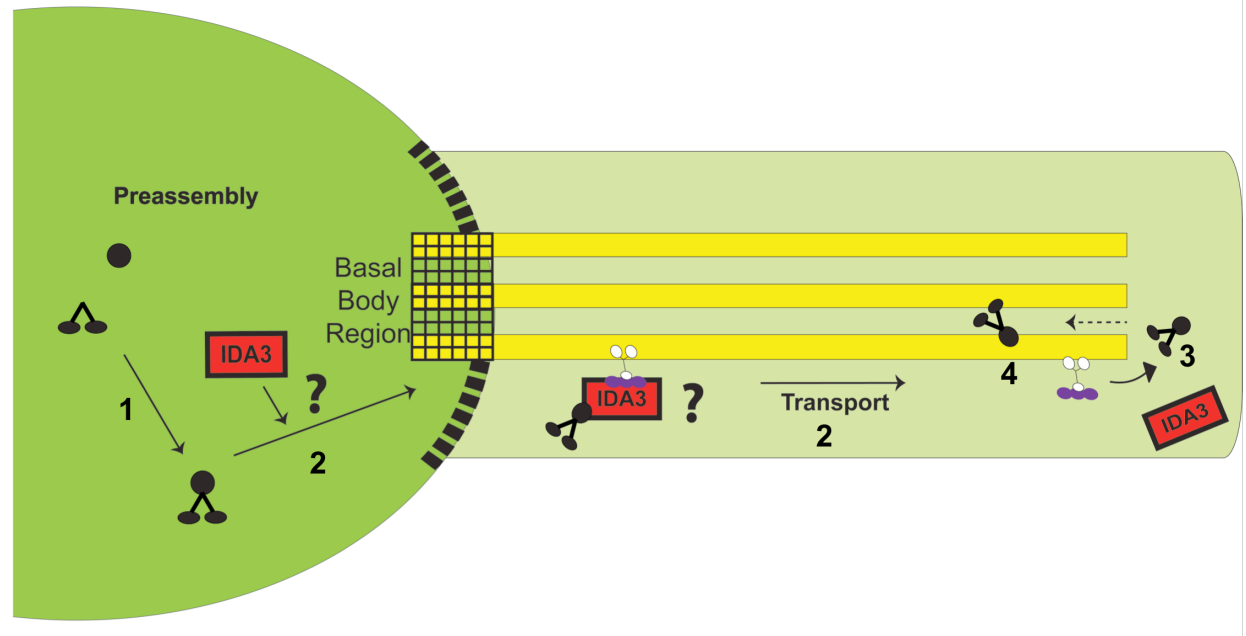
Preassembly
Basal
Body
Region
IDA3
1
?
2
IDA3
?
Transport
2
4
3
IDA3

Figure 4.2. Hypothetical steps leading to I1 dynein assembly in the axoneme. In my dissertation, I demonstrated that I1 dynein preassembles in the cytoplasm (**1**) and the preassembled I1 complex is transported to the distal tip of the cilium by IFT (**2** and **3**). I also hypothesize that IDA3 is an adapter required for I1 dynein entry and transport by IFT. As discussed in Chapter 4, the exact function of IDA3 is not known. IDA3 has been recently cloned and its role in I1 dynein assembly is currently being determined in the Sale lab. The postulated barrier between the cytoplasm and the ciliary compartment is shown as black boxes.


Chromosome 3
Mutation in IDA3
Centromere
Marker 1
Marker 2
Marker 3
Marker 4
BACs

Figure 4.3. Physical map illustrating the mutation in *IDA3*. Traditional mapping by the Kamiya (University of Tokyo) and Dutcher (Washington University, St. Louis) laboratories revealed that the mutation in *ida3* lies within a candidate region (green) between a defined set of marker genes and the centromere on Chromosome 3. Examination of the BAC library has revealed that several overlapping BACs span the candidate region and I predicted that transformation of the *ida3* mutant with a BAC containing *IDA3* would rescue the *ida3* mutant phenotype. Whole genome sequencing of DNA isolated from *ida3* revealed that the mutation (indicated by an "*") maps to a gene (navy blue) within the candidate region (green) estimated to be 4.2kb. As mentioned in Chapter 4, *IDA3* has been cloned from the rescuing BAC and the mutation revealed by whole genome sequencing has been confirmed.

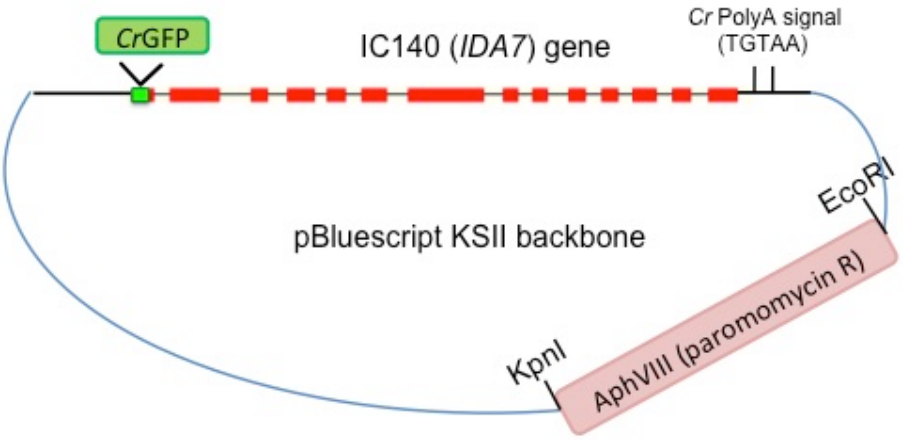

CrGFP GFP codon-optimzed for *Chlamydomonas reinhardtii* (*Cr*)

Figure 4.4. Plasmid map of the IC140-GFP construct used for transformation of *ida7;oda6* cells. The IC140 gene was cloned into the pBluescript KSII vector by Yang and Sale (1998) and was used for transformation-rescue of *ida7* cells by Perrone et al., (1998). Since the N-terminal region of the IC140 protein was shown to be dispensable for rescue of I1 dynein assembly in the axoneme, a codon-optimized version of GFP for use in *Chlamydomonas* (CrGFP) was inserted in Exon 1 (i.e. N-terminus) of the *IC140* gene. A paromomycin resistance cassette (AphVIII) was also subcloned into the vector backbone for selection of transformants.

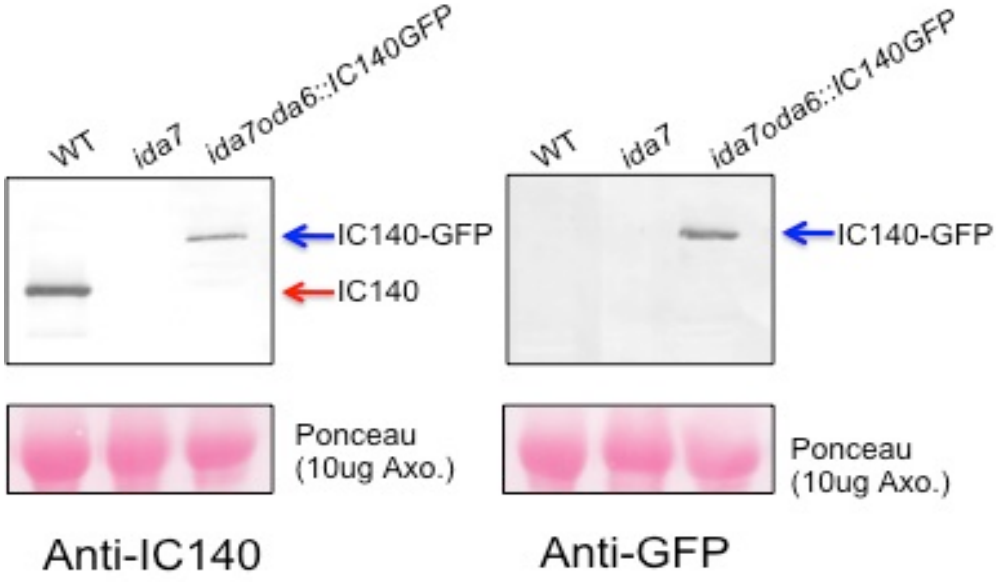
WT
ida7
ida7oda6::IC140GFP
IC140-GFP
IC140
Ponceau
(10ug Axo.)
Anti-IC140
WT
ida7
ida7oda6::IC140GFP
IC140-GFP
Ponceau
(10ug Axo.)
Anti-GFP

Figure 4.5. Western Blot of axonemes isolated from WT, *ida7* and *ida7;oda6*::IC140-GFP cells. The IC140 antibody detects IC140 in wild-type and not in the *ida7* (IC140-null) mutant axonemes. In the *ida7;oda6*::IC140-GFP rescue strain, IC140-GFP migrates at the expected size of ~165kDa. As expected, the GFP antibody also detects the IC140-GFP fusion protein at ~165kDa. The ponceau stain in the bottom panels serves as a loading control.

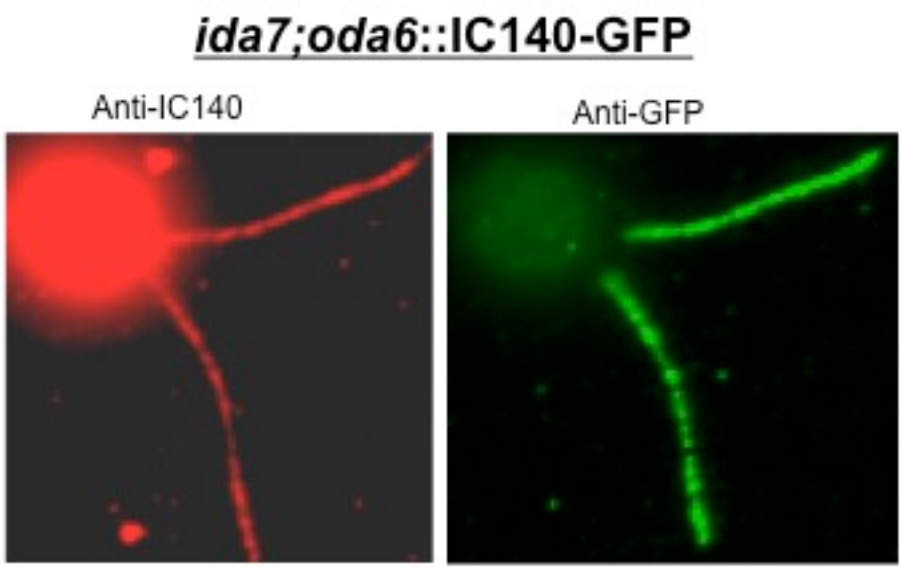
ida7;oda6::IC140-GFP
Anti-IC140
Anti-GFP

Figure 4.6. Immunofluorescence of *ida7;oda6* cells expressing IC140-GFP. Using the IC140 antibody, the IC140-GFP fusion protein is detected along the entire length of the cilia. Immunofluorescence analysis using the GFP antibody also indicates that the IC140-GFP fusion protein is localized along the entire length of the cilium.

***ida7;oda6*::IC140-GFP**

A. KAP-GFP (Zheng

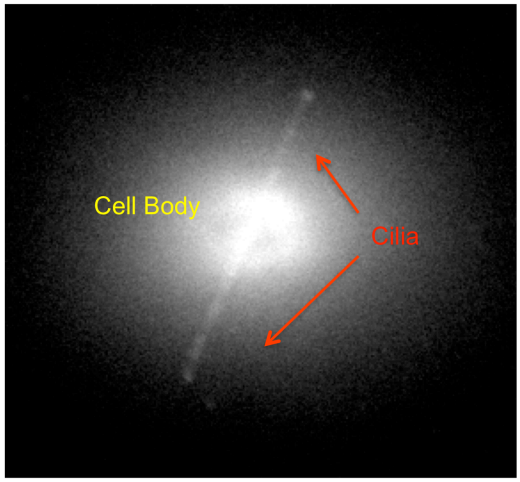

B. IC140-GFP (Lechtreck lab)

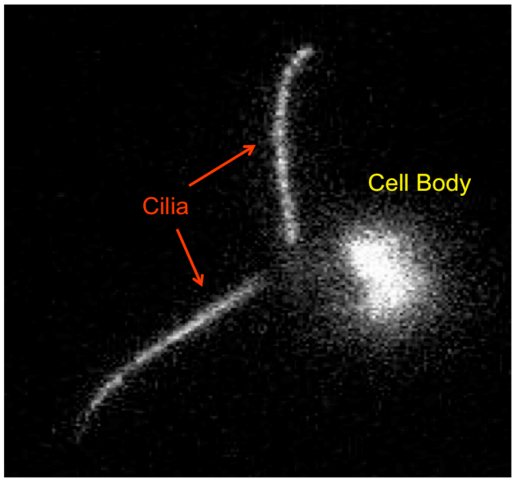

Figure 4.7. TIRF images of a control cell expressing KAP-GFP (A) and IC140-GFP (B). Using the TIRF-M in the Zheng lab (Cell Biology, Emory University), the KAP-GFP cells were used as a positive control. Movement of KAP-GFP, which is representative of IFT, was detected and recorded in real time in both flagella using a 100X objective. (**B**) TIRF imaging of the *ida7oda6::IC140-GFP* cell using the TIRF-M in the Lechtreck lab (UGA), indicated that IC140-GFP is expressed and is localized along the entire length of the cilium. However, as discussed in Chapter 4, no movement of IC140-GFP was detected. This image has modified using specialized software to subtract background fluorescence to show only the cell body and the cilia.

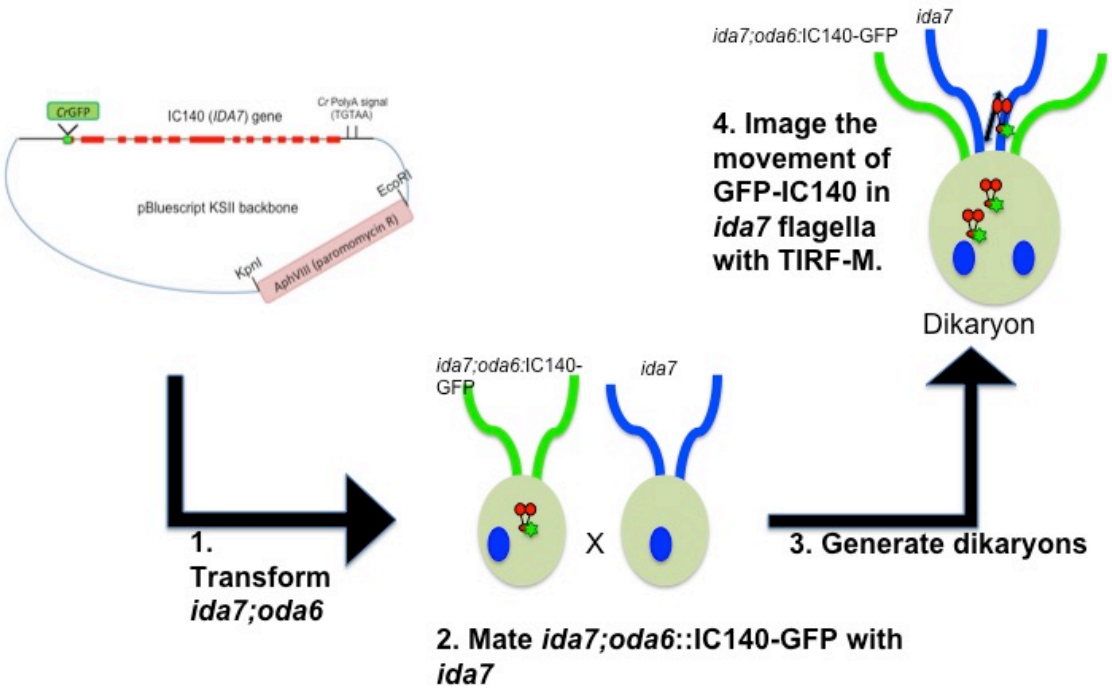
CrGFP
IC140 (IDA7) gene
Cr PolyA signal (TGTAA)
pBluescript KSII backbone
EcoRI
KpnI
AphVIII (paromomycin R)
1. Transform ida7;oda6
ida7;oda6:IC140-GFP
ida7
X
2. Mate ida7;oda6::IC140-GFP with ida7
3. Generate dikaryons
Dikaryon
ida7;oda6:IC140-GFP
ida7
4. Image the movement of GFP-IC140 in ida7 flagella with TIRF-M.

Figure 4.8. Experimental strategy involving dikaryon rescue to examine transport and/or diffusion of IC140-GFP. The first step is to transform *ida7;oda6* cells with a plasmid containing GFP inserted in exon 1 of the IC140 gene (**1**). Initial screening of transformants was carried out using a motility assay described in Methods (Appendix I). Candidate transformants were examined for the assembly of IC140-GFP containing I1 dynein in the ciliary axoneme (data shown in Fig. 4.5 and 4.6). The next step is to mate *ida7;oda6*::IC140-GFP with *ida7* gametes of the opposite mating type (**2**) to generate dikaryons (**3**). The goal is to image the movement of IC140-GFP in the ida7 cilia during the rescue process using TIRF-M (**4**).

Appendix I : Materials and Methods

Cell Strains and Culture

Chlamydomonas strains used in this study were wild-type (CC-125, CC-124, CC-620 and CC-621), *ida3* (CC-2668, CC-2669), *ida7* (CC-3921 5b10; *ida7-1*), *fla10* (CC-1919, CC-4617), *ida3; fla10-1* (this study), *ida1* (CC-2664) and *ida2* (CC-2666). All strains except for *ida3; fla10-1* were obtained from the *Chlamydomonas* Resource Center (University of Minnesota, St. Paul, MN). Cells were grown in tris-acetate-phosphate (TAP) medium with aeration on a 14:10h light/dark cycle. Dikaryons between wild type and I1-deficient cells were generated by mixing gametes produced by differentiating each cell type for 4 hours in M-N medium (Harris 1989). The *ida3; fla10-1* double mutant was generated by crossing *fla10*-1 (-) and *ida3* (+) followed by screening progeny based on the *ida3* motility and ciliary resorption at 32°C. PCR and Sanger sequencing confirmed the selected candidates for the *fla10-1* mutation (Vashishtha et al. 1996).

Preparation of Axonemes and Membrane + Matrix

Cells were grown to mid-log phase and deciliated by treating the cells with 25mM dibucaine (Witman 1986) followed by centrifugation to separate the cilia and cell bodies. To prepare axonemes, the isolated cilia were demembranated by 1% Nonidet P-40 (Darmstadt, Germany) in HMDE + 25mM NaCl (10mM Hepes, 5mM MgSO4, 1mM DTT, 0.5mM EGTA, pH 7.4) and the axonemal pellet was resuspended/dissolved in HMDE + NaCl (10mM Hepes, 5mM $MgSO_4$, 1mM DTT, 0.5mM EDTA, 25mM NaCl and protease inhibitors, pH 7.4) and fixed with Laemmli sample buffer at a concentration of 1mg/mL. The membrane+matrix (M+M) fraction was obtained by demembranating

the pelleted cilia with 1% Nonidet-P40 in HMDE + 25mM NaCl buffer and fixed with Laemmli sample buffer for immunoblotting. For detection of axonemal subunits (IC69, IC140, IC138), the M+M was loaded at five times the relative volume of cilia and axonemes.

Preparation and Fractionation of Axonemal and Cytoplasmic Extracts

Axonemal Extracts: Wild type and I1-deficient axonemes were isolated as described above. Axonemes were then treated with HMDE + 0.6M NaCl for 30 minutes to solubilize the dyneins. The extracted dyneins in the high-salt extract (HSE) were dialyzed against HMDE + 25mM NaCl for 2 x 30mins. Cytoplasmic Extracts from wild type and I1-deficient whole cells were prepared at using the method described in (Alford et al. 2013). Cells were lysed by mechanical agitation by glass beads at room temperature. The axonemal HSE and cytoplasmic extracts were fractionated by velocity sedimentation on 5-20% sucrose gradients as described in Alford et al. 2013 or utilized for reconstitution experiments as described below.

***In vitro* Reconstitution**

Varying amounts of extracts isolated as described above were mixed with a fixed amount of extracted I1-dynein deficient axonemes in the presence of 1mM ATP. The final volumes of all the reconstitutions were equalized with buffer. The reconstitution mixtures were separated by centrifugation into supernatant (S, unbound I1) and pellet (P, bound I1) fractions. The axonemal pellets were resuspended to the original volume and fixed for SDS-PAGE.

Antibodies and Immunoblots

SDS-PAGE and immunoblotting were performed using standard procedures. Primary antibodies used in this study include the following: mouse monoclonal against IC69 (clone 1869A hybridoma, Sigma, St. Louis, MO); rabbit polyclonal antibodies against IC140 (Yang and Sale 1998), IC138 (Hendrickson et al. 2004a), IC97 (Wirschell et al. 2009) and IFT46 clone 17600 (Hou et al. 2007). The secondary antibodies (goat anti-mouse or rabbit) used in immunoblots were purchased from BioRad (Hercules, CA). The secondary anti rabbit or goat conjugated with Alex Fluor 488 or 555 were purchased from Invitrogen (Eugene, OR).

Immunofluorescence microscopy and quantification

For immunofluorescence of whole cells, cells were allowed to adhere for 5 min to poly-L-lysine coated cover slips, excess cells were wicked off, and the cover slips were submerged in -20°C methanol for 5 min. The cover slips were then air-dried, rehydrated with 1X PBS, blocked for 30 min at room temperature with blocking solution (6% fish skin gelatin, 1% BSA, and 0.05% Tween-20 in PBS, pH 7.0), incubated with primary antibodies (4°C overnight), washed 3X with blocking solution, washed 3X, incubated with secondary antibodies (Alexa Fluor–conjugated IgG; 1:1000; Invitrogen, Eugene, OR) for 30 min at RT, washed 3x with PBS, then mounted with ProLong Antifade Gold (Invitrogen, Eugene, OR). Images were captured using a BX60 wide field microscope (Olympus, Tokyo, Japan) under a 60x objective, and with a digital camera (Orca-ER, Hamamatsu, Bridgewater, NJ) and Slidebook software (Intelligent Imaging Innovations, Denver, CO). Quantifying I1 dynein assembly from the tip of mutant cilia in dikaryons was performed as described in Alford et al., (Alford et al. 2013). All the image analysis was performed using Image J (FIJI, National Institutes of Health, Bethesda, MD). For

each combination of dikaryons (Ex. WT x *ida3*, *ida3* x *ida7*), the fluorescence signal (Arbitrary units, AU) starting from the tip of the rescuing cilia was measured as function of distance (μm). The fluorescence intensity values corresponding to every pixel along the length were normalized to the brightest intensity value in the data set and plotted against the length of the cilium (μm) as illustrated in the line scan (Figure 5B). A threshold value of 0.2 was established, and distance at which the normalized fluorescence intensity value dropped and stayed below 0.2 for at least three consecutive data points was recorded as the absolute distance at which the IC140 staining from the tip ended (um). The progressive rescue of I1 dynein assembly from the tip as a function of time after mixing the gametes was plotted using Kaliedograph (Reading, PA). The standard error and p-values were calculated in MS Excel (Redmond, WA).

Dikaryon rescue using the *fla10-1* mutants was performed as described (Piperno et al. 1996). Briefly both gametes, *ida3; fla10-1* and *fla10-1* were preincubated at the restrictive temperature, 32°C, for at least 38 minutes prior to mixing in order to inactivate the kinesin. Secondly, the dikaryons involving *fla10-1* and *ida3; fla10-1* double mutant gametes could be analyzed for I1 assembly for a maximum time of 60 minutes after mixing, after which dikaryons began to lose their cilia due to resorption.

Mapping of IDA3

In the traditional method of mapping genes by tetrad analysis, haploid parent strains (i.e. mutant and S1 D2 cells) are crossed resulting in a 'tetrad' that contains 4 meiotic progeny. Each of the 4 progeny can be classified based on the phenotype. Generally, three types of tetrads can be obtained from a cross: parental ditype (PD) i.e.

progeny exhibiting the same phenotype as the parents; nonparental ditype (NPD) i.e. progeny exhibiting recombinant phenotypes or wild-type; and tetratype (T) i.e. progeny exhibiting both parental and recombinant phenotypes. The relative ratios of these three types of tetrads indicate whether or not the mutant gene is linked to the given marker (i.e. on the same chromosome) or unlinked (i.e. on the same chromosome but distant or on different chromosomes). For example, in this study, the mutant gene in a novel dynein mutant, *ida3*, was mapped to chromosome 3 and additional mapping placed *IDA3* closed to the centromere. Having known the general location of IDA3, in collaboration with Dr. Susan Dutcher (Wash U), we were able to perform further mapping and to identify the mutation in the *IDA3* by whole-genome sequencing (WGS). Further discussion of the mutant and the phenotype are presented in Chapters 2-4.

Appendix II: Tables (Attached at the end of the document)

Table 1: ODA and associated proteins

Table 2: IDA and associated proteins

Table 3: List of mutants used in this study

Table 4: IFT and associated proteins

References

Afzelius BA. 1981. Genetical and ultrastructural aspects of the immotile-cilia syndrome. *American journal of human genetics* **33**: 852-864.

Ahmed NT, Gao C, Lucker BF, Cole DG, Mitchell DR. 2008. ODA16 aids axonemal outer row dynein assembly through an interaction with the intraflagellar transport machinery. *The Journal of cell biology* **183**: 313-322.

Ahmed NT, Mitchell DR. 2005. ODA16p, a Chlamydomonas flagellar protein needed for dynein assembly. *Molecular biology of the cell* **16**: 5004-5012.

Alford LM, Mattheyses AL, Hunter EL, Lin H, Dutcher SK, Sale WS. 2013. The Chlamydomonas mutant pf27 reveals novel features of ciliary radial spoke assembly. *Cytoskeleton (Hoboken)*.

Allen RD, Metuzals J, Tasaki I, Brady ST, Gilbert SP. 1982. Fast axonal transport in squid giant axon. *Science* **218**: 1127-1129.

Austin-Tse C, Halbritter J, Zariwala MA, Gilberti RM, Gee HY, Hellman N, Pathak N, Liu Y, Panizzi JR, Patel-King RS et al. 2013. Zebrafish Ciliopathy Screen Plus Human Mutational Analysis Identifies C21orf59 and CCDC65 Defects as Causing Primary Ciliary Dyskinesia. *American journal of human genetics* **93**: 672-686.

Avasthi P, Marshall WF. 2012. Stages of ciliogenesis and regulation of ciliary length. *Differentiation* **83**: S30-42.

Avasthi P, Onishi M, Karpiak J, Yamamoto R, Mackinder L, Jonikas MC, Sale WS, Shoichet B, Pringle JR, Marshall WF. 2014. Actin is required for IFT regulation in Chlamydomonas reinhardtii. *Curr Biol* **24**: 2025-2032.

Avidor-Reiss T, Maer AM, Koundakjian E, Polyanovsky A, Keil T, Subramaniam S, Zuker CS. 2004. Decoding cilia function: defining specialized genes required for compartmentalized cilia biogenesis. *Cell* **117**: 527-539.

Awata J, Takada S, Standley C, Lechtreck KF, Bellve KD, Pazour GJ, Fogarty KE, Witman GB. 2014. NPHP4 controls ciliary trafficking of membrane proteins and large soluble proteins at the transition zone. *J Cell Sci* **127**: 4714-4727.

Babu D, Roy S. 2013. Left-right asymmetry: cilia stir up new surprises in the node. *Open Biol* **3**: 130052.

Barbar E. 2008. Dynein light chain LC8 is a dimerization hub essential in diverse protein networks. *Biochemistry* **47**: 503-508.

Barber CF, Heuser T, Carbajal-Gonzalez BI, Botchkarev VV, Jr., Nicastro D. 2012. Three-dimensional structure of the radial spokes reveals heterogeneity and interactions with dyneins in Chlamydomonas flagella. *Molecular biology of the cell* **23**: 111-120.

Basu B, Brueckner M. 2008. Cilia multifunctional organelles at the center of vertebrate left-right asymmetry. *Curr Top Dev Biol* **85**: 151-174.

Bayly PV, Lewis BL, Kemp PS, Pless RB, Dutcher SK. 2010. Efficient spatiotemporal analysis of the flagellar waveform of Chlamydomonas reinhardtii. *Cytoskeleton (Hoboken)* **67**: 56-69.

Behal RH, Betleja E, Cole DG. 2009. Purification of IFT particle proteins and preparation of recombinant proteins for structural and functional analysis. *Methods in cell biology* **93**: 179-196.

Behal RH, Cole DG. 2013. Analysis of interactions between intraflagellar transport proteins. *Methods in enzymology* **524**: 171-194.

Belzile O, Hernandez-Lara CI, Wang Q, Snell WJ. 2013. Regulated Membrane Protein Entry into Flagella Is Facilitated by Cytoplasmic Microtubules and Does Not Require IFT. *Current biology : CB* **23**: 1460-1465.

Bhogaraju S, Cajanek L, Fort C, Blisnick T, Weber K, Taschner M, Mizuno N, Lamla S, Bastin P, Nigg EA et al. 2013a. Molecular basis of tubulin transport within the cilium by IFT74 and IFT81. *Science* **341**: 1009-1012.

Bhogaraju S, Engel BD, Lorentzen E. 2013b. Intraflagellar transport complex structure and cargo interactions. *Cilia* **2**: 10.

Bhogaraju S, Weber K, Engel BD, Lechtreck KF, Lorentzen E. 2014. Getting tubulin to the tip of the cilium: one IFT train, many different tubulin cargo-binding sites? *Bioessays* **36**: 463-467.

Bloodgood RA. 1977. Motility occurring in association with the surface of the Chlamydomonas flagellum. *The Journal of cell biology* **75**: 983-989.

-. 1995. Flagellar surface motility: gliding and microsphere movements. *Methods in cell biology* **47**: 273-279.

Bower R, Tritschler D, Vanderwaal K, Perrone CA, Mueller J, Fox L, Sale WS, Porter ME. 2013. The N-DRC forms a conserved biochemical complex that maintains outer doublet alignment and limits microtubule sliding in motile axonemes. *Molecular biology of the cell* **24**: 1134-1152.

Bower R, Vanderwaal K, O'Toole E, Fox L, Perrone C, Mueller J, Wirschell M, Kamiya R, Sale WS, Porter ME. 2009a. IC138 Defines a Sub-Domain at the Base of the

I1 Dynein That Regulates Microtubule Sliding and Flagellar Motility. *Molecular biology of the cell* **20**: 3055-3063.

-. 2009b. IC138 defines a subdomain at the base of the I1 dynein that regulates microtubule sliding and flagellar motility. *Molecular biology of the cell* **20**: 3055-3063.

Bowman AB, Patel-King RS, Benashski SE, McCaffery JM, Goldstein LS, King SM. 1999. Drosophila roadblock and Chlamydomonas LC7: a conserved family of dynein-associated proteins involved in axonal transport, flagellar motility, and mitosis. *The Journal of cell biology* **146**: 165-180.

Brady ST, Lasek RJ, Allen RD. 1982. Fast axonal transport in extruded axoplasm from squid giant axon. *Science* **218**: 1129-1131.

Brazelton WJ, Amundsen CD, Silflow CD, Lefebvre PA. 2001. The *bld*1 mutation identifies the *Chlamydomonas osm*-6 homolog as a gene required for flagellar assembly. *Current biology : CB* **11**: 1591-1594.

Brokaw CJ, Kamiya R. 1987. Bending patterns of *Chlamydomonas* flagella: IV. Mutants with defects in inner and outer dynein arms indicate differences in dynein arm function. *Cell motility and the cytoskeleton* **8**: 68-75.

Brooks ER, Wallingford JB. 2012. Control of vertebrate intraflagellar transport by the planar cell polarity effector Fuz. *The Journal of cell biology* **198**: 37-45.

-. 2014. Multiciliated cells. *Curr Biol* **24**: R973-982.

Brown JM, Witman GB. 2014. Cilia and Diseases. *Bioscience* **64**: 1126-1137.

Brueckner M. 2012. Impact of genetic diagnosis on clinical management of patients with congenital heart disease: cilia point the way. *Circulation* **125**: 2178-2180.

Bui KH, Ishikawa T. 2013. 3D structural analysis of flagella/cilia by cryo-electron tomography. *Methods in enzymology* **524**: 305-323.

Bui KH, Sakakibara H, Movassagh T, Oiwa K, Ishikawa T. 2009. Asymmetry of inner dynein arms and inter-doublet links in Chlamydomonas flagella. *The Journal of cell biology* **186**: 437-446.

Bui KH, Yagi T, Yamamoto R, Kamiya R, Ishikawa T. 2012. Polarity and asymmetry in the arrangement of dynein and related structures in the Chlamydomonas axoneme. *J Cell Biol* **198**: 913-925.

Burgess SA, Walker ML, Sakakibara H, Knight PJ, Oiwa K. 2003. Dynein structure and power stroke. *Nature* **421**: 715-718.

Carter AP. 2013. Crystal clear insights into how the dynein motor moves. *J Cell Sci* **126**: 705-713.

Carter AP, Cho C, Jin L, Vale RD. 2011. Crystal structure of the dynein motor domain. *Science* **331**: 1159-1165.

Carter AP, Vale RD. 2010. Communication between the AAA+ ring and microtubule-binding domain of dynein. *Biochem Cell Biol* **88**: 15-21.

Casey DM, Inaba K, Pazour GJ, Takada S, Wakabayashi K, Wilkerson CG, Kamiya R, Witman GB. 2003a. DC3, the 21-kDa subunit of the outer dynein arm-docking complex (ODA-DC), is a novel EF-hand protein important for assembly of

both the outer arm and the ODA-DC. *Molecular biology of the cell* **14**: 3650-3663.

Casey DM, Yagi T, Kamiya R, Witman GB. 2003b. DC3, the Smallest Subunit of the *Chlamydomonas* Flagellar Outer Dynein Arm-docking Complex, Is a Redox-sensitive Calcium-binding Protein. *The Journal of biological chemistry* **278**: 42652-42659.

Caspary T, Anderson KV. 2003. Patterning cell types in the dorsal spinal cord: what the mouse mutants say. *Nat Rev Neurosci* **4**: 289-297.

Caspary T, Garcia-Garcia MJ, Huangfu D, Eggenschwiler JT, Wyler MR, Rakeman AS, Alcorn HL, Anderson KV. 2002. Mouse Dispatched homolog1 is required for long-range, but not juxtacrine, Hh signaling. *Current biology : CB* **12**: 1628-1632.

Cho C, Vale RD. 2012. The mechanism of dynein motility: insight from crystal structures of the motor domain. *Biochim Biophys Acta* **1823**: 182-191.

Cole DG. 2003. The intraflagellar transport machinery of Chlamydomonas reinhardtii. *Traffic* **4**: 435-442.

Cole DG, Diener DR, Himelblau AL, Beech PL, Fuster JC, Rosenbaum JL. 1998. *Chlamydomonas* kinesin-II-dependent intraflagellar transport (IFT): IFT particles contain proteins required for ciliary assembly in *Caenorhabditis elegans* sensory neurons. *The Journal of cell biology* **141**: 993-1008.

Craft JM, Harris JA, Hyman S, Kner P, Lechtreck KF. 2015. Tubulin transport by IFT is upregulated during ciliary growth by a cilium-autonomous mechanism. *The Journal of cell biology* **208**: 223-237.

Craige B, Tsao CC, Diener DR, Hou YQ, Lechtreck KF, Rosenbaum JL, Witman GB. 2010. CEP290 tethers flagellar transition zone microtubules to the membrane and regulates flagellar protein content. *J Cell Biol* **190**: 927-940.

Davis EE, Katsanis N. 2012. The ciliopathies: a transitional model into systems biology of human genetic disease. *Curr Opin Genet Dev* **22**: 290-303.

Dean AB, Mitchell DR. 2013. Chlamydomonas ODA10 is a conserved axonemal protein that plays a unique role in outer dynein arm assembly. *Molecular biology of the cell* **24**: 3689-3696.

DiBella LM, Benashski SE, Tedford HW, Harrison A, Patel-King RS, King SM. 2001. The Tctex1/Tctex2 class of dynein light chains. Dimerization, differential expression, and interaction with the LC8 protein family. *The Journal of biological chemistry* **276**: 14366-14373.

DiBella LM, Sakato M, Patel-King RS, Pazour GJ, King SM. 2004a. The LC7 Light Chains of Chlamydomonas Flagellar Dyneins Interact with Components Required for Both Motor Assembly and Regulation. *Molecular biology of the cell*.

DiBella LM, Smith EF, Patel-King RS, Wakabayashi K, King SM. 2004b. A novel Tctex2-related light chain is required for stability of inner dynein arm I1 and motor function in the Chlamydomonas flagellum. *The Journal of biological chemistry* **279**: 21666-21676.

Diener DR, Yang P, Geimer S, Cole DG, Sale WS, Rosenbaum JL. 2011. Sequential assembly of flagellar radial spokes. *Cytoskeleton (Hoboken)* **68**: 389-400.

DiPetrillo CG, Smith EF. 2013. Methods for analysis of calcium/calmodulin signaling in cilia and flagella. *Methods in enzymology* **524**: 37-57.

Dishinger JF, Kee HL, Jenkins PM, Fan S, Hurd TW, Hammond JW, Truong YN, Margolis B, Martens JR, Verhey KJ. 2010a. Ciliary entry of the kinesin-2 motor KIF17 is regulated by importin-beta2 and RanGTP. *Nature cell biology* **12**: 703-710.

Dishinger JF, Kee HL, Jenkins PM, Fan SL, Hurd TW, Hammond JW, Truong YNT, Margolis B, Martens JR, Verhey KJ. 2010b. Ciliary entry of the kinesin-2 motor KIF17 is regulated by importin-beta 2 and RanGTP. *Nature Cell Biology* **12**: 703-U164.

Drummond IA. 2012. Cilia functions in development. *Curr Opin Cell Biol* **24**: 24-30.

Dutcher SK. 2014. The awesome power of dikaryons for studying flagella and basal bodies in Chlamydomonas reinhardtii. *Cytoskeleton (Hoboken)* **71**: 79-94.

Eggenschwiler JT, Anderson KV. 2007. Cilia and developmental signaling. *Annual review of cell and developmental biology* **23**: 345-373.

Elam CA, Sale WS, Wirschell M. 2009. The regulation of dynein-driven microtubule sliding in Chlamydomonas flagella by axonemal kinases and phosphatases. *Methods in cell biology* **92**: 133-151.

Elam CA, Wirschell M, Yamamoto R, Fox LA, York K, Kamiya R, Dutcher SK, Sale WS. 2011. An axonemal PP2A B-subunit is required for PP2A localization and flagellar motility. *Cytoskeleton (Hoboken)* **68**: 363-372.

Encalada SE, Goldstein LS. 2014. Biophysical challenges to axonal transport: motor-cargo deficiencies and neurodegeneration. *Annu Rev Biophys* **43**: 141-169.

Engel BD, Ishikawa H, Wemmer KA, Geimer S, Wakabayashi K, Hirono M, Craige B, Pazour GJ, Witman GB, Kamiya R et al. 2012. The role of retrograde intraflagellar transport in flagellar assembly, maintenance, and function. *The Journal of cell biology* **199**: 151-167.

Engel BD, Lechtreck KF, Sakai T, Ikebe M, Witman GB, Marshall WF. 2009a. Total internal reflection fluorescence (TIRF) microscopy of Chlamydomonas flagella. *Methods in cell biology* **93**: 157-177.

Engel BD, Ludington WB, Marshall WF. 2009b. Intraflagellar transport particle size scales inversely with flagellar length: revisiting the balance-point length control model. *The Journal of cell biology* **187**: 81-89.

Ferris PJ, Waffenschmidt S, Umen JG, Lin H, Lee JH, Ishida K, Kubo T, Lau J, Goodenough UW. 2005. Plus and minus sexual agglutinins from Chlamydomonas reinhardtii. *Plant Cell* **17**: 597-615.

Follit JA, Li L, Vucica Y, Pazour GJ. 2010. The cytoplasmic tail of fibrocystin contains a ciliary targeting sequence. *J Cell Biol* **188**: 21-28.

Fowkes ME, Mitchell DR. 1998. The role of preassembled cytoplasmic complexes in assembly of flagellar dynein subunits. *Molecular biology of the cell* **9**: 2337-2347.

Fox LA, Sawin KE, Sale WS. 1994. Kinesin-related proteins in eukaryotic flagella. *Journal of cell science* **107 (Pt 6)**: 1545-1550.

Fu MM, Holzbaur EL. 2014. Integrated regulation of motor-driven organelle transport by scaffolding proteins. *Trends Cell Biol* **24**: 564-574.

Fu MM, Nirschl JJ, Holzbaur EL. 2014. LC3 binding to the scaffolding protein JIP1 regulates processive dynein-driven transport of autophagosomes. *Dev Cell* **29**: 577-590.

Garcia-Garcia MJ, Eggenschwiler JT, Caspary T, Alcorn HL, Wyler MR, Huangfu D, Rakeman AS, Lee JD, Feinberg EH, Timmer JR et al. 2005. Analysis of mouse embryonic patterning and morphogenesis by forward genetics. *Proceedings of the National Academy of Sciences of the United States of America* **102**: 5913-5919.

Gerdes JM, Davis EE, Katsanis N. 2009. The vertebrate primary cilium in development, homeostasis, and disease. *Cell* **137**: 32-45.

Gibbons BH, Gibbons IR. 1972. Flagellar movement and adenosine triphosphatase activity in sea urchin sperm extracted with triton X-100. *The Journal of cell biology* **54**: 75-97.

Gibbons IR. 1963. Studies on the Protein Components of Cilia from Tetrahymena Pyriformis. *Proceedings of the National Academy of Sciences of the United States of America* **50**: 1002-1010.

Gibbons IR, Rowe AJ. 1965. Dynein: A Protein with Adenosine Triphosphatase Activity from Cilia. *Science* **149**: 424-426.

Goduti DJ, Smith EF. 2012. Analyses of functional domains within the PF6 protein of the central apparatus reveal a role for PF6 sub-complex members in regulating flagellar beat frequency. *Cytoskeleton (Hoboken)* **69**: 179-194.

Goetz SC, Anderson KV. 2010. The primary cilium: a signalling centre during vertebrate development. *Nat Rev Genet* **11**: 331-344.

Gokhale A, Wirschell M, Sale WS. 2009. Regulation of dynein-driven microtubule sliding by the axonemal protein kinase CK1 in Chlamydomonas flagella. *The Journal of cell biology* **186**: 817-824.

Goodenough UW, Heuser JE. 1982. Substructure of the outer dynein arm. *The Journal of cell biology* **95**: 798-815.

-. 1985a. Outer and inner dynein arms of cilia and flagella. *Cell* **41**: 341-342.

-. 1985b. Substructure of Inner Dynein Arms, Radial Spokes, and the Central Pair Projection Complex of Cilia and Flagella. *J Cell Biol* **100**: 2008-2018.

-. 1985c. Substructure of inner dynein arms, radial spokes, and the central pair/projection complex of cilia and flagella. *The Journal of cell biology* **100**: 2008-2018.

Gopal R, Foster KW, Yang P. 2012. The DPY-30 domain and its flanking sequence mediate the assembly and modulation of flagellar radial spoke complexes. *Mol Cell Biol* **32**: 4012-4024.

Gupta A, Diener DR, Sivadas P, Rosenbaum JL, Yang P. 2012. The versatile molecular complex component LC8 promotes several distinct steps of flagellar assembly. *The Journal of cell biology* **198**: 115-126.

Hao L, Thein M, Brust-Mascher I, Civelekoglu-Scholey G, Lu Y, Acar S, Prevo B, Shaham S, Scholey JM. 2011. Intraflagellar transport delivers tubulin isotypes to sensory cilium middle and distal segments. *Nat Cell Biol* **13**: 790-798.

Harris EH. 1989. *The Chlamydomonas Sourcebook: A Comprehensive Guide to Biology and Laboratory Use*. Academic Press, San Diego.

Harris EH. 2009. *The Chlamydomonas Sourcebook: Introduction to Chlamydomonas and Its Laboratory Use.* Academic Press, Oxford.

Harrison A, Olds-Clarke P, King SM. 1998. Identification of the t complex-encoded cytoplasmic dynein light chain tctex1 in inner arm I1 supports the involvement of flagellar dyneins in meiotic drive. *The Journal of cell biology* **140**: 1137-1147.

Hendrickson TW, Perrone CA, Griffin P, Wuichet K, Mueller J, Yang P, Porter ME, Sale WS. 2004a. IC138 is a WD-repeat Dynein Intermediate Chain Required for Light Chain Assembly and Regulation of Flagellar Bending. *Molecular biology of the cell* **12**: 5431-5442.

-. 2004b. IC138 is a WD-repeat dynein intermediate chain required for light chain assembly and regulation of flagellar bending. *Molecular biology of the cell* **15**: 5431-5442.

Heuser T, Barber CF, Lin J, Krell J, Rebesco M, Porter ME, Nicastro D. 2012. Cryoelectron tomography reveals doublet-specific structures and unique interactions in the I1 dynein. *Proc Natl Acad Sci U S A* **109**: E2067-2076.

Heuser T, Raytchev M, Krell J, Porter ME, Nicastro D. 2009. The dynein regulatory complex is the nexin link and a major regulatory node in cilia and flagella. *The Journal of cell biology* **187**: 921-933.

Higginbotham H, Eom TY, Mariani LE, Bachleda A, Hirt J, Gukassyan V, Cusack CL, Lai C, Caspary T, Anton ES. 2012. Arl13b in primary cilia regulates the migration and placement of interneurons in the developing cerebral cortex. *Dev Cell* **23**: 925-938.

Hildebrandt F, Benzing T, Katsanis N. 2011. Ciliopathies. *N Engl J Med* **364**: 1533-1543.

Hirokawa N, Tanaka Y, Okada Y. 2012. Cilia, KIF3 molecular motor and nodal flow. *Curr Opin Cell Biol* **24**: 31-39.

Hirokawa N, Tanaka Y, Okada Y, Takeda S. 2006. Nodal flow and the generation of left-right asymmetry. *Cell* **125**: 33-45.

Hjeij R, Onoufriadis A, Watson CM, Slagle CE, Klena NT, Dougherty GW, Kurkowiak M, Loges NT, Diggle CP, Morante NF et al. 2014. CCDC151 mutations cause primary ciliary dyskinesia by disruption of the outer dynein arm docking complex formation. *Am J Hum Genet* **95**: 257-274.

Hom EF, Witman GB, Harris EH, Dutcher SK, Kamiya R, Mitchell DR, Pazour GJ, Porter ME, Sale WS, Wirschell M et al. 2011. A unified taxonomy for ciliary dyneins. *Cytoskeleton (Hoboken)* **68**: 555-565.

Hook P, Vallee RB. 2006. The dynein family at a glance. *Journal of cell science* **119**: 4369-4371.

Hoops HJ, Witman GB. 1983. Outer doublet heterogeneity reveals structural polarity related to beat direction in Chlamydomonas flagella. *The Journal of cell biology* **97**: 902-908.

Horani A, Brody SL, Ferkol TW. 2014. Picking up speed: advances in the genetics of primary ciliary dyskinesia. *Pediatr Res* **75**: 158-164.

Horani A, Brody SL, Ferkol TW, Shoseyov D, Wasserman MG, Ta-shma A, Wilson KS, Bayly PV, Amirav I, Cohen-Cymberknoh M et al. 2013. CCDC65 mutation

causes primary ciliary dyskinesia with normal ultrastructure and hyperkinetic cilia. *PloS one* **8**: e72299.

Horani A, Druley TE, Zariwala MA, Patel AC, Levinson BT, Van Arendonk LG, Thornton KC, Giacalone JC, Albee AJ, Wilson KS et al. 2012. Whole-exome capture and sequencing identifies HEATR2 mutation as a cause of primary ciliary dyskinesia. *American journal of human genetics* **91**: 685-693.

Hornef N, Olbrich H, Horvath J, Zariwala MA, Fliegauf M, Loges NT, Wildhaber J, Noone PG, Kennedy M, Antonarakis SE et al. 2006. DNAH5 mutations are a common cause of primary ciliary dyskinesia with outer dynein arm defects. *Am J Respir Crit Care Med* **174**: 120-126.

Horst CJ, Witman GB. 1993. ptx1, a nonphototactic mutant of Chlamydomonas, lacks control of flagellar dominance. *The Journal of cell biology* **120**: 733-741.

Hou Y, Qin H, Follit JA, Pazour GJ, Rosenbaum JL, Witman GB. 2007. Functional analysis of an individual IFT protein: IFT46 is required for transport of outer dynein arms into flagella. *The Journal of cell biology* **176**: 653-665.

Hu Q, Milenkovic L, Jin H, Scott MP, Nachury MV, Spiliotis ET, Nelson WJ. 2010. A septin diffusion barrier at the base of the primary cilium maintains ciliary membrane protein distribution. *Science* **329**: 436-439.

Hu Q, Nelson WJ. 2011. Ciliary diffusion barrier: the gatekeeper for the primary cilium compartment. *Cytoskeleton (Hoboken)* **68**: 313-324.

Huang L, Lipschutz JH. 2014. Cilia and polycystic kidney disease, kith and kin. *Birth Defects Res C Embryo Today* **102**: 174-185.

Ide T, Owa M, King SM, Kamiya R, Wakabayashi K. 2013. Protein-protein interactions between intermediate chains and the docking complex of Chlamydomonas flagellar outer arm dynein. *FEBS Lett* **587**: 2143-2149.

Ikeda K, Yamamoto R, Wirschell M, Yagi T, Bower R, Porter ME, Sale WS, Kamiya R. 2009. A novel ankyrin-repeat protein interacts with the regulatory proteins of inner arm dynein f (I1) of Chlamydomonas reinhardtii. *Cell motility and the cytoskeleton* **66**: 448-456.

Insinna C, Besharse JC. 2008. Intraflagellar transport and the sensory outer segment of vertebrate photoreceptors. *Dev Dyn* **237**: 1982-1992.

Ishikawa H, Marshall WF. 2011. Ciliogenesis: building the cell's antenna. *Nat Rev Mol Cell Biol* **12**: 222-234.

Ishikawa T. 2012. Structural biology of cytoplasmic and axonemal dyneins. *J Struct Biol* **179**: 229-234.

Jauregui AR, Nguyen KC, Hall DH, Barr MM. 2008. The Caenorhabditis elegans nephrocystins act as global modifiers of cilium structure. *The Journal of cell biology* **180**: 973-988.

Johnson KA, Rosenbaum JL. 1992. Polarity of flagellar assembly in *Chlamydomonas*. *The Journal of cell biology* **119**: 1605-1611.

Jones C, Roper VC, Foucher I, Qian D, Banizs B, Petit C, Yoder BK, Chen P. 2008. Ciliary proteins link basal body polarization to planar cell polarity regulation. *Nature genetics* **40**: 69-77.

Kagami O, Kamiya R. 1992. Translocation and Rotation of Microtubules Caused by Multiple Species of Chlamydomonas Inner-Arm Dynein. *Journal of cell science* **103**: 653-664.

Kamiya R. 1991. Selection of Chlamydomonas dynein mutants. *Methods in enzymology* **196**: 348-355.

Kamiya R, Kurimoto E, Muto E. 1991. Two types of *Chlamydomonas* flagellar mutants missing different components of inner-arm dynein. *The Journal of cell biology* **112**: 441-447.

Kamiya R, Yagi T. 2014. Functional diversity of axonemal dyneins as assessed by in vitro and in vivo motility assays of chlamydomonas mutants. *Zoolog Sci* **31**: 633-644.

Karki S, Holzbaur EL. 1999. Cytoplasmic dynein and dynactin in cell division and intracellular transport. *Current opinion in cell biology* **11**: 45-53.

Keady BT, Samtani R, Tobita K, Tsuchya M, San Agustin JT, Follit JA, Jonassen JA, Subramanian R, Lo CW, Pazour GJ. 2012. IFT25 links the signal-dependent movement of Hedgehog components to intraflagellar transport. *Dev Cell* **22**: 940-951.

Kee HL, Dishinger JF, Blasius TL, Liu CJ, Margolis B, Verhey KJ. 2012. A size-exclusion permeability barrier and nucleoporins characterize a ciliary pore complex that regulates transport into cilia. *Nat Cell Biol* **14**: 431-437.

Kelekar P, Wei M, Yang P. 2009. Isolation and analysis of radial spoke proteins. *Methods in cell biology* **92**: 181-196.

Kennedy MP, Omran H, Leigh MW, Dell S, Morgan L, Molina PL, Robinson BV, Minnix SL, Olbrich H, Severin T et al. 2007. Congenital heart disease and other heterotaxic defects in a large cohort of patients with primary ciliary dyskinesia. *Circulation* **115**: 2814-2821.

Kikkawa M. 2013. Big steps toward understanding dynein. *The Journal of cell biology* **202**: 15-23.

Kim H, Xu H, Yao Q, Li W, Huang Q, Outeda P, Cebotaru V, Chiaravalli M, Boletta A, Piontek K et al. 2014. Ciliary membrane proteins traffic through the Golgi via a Rabep1/GGA1/Arl3-dependent mechanism. *Nature communications* **5**: 5482.

Kim S, Dynlacht BD. 2013. Assembling a primary cilium. *Curr Opin Cell Biol* **25**: 506-511.

King SJ, Dutcher SK. 1997. Phosphoregulation of an inner dynein arm complex in Chlamydomonas reinhardtii is altered in phototactic mutant strains. *The Journal of cell biology* **136**: 177-191.

King SM. 2012. Integrated control of axonemal dynein AAA(+) motors. *J Struct Biol* **179**: 222-228.

-. 2013. Biochemical and physiological analysis of axonemal dyneins. *Methods in enzymology* **524**: 123-145.

King SM, Kamiya R. 2009. Axonemal Dyneins: Assembly, Structure, and Force Generation. in *The Chlamydomonas Sourcebook: Cell Motility and Behavior* (ed. GB Witman), pp. 131-208. Academic Press, Oxford.

Knowles MR, Daniels LA, Davis SD, Zariwala MA, Leigh MW. 2013a. Primary ciliary dyskinesia. Recent advances in diagnostics, genetics, and characterization of clinical disease. *Am J Respir Crit Care Med* **188**: 913-922.

Knowles MR, Leigh MW, Ostrowski LE, Huang L, Carson JL, Hazucha MJ, Yin W, Berg JS, Davis SD, Dell SD et al. 2013b. Exome sequencing identifies mutations in CCDC114 as a cause of primary ciliary dyskinesia. *American journal of human genetics* **92**: 99-106.

Knowles MR, Leigh MW, Zariwala MA. 2012. Cutting edge genetic studies in primary ciliary dyskinesia. *Thorax* **67**: 464; author reply 464.

Knowles MR, Ostrowski LE, Loges NT, Hurd T, Leigh MW, Huang L, Wolf WE, Carson JL, Hazucha MJ, Yin W et al. 2013c. Mutations in SPAG1 cause primary ciliary dyskinesia associated with defective outer and inner dynein arms. *American journal of human genetics* **93**: 711-720.

Kobayashi D, Takeda H. 2012. Ciliary motility: the components and cytoplasmic preassembly mechanisms of the axonemal dyneins. *Differentiation* **83**: S23-29.

Koefoed K, Veland IR, Pedersen LB, Larsen LA, Christensen ST. 2014. Cilia and coordination of signaling networks during heart development. *Organogenesis* **10**: 108-125.

Komatsu Y, Mishina Y. 2013. Establishment of left-right asymmetry in vertebrate development: the node in mouse embryos. *Cell Mol Life Sci* **70**: 4659-4666.

Kon T, Oyama T, Shimo-Kon R, Imamula K, Shima T, Sutoh K, Kurisu G. 2012. The 2.8 A crystal structure of the dynein motor domain. *Nature* **484**: 345-350.

Kon T, Sutoh K, Kurisu G. 2011. X-ray structure of a functional full-length dynein motor domain. *Nat Struct Mol Biol* **18**: 638-642.

Kotani N, Sakakibara H, Burgess SA, Kojima H, Oiwa K. 2007. Mechanical properties of inner-arm dynein-f (dynein I1) studied with in vitro motility assays. *Biophysical journal* **93**: 886-894.

Kozminski KG. 2012. Intraflagellar transport--the "new motility" 20 years later. *Molecular biology of the cell* **23**: 751-753.

Kozminski KG, Beech PL, Rosenbaum JL. 1995. The *Chlamydomonas* kinesin-like protein FLA10 is involved in motility associated with the flagellar membrane. *The Journal of cell biology* **131**: 1517-1527.

Kozminski KG, Forscher P, Rosenbaum JL. 1998. Three flagellar motilities in Chlamydomonas unrelated to flagellar beating. Video supplement. *Cell motility and the cytoskeleton* **39**: 347-348.

Kozminski KG, Johnson KA, Forscher P, Rosenbaum JL. 1993. A motility in the eukaryotic flagellum unrelated to flagellar beating. *Proceedings of the National Academy of Sciences of the United States of America* **90**: 5519-5523.

Kubo T, Yagi T, Kamiya R. 2012. Tubulin polyglutamylation regulates flagellar motility by controlling a specific inner-arm dynein that interacts with the dynein regulatory complex. *Cytoskeleton (Hoboken)* **69**: 1059-1068.

Kurkowiak M, Zietkiewicz E, Witt M. 2015. Recent advances in primary ciliary dyskinesia genetics. *J Med Genet* **52**: 1-9.

Larkins CE, Aviles GD, East MP, Kahn RA, Caspary T. 2011. Arl13b regulates ciliogenesis and the dynamic localization of Shh signaling proteins. *Mol Biol Cell* **22**: 4694-4703.

Larkins CE, Long AB, Caspary T. 2012. Defective Nodal and Cerl2 expression in the Arl13b(hnn) mutant node underlie its heterotaxia. *Dev Biol* **367**: 15-24.

Lechtreck KF. 2013. In vivo imaging of IFT in Chlamydomonas flagella. *Methods in enzymology* **524**: 265-284.

Lechtreck KF, Delmotte P, Robinson ML, Sanderson MJ, Witman GB. 2008. Mutations in Hydin impair ciliary motility in mice. *The Journal of cell biology* **180**: 633-643.

Lechtreck KF, Gould TJ, Witman GB. 2013. Flagellar central pair assembly in Chlamydomonas reinhardtii. *Cilia* **2**: 15.

Lechtreck KF, Johnson EC, Sakai T, Cochran D, Ballif BA, Rush J, Pazour GJ, Ikebe M, Witman GB. 2009. The Chlamydomonas reinhardtii BBSome is an IFT cargo required for export of specific signaling proteins from flagella. *The Journal of cell biology* **187**: 1117-1132.

Lefebvre PA, Nordstrom SA, Moulder JE, Rosenbaum JL. 1978. Flagellar elongation and shortening in *Chlamydomonas*. IV. Effects of flagellar detachment, regeneration, and resorption on the induction of flagellar protein synthesis. *The Journal of cell biology* **78**: 8-27.

Lefebvre PA, Rosenbaum JL. 1986. Regulation of the synthesis and assembly of ciliary and flagellar proteins during regeneration. *Annu Rev Cell Biol* **2**: 517-546.

Lehman JM, Michaud EJ, Schoeb TR, Aydin-Son Y, Miller M, Yoder BK. 2008. The Oak Ridge Polycystic Kidney mouse: modeling ciliopathies of mice and men. *Developmental dynamics : an official publication of the American Association of Anatomists* **237**: 1960-1971.

Li JB, Gerdes JM, Haycraft CJ, Fan Y, Teslovich TM, May-Simera H, Li H, Blacque OE, Li L, Leitch CC et al. 2004. Comparative genomics identifies a flagellar and basal body proteome that includes the BBS5 human disease gene. *Cell* **117**: 541-552.

Lin H, Goodenough UW. 2007. Gametogenesis in the Chlamydomonas reinhardtii minus mating type is controlled by two genes, MID and MTD1. *Genetics* **176**: 913-925.

Lin J, Heuser T, Carbajal-Gonzalez BI, Song K, Nicastro D. 2012. The structural heterogeneity of radial spokes in cilia and flagella is conserved. *Cytoskeleton (Hoboken)* **69**: 88-100.

Lin J, Tritschler D, Song K, Barber CF, Cobb JS, Porter ME, Nicastro D. 2011. Building blocks of the nexin-dynein regulatory complex in Chlamydomonas flagella. *The Journal of biological chemistry* **286**: 29175-29191.

Linck R, Fu X, Lin J, Ouch C, Schefter A, Steffen W, Warren P, Nicastro D. 2014. Insights into the structure and function of ciliary and flagellar doublet microtubules: tektins, Ca2+-binding proteins, and stable protofilaments. *J Biol Chem* **289**: 17427-17444.

Linck RW, Stephens RE. 2007. Functional protofilament numbering of ciliary, flagellar, and centriolar microtubules. *Cell Motil Cytoskeleton* **64**: 489-495.

Loges NT, Olbrich H, Becker-Heck A, Haffner K, Heer A, Reinhard C, Schmidts M, Kispert A, Zariwala MA, Leigh MW et al. 2009. Deletions and point mutations of LRRC50 cause primary ciliary dyskinesia due to dynein arm defects. *American journal of human genetics* **85**: 883-889.

Loges NT, Olbrich H, Fenske L, Mussaffi H, Horvath J, Fliegauf M, Kuhl H, Baktai G, Peterffy E, Chodhari R et al. 2008. DNAI2 mutations cause primary ciliary dyskinesia with defects in the outer dynein arm. *American journal of human genetics* **83**: 547-558.

Luck D, Piperno G, Ramanis Z, Huang B. 1977. Flagellar mutants of Chlamydomonas: studies of radial spoke-defective strains by dikaryon and revertant analysis. *Proceedings of the National Academy of Sciences of the United States of America* **74**: 3456-3460.

Ludington WB, Wemmer KA, Lechtreck KF, Witman GB, Marshall WF. 2013. Avalanche-like behavior in ciliary import. *Proceedings of the National Academy of Sciences of the United States of America* **110**: 3925-3930.

Maday S, Twelvetrees AE, Moughamian AJ, Holzbaur EL. 2014. Axonal transport: cargo-specific mechanisms of motility and regulation. *Neuron* **84**: 292-309.

Malicki J, Avidor-Reiss T. 2014. From the cytoplasm into the cilium: bon voyage. *Organogenesis* **10**: 138-157.

Malicki J, Besharse JC. 2012. Kinesin-2 family motors in the unusual photoreceptor cilium. *Vision Res* **75**: 33-36.

Marshall WF. 2008. The cell biological basis of ciliary disease. *The Journal of cell biology* **180**: 17-21.

-. 2010. Cilia self-organize in response to planar cell polarity and flow. *Nat Cell Biol* **12**: 314-315.

Marshall WF, Kintner C. 2008. Cilia orientation and the fluid mechanics of development. *Curr Opin Cell Biol* **20**: 48-52.

Marszalek JR, Ruiz-Lozano P, Roberts E, Chien KR, Goldstein LS. 1999. Situs inversus and embryonic ciliary morphogenesis defects in mouse mutants lacking the KIF3A subunit of kinesin-II. *Proceedings of the National Academy of Sciences of the United States of America* **96**: 5043-5048.

Mastronarde DN, O'Toole ET, McDonald KL, McIntosh JR, Porter ME. 1992. Arrangement of inner dynein arms in wild-type and mutant flagella of *Chlamydomonas*. *The Journal of cell biology* **118**: 1145-1162.

McGrath J, Brueckner M. 2003. Cilia are at the heart of vertebrate left-right asymmetry. *Curr Opin Genet Dev* **13**: 385-392.

McGrath J, Somlo S, Makova S, Tian X, Brueckner M. 2003. Two populations of node monocilia initiate left-right asymmetry in the mouse. *Cell* **114**: 61-73.

Mitchell B, Stubbs JL, Huisman F, Taborek P, Yu C, Kintner C. 2009. The PCP pathway instructs the planar orientation of ciliated cells in the Xenopus larval skin. *Curr Biol* **19**: 924-929.

Mitchell DR, Nakatsugawa M. 2004. Bend propagation drives central pair rotation in Chlamydomonas reinhardtii flagella. *The Journal of cell biology* **166**: 709-715.

Mitchell DR, Yokoyama R. 2003. Structural Analysis of Central Pair Function in Chlamydomonas Flagella. *Molecular biology of the cell* **14**: 436a.

Mitchison HM, Schmidts M, Loges NT, Freshour J, Dritsoula A, Hirst RA, O'Callaghan C, Blau H, Al Dabbagh M, Olbrich H et al. 2012. Mutations in axonemal dynein assembly factor DNAAF3 cause primary ciliary dyskinesia. *Nature genetics* **44**: 381-389, S381-382.

Moore DJ, Onoufriadis A, Shoemark A, Simpson MA, zur Lage PI, de Castro SC, Bartoloni L, Gallone G, Petridi S, Woollard WJ et al. 2013. Mutations in ZMYND10, a gene essential for proper axonemal assembly of inner and outer dynein arms in humans and flies, cause primary ciliary dyskinesia. *American journal of human genetics* **93**: 346-356.

Moss AG, Pazour GJ, Witman GB. 1995. Assay of Chlamydomonas phototaxis. *Methods in cell biology* **47**: 281-287.

Mourao A, Nager AR, Nachury MV, Lorentzen E. 2014. Structural basis for membrane targeting of the BBSome by ARL6. *Nature structural & molecular biology* **21**: 1035-1041.

Mueller J, Perrone CA, Bower R, Cole DG, Porter ME. 2005. The FLA3 KAP subunit is required for localization of kinesin-2 to the site of flagellar assembly and processive anterograde intraflagellar transport. *Mol Biol Cell* **16**: 1341-1354.

Myster SH, Knott JA, O'Toole E, Porter ME. 1997. The Chlamydomonas Dhc1 gene encodes a dynein heavy chain subunit required for assembly of the I1 inner arm complex. *Molecular biology of the cell* **8**: 607-620.

Myster SH, Knott JA, Wysocki KM, O'Toole E, Porter ME. 1999. Domains in the 1alpha dynein heavy chain required for inner arm assembly and flagellar motility in Chlamydomonas. *The Journal of cell biology* **146**: 801-818.

Nachury MV, Seeley ES, Jin H. 2010. Trafficking to the Ciliary Membrane: How to Get Across the Periciliary Diffusion Barrier? *Annual Review of Cell and Developmental Biology, Vol 26* **26**: 59-87.

Nakazawa Y, Ariyoshi T, Noga A, Kamiya R, Hirono M. 2014. Space-dependent formation of central pair microtubules and their interactions with radial spokes. *PLoS One* **9**: e110513.

Nauli SM, Alenghat FJ, Luo Y, Williams E, Vassilev P, Li X, Elia AE, Lu W, Brown EM, Quinn SJ et al. 2003. Polycystins 1 and 2 mediate mechanosensation in the primary cilium of kidney cells. *Nat Genet* **33**: 129-137.

Nauli SM, Jin X, AbouAlaiwi WA, El-Jouni W, Su X, Zhou J. 2013. Non-motile primary cilia as fluid shear stress mechanosensors. *Methods Enzymol* **525**: 1-20.

Nicastro D. 2009. Cryo-electron microscope tomography to study axonemal organization. *Methods in cell biology* **91**: 1-39.

Nicastro D, Schwartz C, Pierson J, Gaudette R, Porter ME, McIntosh JR. 2006. The molecular architecture of axonemes revealed by cryoelectron tomography. *Science* **313**: 944-948.

Nonaka S, Tanaka Y, Okada Y, Takeda S, Harada A, Kanai Y, Kido M, Hirokawa N. 1998. Randomization of left-right asymmetry due to loss of nodal cilia generating leftward flow of extraembryonic fluid in mice lacking KIF3B motor protein. *Cell* **95**: 829-837.

Oda T, Kikkawa M. 2013. Novel structural labeling method using cryo-electron tomography and biotin-streptavidin system. *J Struct Biol* **183**: 305-311.

Oda T, Yanagisawa H, Kamiya R, Kikkawa M. 2014a. Cilia and flagella. A molecular ruler determines the repeat length in eukaryotic cilia and flagella. *Science* **346**: 857-860.

Oda T, Yanagisawa H, Yagi T, Kikkawa M. 2014b. Mechanosignaling between central apparatus and radial spokes controls axonemal dynein activity. *The Journal of cell biology* **204**: 807-819.

Oh EC, Katsanis N. 2012. Cilia in vertebrate development and disease. *Development* **139**: 443-448.

Oiwa K, Sakakibara H. 2005. Recent progress in dynein structure and mechanism. *Curr Opin Cell Biol* **17**: 98-103.

Okita N, Isogai N, Hirono M, Kamiya R, Yoshimura K. 2005. Phototactic activity in Chlamydomonas 'non-phototactic' mutants deficient in Ca2+-dependent control of flagellar dominance or in inner-arm dynein. *Journal of cell science* **118**: 529-537.

Olbrich H, Schmidts M, Werner C, Onoufriadis A, Loges NT, Raidt J, Banki NF, Shoemark A, Burgoyne T, Al Turki S et al. 2012. Recessive HYDIN mutations cause primary ciliary dyskinesia without randomization of left-right body asymmetry. *American journal of human genetics* **91**: 672-684.

Omoto CK, Witman GB. 1981. Functionally significant central-pair rotation in a primitive eukaryotic flagellum. *Nature* **290**: 708-710.

Omran H, Kobayashi D, Olbrich H, Tsukahara T, Loges NT, Hagiwara H, Zhang Q, Leblond G, O'Toole E, Hara C et al. 2008. Ktu/PF13 is required for cytoplasmic pre-assembly of axonemal dyneins. *Nature* **456**: 611-616.

Onoufriadis A, Shoemark A, Munye MM, James CT, Schmidts M, Patel M, Rosser EM, Bacchelli C, Beales PL, Scambler PJ et al. 2014. Combined exome and whole-genome sequencing identifies mutations in ARMC4 as a cause of primary ciliary dyskinesia with defects in the outer dynein arm. *J Med Genet* **51**: 61-67.

Ori-McKenney KM, McKenney RJ, Vallee RB. 2012. Studies of Lissencephaly and Neurodegenerative Disease Reveal Novel Aspects of Cytoplasmic Dynein Regulation. *Dyneins: Structure, Biology and Disease*: 441-453.

Ostrowski LE, Dutcher SK, Lo CW. 2011. Cilia and models for studying structure and function. *Proc Am Thorac Soc* **8**: 423-429.

Owa M, Furuta A, Usukura J, Arisaka F, King SM, Witman GB, Kamiya R, Wakabayashi K. 2014. Cooperative binding of the outer arm-docking complex underlies the regular arrangement of outer arm dynein in the axoneme. *Proc Natl Acad Sci U S A* **111**: 9461-9466.

Pan J, Snell WJ. 2000. Signal transduction during fertilization in the unicellular green alga, Chlamydomonas. *Curr Opin Microbiol* **3**: 596-602.

-. 2002. Kinesin-II is required for flagellar sensory transduction during fertilization in Chlamydomonas. *Molecular biology of the cell* **13**: 1417-1426.

Panizzi JR, Becker-Heck A, Castleman VH, Al-Mutairi DA, Liu Y, Loges NT, Pathak N, Austin-Tse C, Sheridan E, Schmidts M et al. 2012. CCDC103 mutations cause primary ciliary dyskinesia by disrupting assembly of ciliary dynein arms. *Nature genetics* **44**: 714-719.

Paschal BM, Shpetner HS, Vallee RB. 1987. MAP 1C is a microtubule-activated ATPase which translocates microtubules in vitro and has dynein-like properties. *The Journal of cell biology* **105**: 1273-1282.

Pazour GJ. 2004. Intraflagellar transport and cilia-dependent renal disease: the ciliary hypothesis of polycystic kidney disease. *J Am Soc Nephrol* **15**: 2528-2536.

Pazour GJ, Baker SA, Deane JA, Cole DG, Dickert BL, Rosenbaum JL, Witman GB, Besharse JC. 2002a. The intraflagellar transport protein, IFT88, is essential for vertebrate photoreceptor assembly and maintenance. *The Journal of cell biology* **157**: 103-113.

Pazour GJ, Dickert BL, Vucica Y, Seeley ES, Rosenbaum JL, Witman GB, Cole DG. 2000. Chlamydomonas IFT88 and its mouse homologue, polycystic kidney disease gene tg737, are required for assembly of cilia and flagella. *The Journal of cell biology* **151**: 709-718.

Pazour GJ, Dickert BL, Witman GB. 1998. The DHC1b (DHC2) isoform of cytoplasmic dynein is required for flagellar assembly. *Mol Biol Cell* **9**: 131A-131A.

Pazour GJ, San Agustin JT, Follit JA, Rosenbaum JL, Witman GB. 2002b. Polycystin-2 localizes to kidney cilia and the ciliary level is elevated in orpk mice with polycystic kidney disease. *Current biology : CB* **12**: R378-380.

Pazour GJ, Sineschekov OA, Witman GB. 1995. Mutational analysis of the phototransduction pathway of *Chlamydomonas reinhardtii*. *The Journal of cell biology* **131**: 427-440.

Pazour GJ, Witman GB. 2003. The vertebrate primary cilium is a sensory organelle. *Curr Opin Cell Biol* **15**: 105-110.

Pedersen LB, Rosenbaum JL. 2008. Intraflagellar transport (IFT) role in ciliary assembly, resorption and signalling. *Current topics in developmental biology* **85**: 23-61.

Perrone CA, Myster SH, Bower R, O'Toole ET, Porter ME. 2000. Insights into the structural organization of the I1 inner arm dynein from a domain analysis of the 1beta dynein heavy chain. *Molecular biology of the cell* **11**: 2297-2313.

Perrone CA, Yang P, O'Toole E, Sale WS, Porter ME. 1998. The Chlamydomonas IDA7 locus encodes a 140-kDa dynein intermediate chain required to assemble the I1 inner arm complex. *Molecular biology of the cell* **9**: 3351-3365.

Pigino G, Bui KH, Maheshwari A, Lupetti P, Diener D, Ishikawa T. 2011. Cryoelectron tomography of radial spokes in cilia and flagella. *The Journal of cell biology* **195**: 673-687.

Pigino G, Ishikawa T. 2012. Axonemal radial spokes: 3D structure, function and assembly. *Bioarchitecture* **2**: 50-58.

Piperno G, Mead K. 1997. Transport of a novel complex in the cytoplasmic matrix of *Chlamydomonas* flagella. *Proceedings of the National Academy of Sciences of the United States of America* **94**: 4457-4462.

Piperno G, Mead K, Henderson S. 1996. Inner dynein arms but not outer dynein arms require the activity of kinesin homologue protein KHP1(FLA10) to reach the distal part of flagella in *Chlamydomonas*. *The Journal of cell biology* **133**: 371-379.

Piperno G, Ramanis Z, Smith EF, Sale WS. 1990. Three distinct inner dynein arms in Chlamydomonas flagella: molecular composition and location in the axoneme. *The Journal of cell biology* **110**: 379-389.

Porter ME. 2012. Flagellar Motility and the Dynein Regulatory Complex. *Dyneins: Structure, Biology and Disease*: 337-365.

Porter ME, Bower R, Knott JA, Byrd P, Dentler W. 1999. Cytoplasmic dynein heavy chain 1b is required for flagellar assembly in *Chlamydomonas*. *Molecular biology of the cell* **10**: 693-712.

Porter ME, Power J, Dutcher SK. 1992. Extragenic suppressors of paralyzed flagellar mutations in *Chlamydomonas reinhardtii* identify loci that alter the inner dynein arms. *The Journal of cell biology* **118**: 1163-1176.

Porter ME, Sale WS. 2000. The 9 + 2 axoneme anchors multiple inner arm dyneins and a network of kinases and phosphatases that control motility. *The Journal of cell biology* **151**: F37-42.

Praetorius HA, Spring KR. 2003a. Removal of the MDCK cell primary cilium abolishes flow sensing. *J Membr Biol* **191**: 69-76.

-. 2003b. The renal cell primary cilium functions as a flow sensor. *Curr Opin Nephrol Hypertens* **12**: 517-520.

Qin H, Diener DR, Geimer S, Cole DG, Rosenbaum JL. 2004. Intraflagellar transport (IFT) cargo: IFT transports flagellar precursors to the tip and turnover products to the cell body. *The Journal of cell biology* **164**: 255-266.

Qin H, Rosenbaum JL, Barr MM. 2001. An autosomal recessive polycystic kidney disease gene homolog is involved in intraflagellar transport in C. elegans ciliated sensory neurons. *Current biology : CB* **11**: 457-461.

Rao Damerla R, Gabriel GC, Li Y, Klena NT, Liu X, Chen Y, Cui C, Pazour GJ, Lo CW. 2014. Role of cilia in structural birth defects: insights from ciliopathy mutant mouse models. *Birth Defects Res C Embryo Today* **102**: 115-125.

Reck-Peterson SL, Yildiz A, Carter AP, Gennerich A, Zhang N, Vale RD. 2006. Single-Molecule Analysis of Dynein Processivity and Stepping Behavior. *Cell* **126**: 335-348.

Redwine WB, Hernandez-Lopez R, Zou S, Huang J, Reck-Peterson SL, Leschziner AE. 2012. Structural basis for microtubule binding and release by dynein. *Science* **337**: 1532-1536.

Reiter JF, Blacque OE, Leroux MR. 2012. The base of the cilium: roles for transition fibres and the transition zone in ciliary formation, maintenance and compartmentalization. *EMBO Rep* **13**: 608-618.

Richey E, Qin H. 2013. Isolation of intraflagellar transport particle proteins from Chlamydomonas reinhardtii. *Methods in enzymology* **524**: 1-17.

Roberts AJ, Kon T, Knight PJ, Sutoh K, Burgess SA. 2013. Functions and mechanics of dynein motor proteins. *Nature reviews Molecular cell biology* **14**: 713-726.

Rosenbaum JL, Moulder JE, Ringo DL. 1969. Flagellar elongation and shortening in *Chlamydomonas*. The use of cycloheximide and colchicine to study the synthesis and assembly of flagellar proteins. *The Journal of cell biology* **41**: 600-619.

Rosenbaum JL, Witman GB. 2002. Intraflagellar transport. *Nat Rev Mol Cell Biol* **3**: 813-825.

Satir P. 1998. Keith Roberts Porter: a modern Malpighi. *The Anatomical record* **253**: 39-40.

-. 2012. The new biology of cilia: review and annotation of a symposium. *Developmental dynamics : an official publication of the American Association of Anatomists* **241**: 426-430.

Satir P, Christensen ST. 2007. Overview of structure and function of mammalian cilia. *Annual review of physiology* **69**: 377-400.

Satir P, Heuser T, Sale WS. 2014. A Structural Basis for How Motile Cilia Beat. *Bioscience* **64**: 1073-1083.

Satir P, Pedersen LB, Christensen ST. 2010. The primary cilium at a glance. *Journal of cell science* **123**: 499-503.

Scholey JM. 2008. Intraflagellar transport motors in cilia: moving along the cell's antenna. *The Journal of cell biology* **180**: 23-29.

-. 2012. Kinesin-2 motors transport IFT-particles, dyneins and tubulin subunits to the tips of Caenorhabditis elegans sensory cilia: relevance to vision research? *Vision Res* **75**: 44-52.

-. 2013a. Cilium assembly: delivery of tubulin by kinesin-2-powered trains. *Curr Biol* **23**: R956-959.

-. 2013b. Kinesin-2: a family of heterotrimeric and homodimeric motors with diverse intracellular transport functions. *Annu Rev Cell Dev Biol* **29**: 443-469.

Scholey JM, Anderson KV. 2006. Intraflagellar transport and cilium-based signaling. *Cell* **125**: 439-442.

Scholey JM, Ou G, Snow J, Gunnarson A. 2004. Intraflagellar transport motors in Caenorhabditis elegans neurons. *Biochem Soc Trans* **32**: 682-684.

Schroeder CM, Ostrem JM, Hertz NT, Vale RD. 2014. A Ras-like domain in the light intermediate chain bridges the dynein motor to a cargo-binding region. *Elife* **3**: e03351.

Shaner NC, Lambert GG, Chammas A, Ni Y, Cranfill PJ, Baird MA, Sell BR, Allen JR, Day RN, Israelsson M et al. 2013. A bright monomeric green fluorescent protein derived from Branchiostoma lanceolatum. *Nat Methods* **10**: 407-409.

Sharma N, Berbari NF, Yoder BK. 2008. Ciliary dysfunction in developmental abnormalities and diseases. *Current topics in developmental biology* **85**: 371-427.

Silflow CD, Lefebvre PA. 2001. Assembly and motility of eukaryotic cilia and flagella. Lessons from *Chlamydomonas reinhardtii*. *Plant Physiol* **127**: 1500-1507.

Smith EF, Rohatgi R. 2011. Cilia 2010: the surprise organelle of the decade. *Sci Signal* **4**: mr1.

Smith EF, Sale WS. 1991. Microtubule binding and translocation by inner dynein arm subtype I1. *Cell motility and the cytoskeleton* **18**: 258-268.

-. 1992. Structural and functional reconstitution of inner dynein arms in *Chlamydomonas* flagellar axonemes. *The Journal of cell biology* **117**: 573-581.

Smith EF, Yang P. 2004. The radial spokes and central apparatus: mechano-chemical transducers that regulate flagellar motility. *Cell motility and the cytoskeleton* **57**: 8-17.

Snow JJ, Ou G, Gunnarson AL, Walker MR, Zhou HM, Brust-Mascher I, Scholey JM. 2004. Two anterograde intraflagellar transport motors cooperate to build sensory cilia on C. elegans neurons. *Nat Cell Biol* **6**: 1109-1113.

Song K, Awata J, Tritschler D, Bower R, Witman GB, Porter ME, Nicastro D. 2015. In situ localization of N- and C-termini of subunits of the flagellar nexin-dynein regulatory complex (N-DRC) using SNAP-tag and cryo-electron tomography. *The Journal of biological chemistry*.

Stephens RE. 1994. Tubulin and tektin in sea urchin embryonic cilia: pathways of protein incorporation during turnover and regeneration. *Journal of cell science* **107 (Pt 2)**: 683-692.

Supp DM, Witte DP, Potter SS, Brueckner M. 1997. Mutation of an axonemal dynein affects left-right asymmetry in inversus viscerum mice. *Nature* **389**: 963-966.

Takada S, Kamiya R. 1994. Functional reconstitution of Chlamydomonas outer dynein arms from alpha-beta and gamma subunits: requirement of a third factor. *The Journal of cell biology* **126**: 737-745.

Takada S, Sakakibara H, Kamiya R. 1992. Three-headed outer arm dynein from Chlamydomonas that can functionally combine with outer-arm-missing axonemes. *J Biochem* **111**: 758-762.

Takada S, Wilkerson CG, Wakabayashi K, Kamiya R, Witman GB. 2002. The outer dynein arm-docking complex: composition and characterization of a subunit

(oda1) necessary for outer arm assembly. *Molecular biology of the cell* **13**: 1015-1029.

Takao D, Dishinger JF, Kee HL, Pinskey JM, Allen BL, Verhey KJ. 2014. An assay for clogging the ciliary pore complex distinguishes mechanisms of cytosolic and membrane protein entry. *Curr Biol* **24**: 2288-2294.

Takeda S, Yonekawa Y, Tanaka Y, Okada Y, Nonaka S, Hirokawa N. 1999. Left-right asymmetry and kinesin superfamily protein KIF3A: new insights in determination of laterality and mesoderm induction by kif3A-/- mice analysis. *J Cell Biol* **145**: 825-836.

Takiar V, Caplan MJ. 2011. Polycystic kidney disease: pathogenesis and potential therapies. *Biochim Biophys Acta* **1812**: 1337-1343.

Tanaka Y, Okada Y, Hirokawa N. 2005. FGF-induced vesicular release of Sonic hedgehog and retinoic acid in leftward nodal flow is critical for left-right determination. *Nature* **435**: 172-177.

Tanner CA, Rompolas P, Patel-King RS, Gorbatyuk O, Wakabayashi K, Pazour GJ, King SM. 2008. Three members of the LC8/DYNLL family are required for outer arm dynein motor function. *Molecular biology of the cell* **19**: 3724-3734.

Taulman PD, Haycraft CJ, Balkovetz DF, Yoder BK. 2001. Polaris, a protein involved in left-right axis patterning, localizes to basal bodies and cilia. *Mol Biol Cell* **12**: 589-599.

Thomas S, Cantagrel V, Mariani L, Serre V, Lee JE, Elkhartoufi N, de Lonlay P, Desguerre I, Munnich A, Boddaert N et al. 2014. Identification of a novel

ARL13B variant in a Joubert syndrome-affected patient with retinal impairment and obesity. *Eur J Hum Genet*.

Toba S, Fox LA, Sakakibara H, Porter ME, Oiwa K, Sale WS. 2011. Distinct roles of 1alpha and 1beta heavy chains of the inner arm dynein I1 of Chlamydomonas flagella. *Molecular biology of the cell* **22**: 342-353.

Vallee RB, Williams JC, Varma D, Barnhart LE. 2004. Dynein: An ancient motor protein involved in multiple modes of transport. *Journal of neurobiology* **58**: 189-200.

VanderWaal KE, Yamamoto R, Wakabayashi K, Fox L, Kamiya R, Dutcher SK, Bayly PV, Sale WS, Porter ME. 2011. bop5 Mutations reveal new roles for the IC138 phosphoprotein in the regulation of flagellar motility and asymmetric waveforms. *Molecular biology of the cell* **22**: 2862-2874.

Vashishtha M, Walther Z, Hall JL. 1996. The kinesin-homologous protein encoded by the Chlamydomonas FLA10 gene is associated with basal bodies and centrioles. *Journal of cell science* **109 (Pt 3)**: 541-549.

Veland IR, Awan A, Pedersen LB, Yoder BK, Christensen ST. 2009. Primary cilia and signaling pathways in mammalian development, health and disease. *Nephron Physiol* **111**: p39-53.

Verhey KJ, Dishinger J, Kee HL. 2011. Kinesin motors and primary cilia. *Biochem Soc Trans* **39**: 1120-1125.

Viswanadha R, Hunter EL, Yamamoto R, Wirschell M, Alford LM, Dutcher SK, Sale WS. 2014. The ciliary inner dynein arm, I1 dynein, is assembled in the

cytoplasm and transported by IFT before axonemal docking. *Cytoskeleton (Hoboken)* **71**: 573-586.

Wallingford JB. 2012. Planar cell polarity and the developmental control of cell behavior in vertebrate embryos. *Annual review of cell and developmental biology* **28**: 627-653.

Wallingford JB, Mitchell B. 2011. Strange as it may seem: the many links between Wnt signaling, planar cell polarity, and cilia. *Genes Dev* **25**: 201-213.

Walther Z, Vashishtha M, Hall JL. 1994. The Chlamydomonas FLA10 gene encodes a novel kinesin-homologous protein. *The Journal of cell biology* **126**: 175-188.

Wang Q, Pan J, Snell WJ. 2006. Intraflagellar transport particles participate directly in cilium-generated signaling in Chlamydomonas. *Cell* **125**: 549-562.

Warner FD, Satir P. 1974. The structural basis of ciliary bend formation. Radial spoke positional changes accompanying microtubule sliding. *The Journal of cell biology* **63**: 35-63.

Werner ME, Mitchell BJ. 2012. Planar cell polarity: microtubules make the connection with cilia. *Curr Biol* **22**: R1001-1004.

Wheway G, Parry DA, Johnson CA. 2014. The role of primary cilia in the development and disease of the retina. *Organogenesis* **10**: 69-85.

Wickstead B, Gull K. 2007. Dyneins across eukaryotes: a comparative genomic analysis. *Traffic* **8**: 1708-1721.

Wirschell M, Hendrickson T, Sale WS. 2007a. Keeping an eye on I1: I1 dynein as a model for flagellar dynein assembly and regulation. *Cell motility and the cytoskeleton* **64**: 569-579.

-. 2007b. Keeping an eye on I1: I1 dynein as a model for flagellar dynein assembly and regulation. *Cell motility and the cytoskeleton* **64**: 569-579.

Wirschell M, Pazour G, Yoda A, Hirono M, Kamiya R, Witman GB. 2004. Oda5p, a novel axonemal protein required for assembly of the outer dynein arm and an associated adenylate kinase. *Molecular biology of the cell* **15**: 2729-2741.

Wirschell M, Yang C, Yang P, Fox L, Yanagisawa HA, Kamiya R, Witman GB, Porter ME, Sale WS. 2009. IC97 is a novel intermediate chain of I1 dynein that interacts with tubulin and regulates interdoublet sliding. *Molecular biology of the cell* **20**: 3044-3054.

Witman GB. 1975. The site of in vivo assembly of flagellar microtubules. *Annals of the New York Academy of Sciences* **253**: 178-191.

-. 1986. Isolation of Chlamydomonas flagella and flagellar axonemes. *Methods in enzymology* **134**: 280-290.

Wood CR, Rosenbaum JL. 2014. Proteins of the ciliary axoneme are found on cytoplasmic membrane vesicles during growth of cilia. *Current biology : CB* **24**: 1114-1120.

Wren KN, Craft JM, Tritschler D, Schauer A, Patel DK, Smith EF, Porter ME, Kner P, Lechtreck KF. 2013. A differential cargo-loading model of ciliary length regulation by IFT. *Current biology : CB* **23**: 2463-2471.

Yagi T, Minoura I, Fujiwara A, Saito R, Yasunaga T, Hirono M, Kamiya R. 2005. An axonemal dynein particularly important for flagellar movement at high viscosity. Implications from a new Chlamydomonas mutant deficient in the

dynein heavy chain gene DHC9. *The Journal of biological chemistry* **280**: 41412-41420.

Yamamoto R, Song K, Yanagisawa HA, Fox L, Yagi T, Wirschell M, Hirono M, Kamiya R, Nicastro D, Sale WS. 2013. The MIA complex is a conserved and novel dynein regulator essential for normal ciliary motility. *The Journal of cell biology* **201**: 263-278.

Yamamoto R, Yagi T, Kamiya R. 2006. Functional binding of inner-arm dyneins with demembranated flagella of Chlamydomonas mutants. *Cell motility and the cytoskeleton* **63**: 258-265.

Yang C, Compton MM, Yang P. 2005. Dimeric novel HSP40 is incorporated into the radial spoke complex during the assembly process in flagella. *Molecular biology of the cell* **16**: 637-648.

Yang P, Diener DR, Rosenbaum JL, Sale WS. 2001. Localization of calmodulin and dynein light chain LC8 in flagellar radial spokes. *The Journal of cell biology* **153**: 1315-1326.

Yang P, Diener DR, Yang C, Kohno T, Pazour GJ, Dienes JM, Agrin NS, King SM, Sale WS, Kamiya R et al. 2006. Radial spoke proteins of Chlamydomonas flagella. *Journal of cell science* **119**: 1165-1174.

Yang P, Sale WS. 1998. The Mr 140,000 intermediate chain of Chlamydomonas flagellar inner arm dynein is a WD-repeat protein implicated in dynein arm anchoring. *Molecular biology of the cell* **9**: 3335-3349.

Yang P, Yang C, Wirschell M, Davis S. 2009. Novel LC8 mutations have disparate effects on the assembly and stability of flagellar complexes. *The Journal of biological chemistry* **284**: 31412-31421.

Ye F, Breslow DK, Koslover EF, Spakowitz AJ, Nelson WJ, Nachury MV. 2013. Single molecule imaging reveals a major role for diffusion in the exploration of ciliary space by signaling receptors. *Elife* **2**: e00654.

Yoder BK. 2007. Role of primary cilia in the pathogenesis of polycystic kidney disease. *Journal of the American Society of Nephrology : JASN* **18**: 1381-1388.

Yoder BK, Hou X, Guay-Woodford LM. 2002. The polycystic kidney disease proteins, polycystin-1, polycystin-2, polaris, and cystin, are co-localized in renal cilia. *Journal of the American Society of Nephrology : JASN* **13**: 2508-2516.

Yoshiba S, Hamada H. 2014. Roles of cilia, fluid flow, and Ca2+ signaling in breaking of left-right symmetry. *Trends Genet* **30**: 10-17.

Yuan S, Zhao L, Sun Z. 2013. Dissecting the functional interplay between the TOR pathway and the cilium in zebrafish. *Methods in enzymology* **525**: 159-189.

Zaghloul NA, Katsanis N. 2009. Mechanistic insights into Bardet-Biedl syndrome, a model ciliopathy. *The Journal of clinical investigation* **119**: 428-437.

Zariwala MA, Knowles MR, Omran H. 2007. Genetic defects in ciliary structure and function. *Annual review of physiology* **69**: 423-450.

Zariwala MA, Leigh MW, Ceppa F, Kennedy MP, Noone PG, Carson JL, Hazucha MJ, Lori A, Horvath J, Olbrich H et al. 2006. Mutations of DNAI1 in primary ciliary dyskinesia: evidence of founder effect in a common mutation. *Am J Respir Crit Care Med* **174**: 858-866.

Zariwala MA, Omran H, Ferkol TW. 2011. The emerging genetics of primary ciliary dyskinesia. *Proc Am Thorac Soc* **8**: 430-433.

Zhang Q, Murcia NS, Chittenden LR, Richards WG, Michaud EJ, Woychik RP, Yoder BK. 2003. Loss of the Tg737 protein results in skeletal patterning defects. *Dev Dyn* **227**: 78-90.

Zhou J. 2009. Polycystins and primary cilia: primers for cell cycle progression. *Annu Rev Physiol* **71**: 83-113.

Table 1: Outer Dynein Arms (ODAs) and Associated Proteins

Outer Dynein Arms (ODA)	Protein and aliases[a]	*Chlamydomonas* Gene (Original)	Mutant strains	*Chlamydomonas* Gene (Current)	Human Gene	Properties	References[d]
Heavy Chains	HC1α	*ODA11*	*oda11*	*DHC13*	-	ATPase/Microtubule motor	Kamiya (1988), Mitchell and Brown (1994; 1997)
	HC1β	*ODA4*	*oda4*	*DHC14*	*DNAH9,11,17*	ATPase/Microtubule motor	Kamiya (1988), Mitchell and Brown (1994)
	HC1γ	*ODA2*	*pf28*	*DHC15*	*DNAH5,8*	ATPase/Microtubule motor	Kamiya (1988), Mitchell and Rosenbaum (1985) Wilkerson et al. (1994)
Intermediate chains	**IC1**, IC78, IC80	*ODA9*	*oda9-1, oda9-2 (V5), oda9-3 (V8), oda9-4 (V24), oda9-5 (V27)*	*DIC1*	*DNAI1*	WD-repeat protein, binds a-tubulin, associates with multiple LCs	Kamiya (1988), Wilkerson et al. (1995)
	IC2, IC69, IC70	*ODA6*	*oda6-1, oda6-2*	*DIC2*	*DNAI2*	WD-repeat + coiled-coil protein, associates with multiple ICs	Kamiya (1988), Mitchell and Kang (1991)
Light Chains	LC1	-	-	*DLU1*	*DNAL1*	Leucine-rich repeat, binds **γ** HC motor domain	Patel-King and King (2009)
	LC2	*ODA12*	*oda12-1*[c] *,oda12-2*	*DLT2*	*TCTE3*	Homologue of Tctex2, required for outer arm assembly	Pazour et al. (1999)
	LC3	-	-	*DLX1*	-	Thioredoxin, associates with **β** and **γ** HCs and LC7b	Dibella et al. (2004), Wakabayashi and King (2006)
	LC4	-	-	*DLE1*	-	Ca^{2+} binding, **γ**HC-associated	Sakato et al. (2007)
	LC5	-	-	*DLX2*	-	Thioredoxin, associates with a HCs	Wakabayashi and King (2006)
	LC6	*ODA13*	*oda13*	*DLL2*	-	LC8 homologue, dimer interacts with ICs and LC2	King and Patel-King (2005)
	LC7a	*ODA15*	*oda15*	*DLR1*	*DYNLRB1*	Roadblock homologue, interacts with ICs	Dibella et al. (2004a)
	LC7b	-	-	*DLR2*	*DYNLRB2*	Roadblock homologue, interacts with DC2 and LC3	Dibella et al. (2004a)
	LC8	*FLA14*	*fla14-1,2,3*	*DLL1*	*DYNLL1*	Highly conserved, dimer interacts with ICs, also present in inner arm I1/f and radial spokes, retrograde IFT motor	King and Patel-King (1995), Pazour et al. (1998)
	LC9 (Tctex1 -like)	-	-	*DLT1*	*DYNLT1*[c]	Tctex1 homologue, dimeric, interacts with IC1 and IC2	Dibella et al. (2005)
	LC10, MOT24	*ODA12*	*oda12-1*[b]	*DLL3*	*DNAL4*	Tctex2, interacts with ICs and LC6 LC8 homologue, dimeric	Patel-King et al. (1997)
Docking Complex	DC1	*ODA3*	*oda3-1→ oda3-5*	*DCC1*	-	Docking complex, coiled-coil protein	Kamiya (1988), Takada and Kamiya (1994), Koutoulis et al. (1997)
	DC2	*ODA1*	*oda1*	*DCC2*	*CCDC114*	Docking complex, coiled-coil protein	Kamiya (1988), Takada and Kamiya (1994), Takada et al. (2002)
	DC3	*ODA14*	*oda14-1 (V06), oda14-2 (V16), oda14-3 (F28), oda14-11*	*DLE3*	-	Docking complex, binds Ca2+ in a redox-sensitive manner	Koutoulis et al. (1997), Pazour et al. (2003), Casey et al. (2003a)
Assembly Factors	DCC3	*ODA5*	*oda5-1, oda5-2*	*DCC3*	*CCDC63*	Coiled-coil protein, required for outer arm assembly	Wirschell et al. (2004)
	ODA7	*ODA7*	*oda7*	*DAU1*	*DNAAF1 (LRRC50)*	Leucine-rich repeats, purifies with the outer arm in the absence of I1/f; Putative ODA-I1 linker, required for the assembly of outer arms	Freshour et al. (2007)
	ODA8	*ODA8*	*oda8*	*DLU2*	*LRRC56*	Leucine-rich repeat protein, required for outer arm assembly	Kamiya (1988), Kamiya (1995)
	ODA10	*ODA10*	*Oda10*	-	-	Coiled-coil protein, required for outer arm assembly	Kamiya (1988), Dean and Mitchell (2013)
	ODA16	*ODA16*	*oda16*	*DAW1*	*WDR69*	WD-repeat, required for outer arm transport to the cilium	Ahmed and Mitchell (2005)
	PF13	*PF13*	*pf13-1→pf13-3*	*DAP1*	*DNAAF2*	PIH domain-containing, required for preassembly of outer arms and a subset of inner arms	Omran et al. (2008)
	PF22	*PF22*	*pf22, pf22A*	*DAB1*	*DNAAF3*	Required for outer arm assembly	Huang et al. (1979); Mitchison et al. (2012)
	-	-	-	-	*TXNDC3 (Sptrx2)*[c]	Thioredoxin-nucleoside diphosphate kinase, Partial lack of ODA	Dureiz et al. (2007)

[a]The current preferred protein name is indicated first in bold type

[b]The DLT2 and DLL3 genes are adjacent; both are completely deleted in *oda12-1*

[c]Human patients containing a mutation in this gene demonstrate a wide range of ciliopathies including PCD

[d]Unless cited in the text, these references are not included in the reference list

Table 2: Inner Dynein Arms (IDAs) and Associated Proteins

Inner Dynein Arms (IDA)	Protein and aliases[a]	*Chlamydomonas* Gene (Original)	*Chlamydomonas* Gene (Current)	Mutant strains	Human Gene	Properties	References
I1/f Heavy Chains	HC1α	*IDA1*	*DHC1*	*ida1-1 →ida1-6/pf9-1→pf9-4/pf30*	*DNAH10*	ATPase/Microtubule motor	Kamiya et al. (1991), Piperno et al. (1990), Myster et al. (1997), Myster et al. (1999), Porter et al. (1992)
	HC1β	*IDA2*	*DHC10*	*ida2-1→ida2-6*	*DNAH2*	ATPase/Microtubule motor	Kamiya et al. (1991), Perrone et al. (2000)
I1/f Intermediate Chains	IC140	*IDA7*	*DIC3*	*ida7*	*WDR63*	WD-repeat protein, associates with tubulin and other ICs	Perrone et al. (1998); Yang and Sale (1998)
	IC138	*BOP5*	*DIC4*	*bop5-1→bop5-6*	*WDR78*	WD-repeat protein involved in phosphorylation-based regulation, forms a complex with IC97, FAP120 and LC7b	King and Dutcher, (1997); Hendrickson et al. (2004a); Bower et al. (2009a); Bower et al. (2009b); Ikeda et al. (2009), VanderWaal et al. (2011)
	IC97, IC110	-	*DII6*	-	*LAS1*[b]	Interacts with IC140, IC138, and tubulin	Wirschell et al. (2009)
	FAP120[c]	-	*DII7*	-	-	Present in the IC138 subcomplex	Ikeda et al. (2009)
I1/f Light Chains	Tctex 1	-	*DLT3*	-	*DYNLT3 (rp3)*	Dimeric, LC9 homologue	Harrison et al. (1998), Dibella et al. (2001), Dibella et al. (2004a)
	Tctex 2b	-	*DLT4*	*pf16(D2)*[d]	*TCTEX1D2*	LC2 homologue	Dibella et al. (2004b)
	LC7a, LC7	*ODA15*	*DLR1*	*oda15*	*DYNLRB1*	Shared with outer arm dynein	Dibella et al. (2004a)
	LC7b	-	*DLR2*	-	*DYNLRB2*	Shared with outer arm dynein and interacts with IC138	Dibella et al. (2004a)
	LC8	*FLA14*	*DLL1*	*fla14-1, fla14-2*	*DYNLL1, DYNLL2*	Shared with outer arm dynein, dimeric	Wirschell et al. (2009)
I1/f Associated proteins	FAP73	*MIA1*	*MIA1*	*mia1*	-	Associates with FAP100 in the MIA complex and with IC138	King and Dutcher (1997) and Yamamoto et al. (2013)
	FAP100	*MIA2*	*MIA2*	*mia2*	-	Associates with FAP73 in the MIA complex and with IC138	King and Dutcher (1997) and Yamamoto et al. (2013)
Monomeric inner dynein arm Heavy Chains	DHC6	*DHC6*	*DHC6*	-	*DNAH12*	ATPase/microtubule motor, monomeric species a	Porter et al. (1996)
	DHC5	*DHC5*	*DHC5*	-	*DNAH7*	ATPase/microtubule motor, monomeric species b	Porter et al. (1996), Bui et al. (2012)
	DHC9	*IDA9*	*DHC9*	*ida9*	-	ATPase/microtubule motor, monomeric species c	Porter et al., (1996), Yagi et al. (2005),
	DHC2	*DHC2*	*DHC2*	-	*DNAH1, 6*	ATPase/microtubule motor, monomeric species d	Porter et al. (1996), Bui et al. (2012)
	DHC8	*DHC8*	*DHC8*	-	*DNAH14*	ATPase/microtubule motor, monomeric species e	Porter et al. (1996), Kato et al. (1993)
	DHC7	*DHC7*	*DHC7*	-	-	ATPase/microtubule motor, monomeric species g	Porter et al. (1996)
	DHC4	*DHC4*	*DHC4*	-	*DNAH3*	ATPase/microtubule motor, minor monomeric species of unknown composition	Porter et al. (1996), Yagi et al. (2009)
	DHC11	*DHC11*	*DHC11*	-	-	ATPase/microtubule motor, minor monomeric species of unknown composition	Porter et al. (1999), Yagi et al. (2009)
	DHC3	*DHC3*	*DHC3*	-	-	ATPase/microtubule motor, minor monomeric species of unknown composition	Porter et al. (1996), Yagi et al. (2009)
Monomeric inner dynein arm Associated proteins	Actin	*IDA5*	*DII4 (ACT1)*	*ida5*	*Actin*[e]	Essential for the assembly of species a, c, f, e and one minor dynein	Kato-Minoura (1997)
	NAP1	*NAP1*	*DII5 (ARP12)*	-	-	Novel actin-related protein that can functionally replace actin for species b and g assembly	Hirono et al. (2003)
	p28	*IDA4*	*DII1*	*ida4-1→ida4-3*	*DNALI1*	Essential for assembly of species a, c, and d; dimeric and binds N-terminal region of HC	Kamiya et al. (1991), LeDizet and Piperno (1995a)
	Centrin	*VFL2*	*DLE2 (CNT1)*	*vfl2-1, vfl2-R1,vfl2-R5,vfl2-R8, vfl2-R10, vfl2-R11, vfl2-R13*	*CETN1, CETN2, CETN3*	Ca2+ - binding protein, associates with N-terminal portion of heavy chain and actin	Huang et al., 1988; Sanders and Salisbury (1989), Yanagisawa and Kamiya (2001)
	p38	-	*DII2*	-	*ZMYND12*	Associates with species d only	Yamamoto et al. (2006)
	p44	-	*DII3*	-	*TTC28*	Associates with species d only	Yamamoto et al. (2008)
Monomeric inner dynein arm Assembly Factors	MOT48	*IDA10*	*DAP2*	*ida10-1*	*PIH1D1*	PIH protein, required for the preassembly of a subset of inner arms	Yamamoto et al. (2010)

[a] The current preferred protein name is indicated first in bold type

[b] Related to vertebrate Las1

[c] FAP120 is listed here as an intermediate chain subunit

[d] *pf16(D2)* lacks both the DLT4 and PF16 genes; the latter encodes a component of the central pair apparatus

[e] For organisms which express multiple actin isoforms, it has not been determined which isoform(s) is present in the cilia/flagella

Table 3: List of strains used in this study

Mutant	Mutated Gene (s)	Description of Gene Product	I1 assembly Phenotype	
			Cytoplasm	Axoneme
WT	-	-	+	+
ida1	HC1 alpha	Required for preassembly of the 20S I1 complex in the cytoplasm, and for assembly in the axoneme.	-	-
ida2	HC1 beta	Required for preassembly of the 20S I1 complex in the cytoplasm, and for assembly in the axoneme.	-	-
ida7	IC140	Required for preassembly of the 20S I1 complex in the cytoplasm, and for assembly in the axoneme.	-	-
ida3	IDA3	Predicted IFT adapter	+	-
bld-1	IFT52	Required for ciliogenesis	+	-
bop5-3	IC138	Phosphoprotein required for control of normal waveform	-/+	-/+
fla14-3	LC8	Required for complete assembly of 20S I1 dynein	-/+	-/+
fla10-1^{ts}	FLA10	Encodes kinesin II required for anterograde IFT. Kinesin II is fully functional at permissive temperature (21°C) but is inactivated at restrictive temperature (32°C).	+	+
fla10;ida3^{ts}	FLA10, IDA3	Lacks IDA3 and kinesin II at restrictive temperature.	+	-

"-" : No assembly of the 20S I1 dynein
"+": Assembly of the 20S I1 dynein
"-/+": Assembly of partial I1 dynein complexes in the 10-18S range

Table 4: IFT and associated proteins

	***Chlamydomonas* Protein**	**Domain structure**	**Known/Predicted Function in *Chlamydomonas***	**References**
Kinesin-II	FLA8	Kinesin-II motor	Anterograde IFT	Miller et al., 2005
	FLA10	Kinesin-II motor	Anterograde IFT	Kozminski et al., 1995
	FLA3	Kinesin-II associated	Anterograde IFT	Mueller et al., 2005
Dynein 2b	cDHC1b	Dynein heavy chain	Retrograde IFT	Pazour et al., 1999
	D1bLIC	Coiled-coil	Retrograde IFT	Hou et al., 2004
IFT Particle Complex B	IFT172	WD40[1], TPR[1]	Interacts with EB1 at the tip and controls assembly and disassembly of components at the tip.	Pederson et al., 2005
	IFT88	TPR	Required for flagellar assembly	Pazour et al., 2000
	IFT81	Coiled-coil[1]	N-terminus interacts with IFT74 to form a tubulin-binding module	Bhogaraju et al., 2013
	IFT80	WD40	-	
	IFT74/72	Coiled-coil	N-terminus interacts with IFT81 to form a tubulin-binding module	Bhogaraju et al., 2013
	IFT57/55	Coiled-coil	-	Lucker et al., 2005
	IFT54	-	-	-
	IFT52	GIFT domain	Required for flagellar assembly	Deane et al., 2001
	IFT46	-	Transport of ODA	Hou et al., 2007; Ahmed et al., 2008
	IFT22	Small GTPase	Controls pool size of IFT A and B particles	Silva et al., 2012
	IFT25	Ca2+ binding	Transport of Hedgehog signals	Keady et al., 2012
	IFT27	Small GTPase	Required for cargo loading onto retrograde IFT	Huet et al., 2014
	IFT20	GTPase	Traffics membrane proteins from Golgi to cilium	Follit et al., 2006
	IFT70	-	Predicted to be required for the polyglutamylation of axonemal tubulin	Pathak et al., 2007, Dave et al., 2009
IFT Particle Complex A	IFT144	WD40	Retrograde IFT[2]	Piperno et al., 1998
	IFT140	WD40, TPR	Retrograde IFT[2]	Piperno et al., 1998
	IFT139	-	Retrograde IFT[2]	Piperno et al., 1998
	IFT121	WD40, TPR	Required for flagellar assembly and for stability of IFT complex A	Behal et al., 2011
	IFT122	WD40	Required for flagellar assembly and for stability of IFT complex A	Behal et al., 2011
	IFT43	-	Retrograde IFT[2]	Piperno et al., 1998
	FAP259	TPR, coiled-coil	-	Merchant et al., 2007

Other putative IFT proteins	FAP259	TPR, coiled-coil	-	Merchant et al., 2007
	FAP66	WD40, TPR	-	Merchant et al., 2007
	FAP22	Coiled-coil	-	Pazour et al., 2005
	TTC26/DYF13/IFT 56	-	Transport of specific IDAs	Ishikawa et al., 2014
	FAP118	WD-40	-	Merchant et al., 2007

[1] WD repeats, tetratricopeptide (TPR) and coiled-coils are protein-protein interaction motifs. Such motifs may faciliate formation of the multi-subunit IFT particle complexes and/or be involved in associating cargoes to IFT complexes.

[2]Mutants defective in IFT 144, 140, 139 and 43 subunits demonstrate distinct bulging of the flagellar membranes, decrease in IFT Complex A components in the flagella, and decreased retrograde velocities of IFT; suggesting their role in retrograde IFT.